Earth-Science Reviews 246 (2023) 104588

Contents lists available at ScienceDirect

Earth-Science Reviews

journal homepage: www.elsevier.com/locate/earscirev

Petrology and geochemistry of Canadian diamonds: An up-to-date review

Andrea Curtolo [a,*], Davide Novella [a,*], Alla Logvinova [b], Nikolay V. Sobolev [b,1], Rondi M. Davies [c], Maxwell C. Day [a], Martha G. Pamato [a], Fabrizio Nestola [a]

[a] Department of Geosciences, University of Padova, Padova, Italy
[b] V.S. Sobolev Institute of Geology and Mineralogy SB RAS, Novosibirsk, Russia
[c] Queensborough Community College, City University New York, USA

ARTICLE INFO

Keywords:
Diamond
Canada
Inclusions
Isotopes
Geochemistry
Petrology

ABSTRACT

Canada is one of the most important diamonds producers in the world despite the first diamond mine opening relatively recently in 1998 in the Slave craton. Given the increasing economic and scientific interest towards Canadian diamonds, an investigation of their geochemical and petrological properties was needed to better understand their genesis. A detailed review is given of all available petrological and geochemical data from >3000 Canadian diamonds and their silicate, oxide and sulfide inclusions from published literature and unpublished datasets, compared with data from worldwide datasets.

Based on the available published data, different abundances of peridotites and eclogites in the lithosphere of the Canadian cratons are indicated by mineral inclusions, with the Slave craton exhibiting a high amount of eclogitic diamonds, and the Superior craton exhibiting a strong prevalence of peridotitic diamonds.

Diamond formation from extremely ^{13}C-depleted subducted organic matter is necessary to explain the extremely low $\delta^{13}C$ observed in some samples from the Canadian lithosphere, which, as of today, are the lowest values ever recorded in mantle diamonds. Core-to-rim $\delta^{13}C$ analyses revealed progressive rimward enrichment in ^{13}C for some of the samples, a behavior which is associated to the crystallization of diamonds from oxidized C species (e.g., CO_2).

Using the available data geothermobarometric calculations were performed on both single inclusions and inclusion pairs and provide a formation window for Canadian lithospheric diamonds from ~140 to ~210 km, with temperatures ranging from 900 to 1400 °C, which are generally higher than mantle residence temperature given by N aggregation geothermometry. Sub-lithospheric diamonds are sampled from ~240 km to >660 km based on geobarometry on majoritic garnets and observations of inclusion assemblages. The age range of Canadian diamonds suggest numerous diamond-forming events that took place from the Paleo-Archean to the Neoproterozoic.

1. Introduction

Natural diamonds are unique specimens that allow one to study the deep (>140 km), inaccessible mantle where they form. Studies of their mineral inclusions, in particular, have drastically improved our understanding of deep mantle processes and the petrology and geochemistry of the cratonic lithosphere, where most diamonds form (Clifford, 1966). Most studies of diamonds focus on a specific set of specimens from a particular locality, or localities, likely due to the rarity and poor accessibility of the samples. Nevertheless, many recent studies have addressed specific geological questions related to most cratonic areas, especially when combined with data from kimberlite-hosted xenoliths and/or xenocrysts. For example, many impactful studies have been completed with focus on different aspects of diamonds including their physical, chemical, and isotopic characteristics (Harris, 1987; Cartigny, 2005; Stachel and Harris, 2009; Shirey et al., 2013; Shirey et al., 2019; Howell et al., 2020; Stachel et al., 2022a), their formation processes (Bulanova, 1995; Navon, 1999) and the types of mineral inclusions they contain (Meyer and Boyd, 1972; Sobolev, 1977; Meyer, 1987; Stachel and Harris, 2008; Stachel et al., 2022b). Other works focus on the age determination of diamonds (Pearson and Shirey, 1999; Smit et al., 2022a), the trace element contents of their mineral inclusions (Stachel

* Corresponding authors.
E-mail addresses: andrea.curtolo.2@phd.unipd.it (A. Curtolo), davide.novella@unipd.it (D. Novella).
[1] Deceased

https://doi.org/10.1016/j.earscirev.2023.104588
Received 17 July 2023; Received in revised form 21 September 2023; Accepted 3 October 2023
Available online 10 October 2023

et al., 2004) and on sub-lithospheric inclusions (Stachel et al., 2005; Walter et al., 2022).

Of particular importance are compilations and descriptions of large datasets to provide a global perspective on diamond genesis. Meyer and Boyd (1972) were the first to investigate a large number of mineral inclusions (several hundreds) in diamonds from different localities worldwide, i.e., Sierra Leone, Ghana, South-West Africa, Venezuela, and Thailand. By using X-ray diffraction and electron microprobe techniques, these authors were able to compare the composition of olivine, garnet, magnesiochromite, enstatite and diopside inclusions in diamonds with minerals in xenoliths from the corresponding kimberlites. Differences were observed for garnet and diopside which showed a lower Cr_2O_3 content for the inclusions with respect to the xenoliths, suggesting that diamonds may form in environments with eclogitic paragenesis.

Sobolev (1977) described deep-seated kimberlites and mineral inclusions in diamonds from Russia expanding the dataset of Meyer and Boyd (1972). Sobolev (1977) compared geochemical data of garnet, olivine, magnesiochromite, enstatite and clinopyroxene inclusions with results from published literature. Through analysis of the Cr_2O_3 and CaO content of garnet and clinopyroxene, Sobolev (1977) assigned an eclogitic or peridotitic (harzburgitic, lherzolitic or wehrlitic) paragenesis to different mineral inclusions. These two studies provided crucial insights into the understanding of diamond formation.

Meyer (1987) published the first comprehensive review of mineral inclusions in diamonds in which all data available in the literature was included. This work emphasized the existence of different parageneses to which inclusions in diamonds belong, and further highlighted the compositional differences between clinopyroxene and garnet from eclogitic and peridotitic suites. The work of Meyer (1987) remained a reference point for all the studies on mineral inclusions in diamonds for more than three decades.

Later, Stachel and Harris (2008) published an updated review of mineral inclusions in diamonds, including chemical analyses for nearly 5000 mineral inclusions in diamonds from all over the world. Stachel and Harris (2008) provided unique and statistically sound information regarding the genesis of diamonds, including the relative abundance of lithospheric and sub-lithospheric diamonds, the relative proportions of various parageneses and the ranges of major element compositions for the minerals included in diamonds.

Recently, an entire volume of the Reviews in Mineralogy and Geochemistry from the Mineralogical Society of America about diamonds has been published (vol. 88: Diamond: Genesis, Mineralogy and Geochemistry, Smit et al., 2022b). This book consists of a number of review works covering all aspects of diamond research and represents the most up-to-date, comprehensive, and in-depth resource for information regarding diamonds. Such works are all based on large global databases as they allow one to make important general conclusions regarding the processes and agents involved in diamond formation. However, large databases can hide data trends local to particular cratonic areas. Smaller-scale reviews, focused on diamonds from specific localities, are therefore necessary to better assess diamond-related processes at the scale of the cratonic lithosphere.

In past decades, different countries have become increasingly prominent in terms of annual diamond production, in particular Australia and Canada. Today, Canada is one of the main diamond producers in the world (Fig. 1) ranking second, after Russia, in terms of millions of carats of diamonds produced in 2017 and third in both 2018 and 2019, after Russia and Botswana (Brown et al., 2021).

Canada provided approximately 14–15% of the total world diamond production in 2017 to 2019. Given the increasingly important role of Canada in global diamond production, an investigation of the petrology and geochemistry of Canadian diamonds is warranted to further constrain the genesis of such diamonds and to better understand the petrological and geochemical processes associated with diamond formation in the Canadian cratonic lithosphere.

The study focuses on the type of mineral inclusions in diamonds and on the chemical and isotopic composition of diamonds, i.e., the C and N isotopic composition, the N content, and its aggregation state.

The results presented here provide an updated benchmark for future studies of diamonds, particularly Canadian diamonds, and will better our understanding of the environment of formation of diamonds. Furthermore, our results can be used to compare different cratonic areas worldwide to identify local differences related to the formation and features (e.g., formation processes, isotopic and petrologic features) of diamonds, and the nature of their host cratons.

2. Materials and methods

2.1. Database construction

A critical step in this study was to construct a database that includes all published literature for diamonds from Canadian cratons. To do this, the online scientific database *Scopus* (*www.scopus.com*) was used to collect the published material. To ensure that no published data were missing from our collection, an alternative international database, *ISI Web of Science* (*www.webofscience.com*), was checked. The literature survey was conducted using the specific keywords "*diamond*" and "*Canada*" in the search engine, which provided a total of 845 published manuscripts from as early as 1934. This large body of literature was filtered by restricting the subject area to "*Earth and Planetary Sciences*", reducing the number of manuscripts to 563. Manuscripts were considered relevant, and therefore included in this review, only if one or more of the following types of geological data were reported:

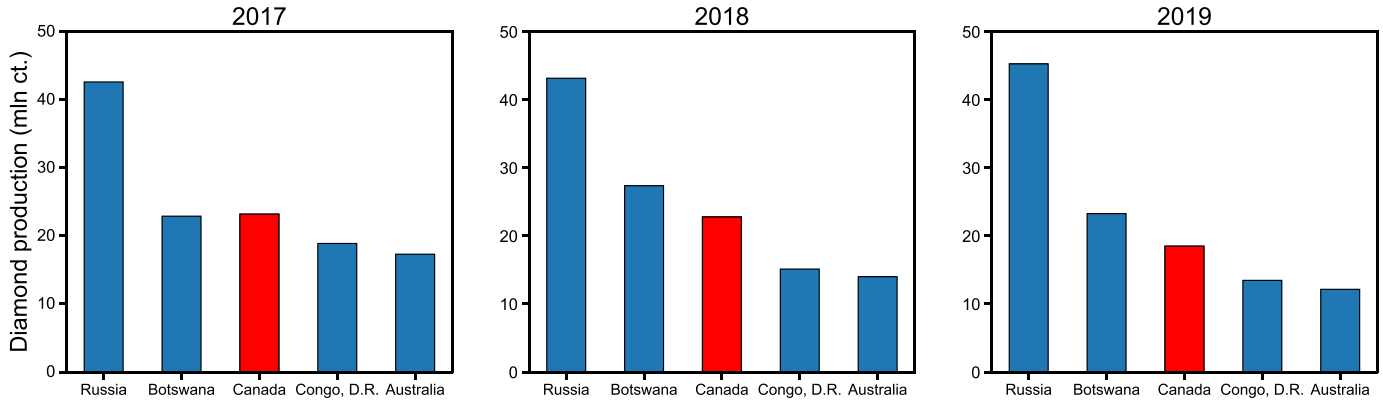

Fig. 1. Annual diamond production (expressed as millions of carats) for the five most important diamond-producing countries in the years 2017, 2018 and 2019 (data from Brown et al., 2021). Canada is highlighted in red in the three images. (For interpretation of the references to colour in this figure legend, the reader is referred to the web version of this article.)

- Diamond C isotopes
- Diamond N content and aggregation state
- Diamond N isotopes
- Presence of mineral inclusions
- Composition of mineral inclusions (major, minor and trace elements)
- Paragenesis

These types of data provide crucial information regarding the origin of diamonds: C and N isotopes provide information about the geochemistry of the environment in which the diamond formed and the processes that formed it; the N content and N aggregation state constitutes the basis for classification of diamonds and serves as a geothermometer that allows determination of the mantle residence temperature; the presence and chemical composition of mineral inclusions provides direct information on the composition of the Earth's mantle; lastly, the paragenesis describing the type of rock in which the diamond formed, provides information on the petrological composition of the mantle.

This review includes 52 manuscripts on natural diamonds from Canadian cratons published since 1998 (Table 1), the opening year of Canada's first diamond mine. While most manuscripts report geochemical data for each individual sample that was analyzed, some studies only provide representative or averaged data, limiting the amount of available data and impacting the statistical analyses of data from Canadian samples (Davies et al., 1998; Davies et al., 2004b; Pokhilenko et al., 2001; Pokhilenko et al., 2004; Sobolev et al., 2008; Ivanova et al., 2017). This issue was addressed by compiling a complete dataset that includes individual sample analyses provided by the authors of these manuscripts. Combination of data from the published literature with unpublished data (as described above), resulted in a database of 3071 diamonds. The geochemical data of these specimens is described in the following sections.

Table 1
Published literature considered in the present study listed from oldest to most recent.

	C isotopes	N content	N isotopes	Inclusions	Inclusions composition*	Inclusion traces^	Paragenesis
Davies et al., 1998	yes	yes	no	yes	yes	no	yes
Pokhilenko et al., 2001	no	no	no	yes	yes	no	yes
Stachel et al., 2003	no	yes	no	yes	yes	no	yes
Davies et al., 2004a	yes	yes	no	yes	yes	yes	yes
Davies et al., 2004b	yes	yes	no	yes	yes	yes	yes
Pokhilenko et al., 2004	yes	no	no	yes	yes	no	yes
Promprated et al., 2004	no	no	no	no	no	yes	no
Tappert et al., 2005	no	yes	no	yes	yes	yes	yes
De Stefano et al., 2006	no	yes	no	yes	yes	no	yes
Stachel et al., 2006	yes	yes	no	yes	yes	no	yes
Tomlinson et al., 2006	no	yes	no	yes	yes	no	yes
Westerlund et al., 2006	no	yes	no	yes	yes	yes	yes
Banas et al., 2007	yes	yes	no	yes	yes	no	yes
Donnelly et al., 2007	yes	yes	no	yes	yes	yes	yes
Klein-BenDavid et al., 2007	yes	yes	yes	no	no	no	no
Creighton et al., 2008	yes	yes	no	no	no	no	yes
Sobolev et al., 2008	no	no	no	yes	yes	no	yes
Aulbach et al., 2009	yes	yes	no	yes	yes	yes	yes
Burgess et al., 2009	yes	yes	yes	no	no	no	no
Cartigny et al., 2009	yes	yes	yes	no	no	no	yes
De Stefano et al., 2009	no	yes	no	yes	yes	yes	yes
Van Rythoven and Schulze, 2009	no	no	no	yes	yes	no	yes
Bruce et al., 2011	no	yes	no	no	no	no	no
Fedortchouk and Zhang, 2011	no	yes	no	no	no	no	no
Smart et al., 2011	yes	yes	no	no	no	no	yes
Van Rythoven et al., 2011	no	no	no	yes	yes	no	yes
Aulbach et al., 2012	no	yes	no	no	no	no	yes
Hunt et al., 2012	yes	yes	no	yes	yes	no	yes
Johnson et al., 2012	yes	yes	no	no	no	no	no
Miller et al., 2012	yes	no	no	yes	yes	no	yes
Nestola et al., 2012	no	no	no	yes	no	no	no
Peats et al., 2012	yes	yes	no	no	no	no	no
Smart et al., 2012	no	no	no	yes	yes	yes	yes
Zhang and Fedortchouk, 2012	no	yes	no	no	no	no	no
Melton et al., 2013	yes	yes	no	no	no	no	no
Smit et al., 2014	yes	yes	no	no	no	no	no
Petts et al., 2015	yes	yes	yes	no	no	no	yes
Hogberg et al., 2016	yes	yes	yes	no	no	no	no
Krebs et al., 2016	yes	yes	no	no	no	no	no
Petts et al., 2016	yes	yes	yes	no	no	no	no
Sobolev et al., 2016	no	no	no	yes	yes	yes	yes
Ivanova et al., 2017	no	no	no	yes	yes	no	yes
Van Rythoven et al., 2017	yes	yes	no	no	no	no	no
Aulbach et al., 2018	no	no	no	no	no	yes	yes
Li et al., 2018	no	yes	no	no	no	no	no
Stachel et al., 2018	no	yes	no	yes	yes	yes	yes
Krebs et al., 2019	no	no	no	yes	no	no	yes
Lai et al., 2020	yes	yes	no	no	no	no	no
Pamato et al., 2021	no	no	no	yes	yes	no	no
Elazar et al., 2022	no	yes	no	no	no	no	no
Timmerman et al., 2022	yes	yes	yes	no	no	no	no
Van Rythoven et al., 2022	yes	yes	no	no	no	no	no

*Major and minor elements; ^Trace elements

2.2. Geological setting and samples

Most of the Canadian lithosphere consists of the Canadian Shield, the exposed north-eastern part of Laurentia, a large craton that makes up most of the North American lithosphere. The Canadian Shield extends north-south from Baffin Island to the Great Lakes, and east-west from the Greenville Province to the Cordilleras (Mints, 2017). The Shield is overlain by a Phanerozoic sedimentary cover in the most western area which is bordered (north to south) by Great Bear Lake, Great Slave Lake, and Lake Winnipeg. The Canadian Shield is composed of Archean provinces welded together by Paleoproterozoic orogens (the most important being the Trans-Hudson Orogen, 2.0–1.8 Ga, welding together the Hearne-Wyoming provinces to the Superior province; Hoffman, 1988) occasionally containing accreted back-arc terrains and sedimentary basins. The Archean provinces of the Shield are six, from west to east: 1) Slave, 2) Rae, 3) Hearne, 4) Wyoming, 5) Superior and 6) Nain. These provinces represent Archean continents or fragments of Archean continental lithosphere (Whitmeyer and Karlstrom, 2007), and each province represents cratonic basement material, specifically granites and greenstones or their high-grade metamorphic equivalents (Hoffman, 1988).

The majority of diamonds described in this study are from the Slave and Superior cratons and the minority are from the Nain and Rae cratons (Fig. 2). The Hearne and Wyoming cratons will not be discussed in this work as no diamonds are recorded in the Canadian part of these cratons. Both micro (<0.5 mm) and macro (>0.5 mm) diamonds, as well as diamonds with and without inclusions are included in this database and exhibit a wide range of different morphologies: octahedral, dodecahedral, cubic, aggregates, twins, macles, coated and fibrous. Inclusion-bearing diamonds usually show more than a single mineral inclusion with up to 15 or more inclusions described in some instances.

2.3. Data treatment

The N content and aggregation state of each diamond sample, as well as the isotopic and chemical composition of the inclusions have not been modified in any way with respect to the original manuscripts. No data have been discarded from the statistics reported in this study unless clearly stated and justified in the text.

In one instance, three different manuscripts (Tappert et al., 2005; Cartigny et al., 2009; Melton et al., 2013) report analyses of the N content and aggregation state of the same set of diamonds from the Panda kimberlite (Slave craton). For these samples, the data from Tappert et al. (2005) were considered as they were the first to be published and were found to be in good agreement with those presented in Cartigny et al. (2009).

For some mineral inclusions in this database, principal component analysis (PCA) was performed to highlight possible correlations and groupings with respect to the major and minor element composition. This procedure involves reorientation and projection of the n-dimensional space (n = number of variables) that fully describes the dataset of interest. This approach allows for evaluation of correlation (or lack thereof) among all variables at the same time. A detailed explanation of this data treatment procedure is given by Wold et al. (1987). In the present study all calculations necessary for PCA were performed in Python with the *scikit-learn* library (Pedregosa et al., 2011).

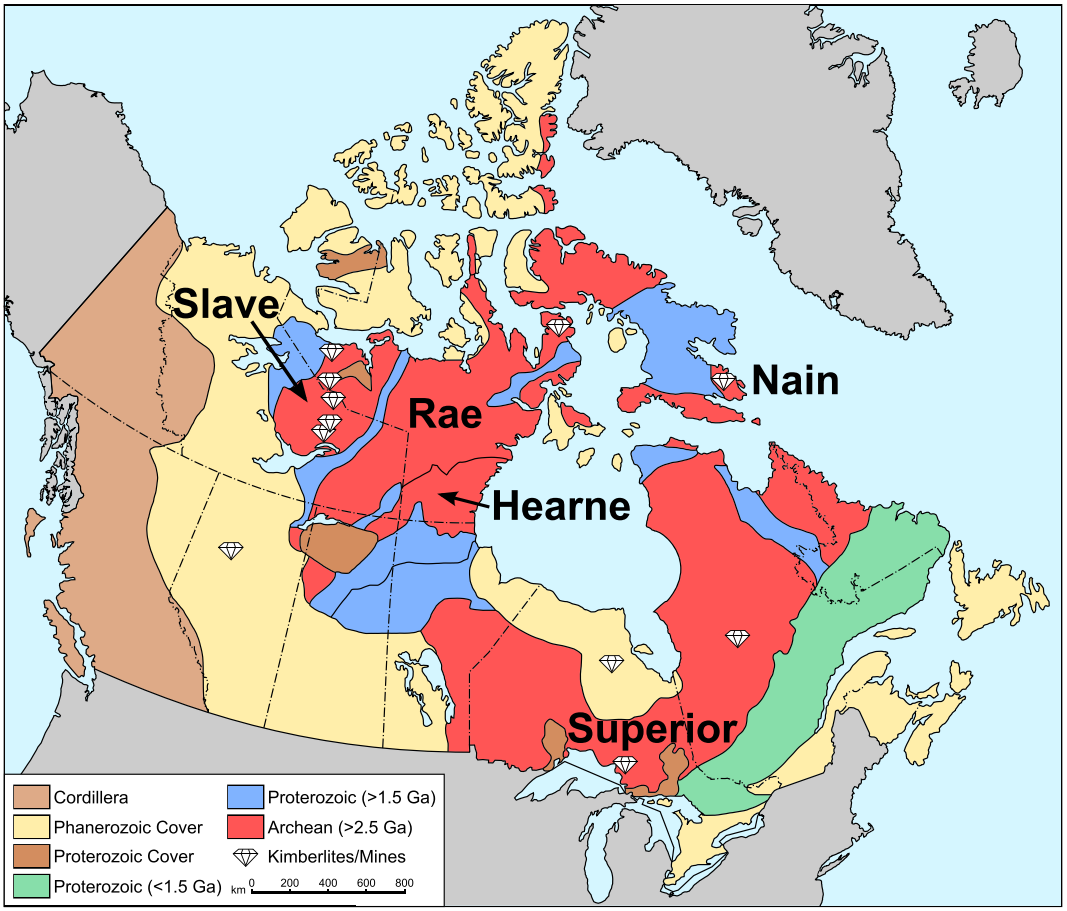

Fig. 2. Geological map of Canada showing the different cratonic areas. Diamond symbols indicate the localities where the diamonds described in this work were collected. For the purpose of clarity, and since its Canadian part is overlain by a Phanerozoic cover, the Wyoming craton is not highlighted. Modified after Woodland et al., 2021.

3. Results and discussion

3.1. Paragenesis

The paragenesis of a diamond refers to the type of rock in which the diamond formed. Diamonds can form in one of three substrates (or suites): peridotitic, eclogitic, websteritic. The peridotitic suite can be further differentiated into three different paragenesis: lherzolitic, harzburgitic, wehrlitic. The paragenesis of a diamond can be determined either from the inclusions (and their composition) hosted inside the stone or based on the paragenesis of the xenolith from which the diamond was extracted. A table of the inclusions that can be found in diamonds from every suite can be found in Stachel et al. (2022b).

In this section, the paragenesis of Canadian diamonds will be discussed, along with their origin in the lithospheric mantle, or in the deeper, convective mantle.

Out of 3071 diamonds in the dataset, 1075 have a known paragenesis. For 964 of these, the paragenesis was retrieved from mineral inclusions, while 108 were classified based on the paragenesis of the corresponding xenolith, and 3 (samples AB65, AB70 and Lynx28 from Van Rythoven et al., 2017) were classified in the original manuscript but no data regarding the presence of inclusions or the paragenesis of the host xenoliths were reported. Of the 1075 diamonds with known paragenesis, two contain inclusions that are recognized as epigenetic (samples 13544 from Hunt et al., 2012 and Ash-106A from Davies et al., 2004a) and four are classified as having mixed paragenesis due to incorporation of eclogitic clinopyroxene and olivine (De Stefano et al., 2006). These diamonds are therefore excluded from further consideration, reducing the number of inclusion-bearing diamonds to 1069.

In total, 49 diamonds were identified as sub-lithospheric due to the presence of one or more of the following mineral inclusions: majoritic garnet, ferropericlase, low Ni-enstatite (former bridgmanite) and breyite (former $CaSiO_3$-perovskite). These 49 diamonds amount to 4.6% of all studied Canadian diamonds with a known paragenesis, the remaining 95.4% are classified as lithospheric (Fig. 3).

Stachel and Harris (2008) calculated a 90:10 proportion of lithospheric to sub-lithospheric diamonds for a worldwide database but identified a selection bias due to a strong scientific interest towards sub-lithospheric diamonds that cause these specimens to be statistically overrepresented. Accounting for this bias, Stachel and Harris (2008) recalculated this proportion and obtained a 99:1 ratio for lithospheric to sub-lithospheric diamonds. This ratio was recently changed to 98:2 by Stachel et al. (2022b), after the recognition that CLIPPIR (Cullinan-like, Large, Inclusion-Poor, Pure, Irregular, Resorbed) diamonds form in the transition zone or lower mantle (Smith et al., 2016). Importantly, further work is required to determine whether the higher abundance of superdeep diamonds from Canada is due to a selection bias or is statistically representative.

Of the 49 sub-lithospheric diamonds, 40 (82%) are from the Slave craton (Lac de Gras area, in particular the DO27 pipe, which alone produced approximately half of all Canadian sub-lithospheric diamonds), the remaining 9 (18%) are from the Superior (5) and Rae (4) cratons. The Slave craton has a layered structure, with a highly depleted, oxidized shallow layer, and a less depleted, more reduced deep layer (Griffin et al., 1999; Kopylova and Caro, 2004; Snyder et al., 2014). This peculiar structure was attributed to mantle plume activity that thickened the proto-craton, forming the lower, less depleted layer and may have transported the sub-lithospheric diamonds from the convective mantle into the lithosphere (Davies et al., 2004b). However, Timmerman et al. (2022) shows that mantle plumes were not involved in the formation of the Slave craton, which accreted by imbrication of subducted oceanic lithosphere under a pre-existing cratonic nucleus. This implies that plume activity responsible for the transport of the sub-lithospheric diamonds into the lithosphere was operative after the formation of the Slave craton. This agrees with the observation that all sub-lithospheric diamonds, dated as of today, are Mesoproterozoic or younger (Smit et al., 2022a). It follows that the mantle plume that transported diamonds into the lithosphere must also be Mesoproterozoic or younger, and thus subsequent to the formation of the craton. Moreover, the kimberlites of the Lac de Gras area have been dated, and are among the youngest kimberlites in the world, with emplacement ages ranging from 45 to 74 Ma (Scott Smith, 2008; Heaman et al., 2019), giving us a lower boundary for the diamond formation age. It is important to note, however, that all dated sub-lithospheric diamonds, as of today, come from the Juina area (Brazil), apart from a single dating attempt of sub-lithospheric inclusions from Letseng, (Lesotho; Smit et al., 2022a). Therefore, the possibility that the young age of sub-lithospheric diamonds is simply a local characteristic cannot be ruled out, but new data regarding the age of diamonds from different areas are needed to support this.

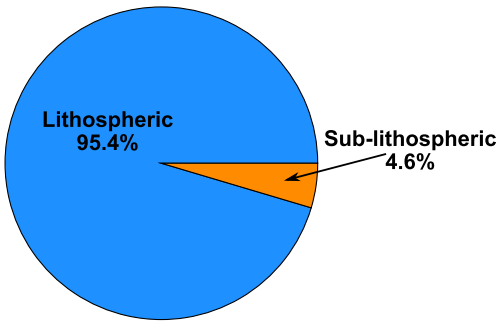

Fig. 3. Relative abundances (see text for statistical interpretation) of lithospheric and sub-lithospheric Canadian diamonds calculated from a dataset of 1069 diamonds.

The five diamonds from the Superior province come mainly from the Wawa area and have been classified as sub-lithospheric based on geobarometry of majoritic garnet inclusions (see section 3.6.1). These samples have a pressure of formation (minimum estimates) ranging from 8.6 to 11.4 GPa, compatible with the sub-lithospheric mantle. However, Stachel et al. (2006) studied three of these diamonds and suggested an origin in a portion of lithospheric mantle extending into the majoritic garnet stability field. This would require extension of the lithospheric mantle up to depths >350 km, which there is no evidence for (Pearson et al., 2021). However, the regular shape of such diamonds suggests a lithospheric origin. If all five diamonds from the Superior province are assigned a lithospheric origin, the proportion of sub-lithospheric to lithospheric diamonds in Canada decreases by only ~0.5%. Thus, this uncertainty has minimal statistical relevance and does not affect the validity of comparisons made between the proportion of sub-lithospheric diamonds in Canada and in the worldwide database of Stachel et al. (2022b).

The 1020 lithospheric diamonds in this database have been grouped into peridotitic (harzburgitic, lherzolitic and wehrlitic), eclogitic and websteritic suites to obtain information regarding the composition of the Canadian lithosphere. The studied diamonds from Canada exhibit an almost perfect 2:1 ratio between the peridotitic and eclogitic suites, where 34.8% and 64.3% of the diamonds belong to eclogitic and peridotitic suites, respectively (Fig. 4). The remaining 0.9% accounts for the websteritic suite, which is very poorly represented in the available Canadian specimens (9 out of 1020 diamonds) with respect to the global database, which reports 2.3% of the total diamonds as websteritic (Stachel and Harris, 2008).

This proportion almost perfectly matches the global dataset of Stachel and Harris (2008), who report 32.8% and 65.0% of diamonds are eclogitic and peridotitic, respectively.

Recent estimates based on geophysical constraints (Garber et al., 2018) are contradictory and suggest the cratonic lithosphere is unlikely to consist of >20% eclogite. The higher abundance of eclogite lithologies in diamonds compared to the cratonic lithosphere may be due to

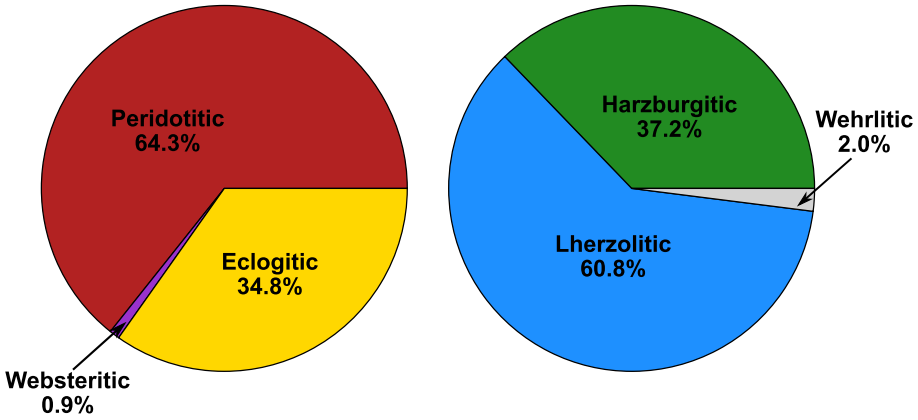

Fig. 4. (Left) Relative abundances of Canadian diamond parageneses. (Right) Relative abundances of the parageneses in the peridotitic suite. A precise paragenesis could not be assigned to most (78%) of the diamonds in the peridotitic suite as they do not host garnet inclusions.

preferential sampling of eclogitic substrates during kimberlite eruption, to eclogite being preferentially preserved compared to peridotite in diamond-forming environments (Stachel et al., 2022b) or to eclogites having on average higher diamond grade then peridotites.

Of the studied peridotitic diamonds from Canada, 60.8% have lherzolitic paragenesis 37.2% have harzburgitic paragenesis and 2% have wehrlitic paragenesis. Peridotitic parageneses can be better assessed by considering garnet exclusively, which is the only inclusion that can be assigned to the harzburgitic, lherzolitic and wehrlitic parageneses using its major element composition (see Stachel and Harris, 2008). Considering only parageneses based on the composition of garnet inclusions (130 samples), we observe 55% lherzolitic, 42.6% harzburgitic and 2.3% wehrlitic diamonds. This is in stark contrast with a database of 1175 garnets from worldwide diamonds, studied by Stachel et al. (2022b), which show predominately harzburgitic paragenesis (81%) compared to lherzolitic (18%) and wehrlitic (1%) paragenesis. This discrepancy is mainly due to the large set of inclusion bearing diamonds from the Victor Mine (Superior craton) analyzed by Stachel et al. (2018), who reported 63 out of 102 diamonds as lherzolitic, and not a single diamond assigned to a harzburgitic paragenesis. The lherzolite-rich nature of the samples from Victor Mine is due to a combination of efficient kimberlite sampling from a narrow lherzolite layer and sub-solidus diamond precipitation from a metasomatic C-O-H fluid that refertilized the mantle. A cold geotherm in the area allowed lherzolite + fluid to be stable at the depths of diamond stability, typically, along a normal geotherm, lherzolite + fluid would melt at depths >140 km (Stachel et al., 2018). Individual mines with anomalous diamond parageneses are well described, a notorious example is Pipe 50 (Fuxian kimberlite field, Liaoning province, China; Harris et al., 1991) which also exhibits a predominantly lherzolitic paragenesis. Without considering the diamonds from the Victor Mine, the relative proportions of harzburgitic, lherzolitic and wehrlitic parageneses become 80.9%, 17.6% and 1.5% respectively, and are in excellent agreement with the global data of Stachel et al. (2022b).

3.2. *Nitrogen content and aggregation state*

Nitrogen is the most abundant impurity in natural diamonds (Green et al., 2022) and serves as the basis for the diamond *type* classification (Robertson et al., 1934) that distinguishes diamonds that contain measurable amounts of N as Type I diamonds from those that have no detectable N as Type II diamonds (Shirey et al., 2013). Typically, the N content of diamonds is measured using Fourier-Transformed Infrared (FTIR) spectroscopy and the detection limit for this method is ~10 at.ppm, depending on the instrument and the sample. In this database, The N content of a small number of diamonds was measured using Secondary Ion Mass Spectrometry (SIMS), allowing measurement of N content below the FTIR detection limit. However, in order to compare specimens and organize the database, all diamonds with a N content <10 at.ppm were classified as Type II, in line with Stachel et al. (2022a) as further Type classification requires interpretable signal in the one-phonon region and in most cases, N concentrations ≥10 at.ppm.

Of the 3071 samples in the database, the N content of 2567 diamonds is determined and reported in the corresponding literature. Based on the available data, most Canadian diamonds (82.5%) are Type I, the remaining 17.5% have N contents <10 at.ppm, and are therefore classified as Type II (Fig. 5).

Following the results of Dyer et al. (1965), who analyzed a database of 500 diamonds, authors (e.g., Pearson et al., 2003; Banas et al., 2007; Johnson et al., 2012) often report that Type II diamonds comprise ~2% of global diamonds. Harris (1987) suggested that the N content observed in diamonds may be dependent upon their place of origin. In fact, Stachel and Harris (2009) calculated that 10% of all eclogitic and 24% of all peridotitic diamonds are Type II. Shirey et al. (2013) showed that only ~70% of diamonds have an N content >20 at.ppm, suggesting that the earlier estimate of Dyer et al. (1965) is not representative of the true abundance of Type II diamonds. In this regard, the percentage of Type II diamonds in this study is in agreement with the worldwide value.

The highest N concentration observed in a Canadian diamond is 3833 at.ppm (Fig. 6) found in an eclogitic sample from the Slave craton (Donnelly et al., 2007) which is also, as of today, the highest N concentration ever recorded in a diamond from the Earth's mantle (Stachel et al., 2022a). The median N content for the database is 380 at.ppm, more than twice what is observed in the global database (160 at.ppm; Stachel et al., 2022a). The higher median and maximum N concentrations with respect to global database suggest a higher N concentration in

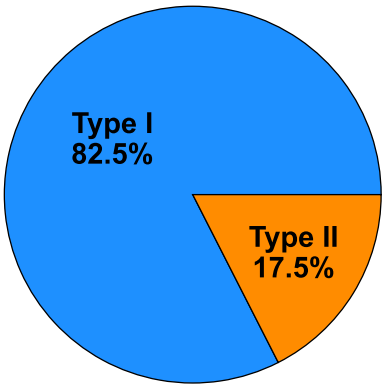

Fig. 5. Relative proportions of 2567 Canadian diamond Types based on their N content.

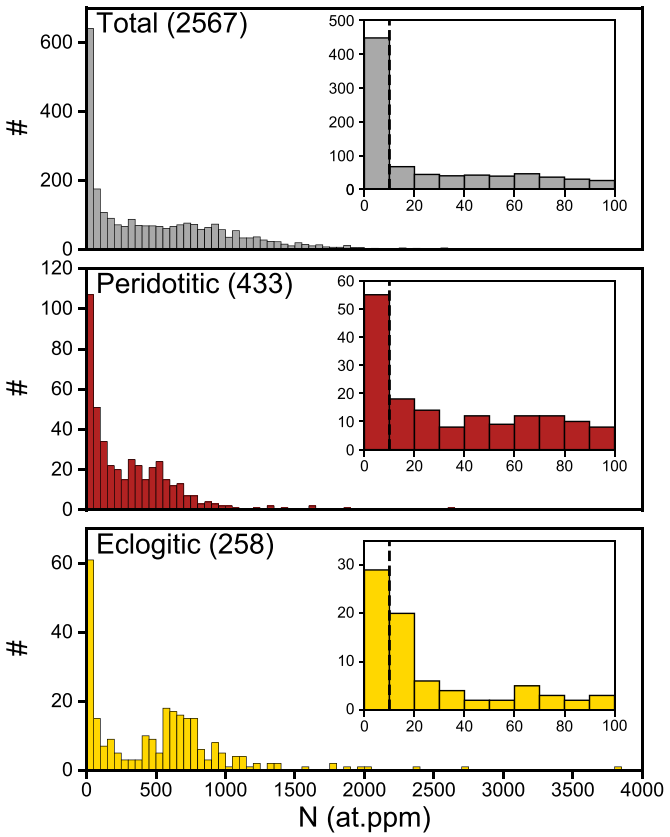

Fig. 6. The distribution of N in Canadian diamonds with a bin size of 50 at. ppm. The insets on the upper right of every plot represent the distribution of the N concentration between 0 and 100 at.ppm, with a bin size of 10 at.ppm. The black dashed line represents the boundary between Type I and Type II diamonds.

Canadian diamond-forming environments with respect to the rest of the world.

Of the 2567 diamonds with a known N content, 691 also have known paragenesis allowing comparison of the N content in peridotitic and eclogitic diamonds (Fig. 6).

Based on the present data, peridotitic diamonds from Canada show N contents up to 2636 at.ppm with a median of 201 at.ppm, 12.7% of the diamonds are Type II as they have an N content <10 at.ppm. These data are in stark contrast with the global database, where the median N content for peridotitic diamonds is 109 at.ppm (Stachel et al., 2022a) and the percent of Type II diamonds (24%) is almost twice that observed in Canadian diamonds (Stachel and Harris, 2009).

For eclogitic Canadian diamonds, the highest N content is 3833 at. ppm (which is also the highest N content in this database) with a median of 523 at.ppm, 11% of eclogitic diamonds are Type II. The median N content is higher than what is reported in the global database (454 at. ppm; Stachel et al., 2022a) but the abundance of Type II is in close agreement with the published literature (10%; Stachel and Harris, 2009).

Despite the proportion of Type II diamonds being similar for peridotitic and eclogitic paragenesis, the N content of Type I diamonds is relatively lower for peridotitic samples suggesting that the formation of Type II diamonds may be unrelated to the concentration of N in the environment of diamond formation. This would imply non-equilibrium incorporation of N into the diamond lattice during growth. Kinetic processes related to incorporation of impurities during diamond formation have been theorized by different authors (e.g., Reutsky et al., 2017; Kueter et al., 2020). The mechanisms of incorporation of N into the diamond lattice however is subject to debate, and the validity of kinetic models have been questioned (Stachel et al., 2022a). An interesting model explaining the incorporation of N in diamonds is provided by Mikhail and Howell (2016). Their model suggests that N behaves as a compatible element in diamonds only when it is present in a monoatomic state, and this occurs mainly during redox reactions involving N species. In this scenario, N-poor (and N-free) diamonds would form in the presence of a redox gradient that does not cross the boundary between different N species and thus does not generate monoatomic N. It is not possible to assign a paragenesis to most of the observed Type II Canadian diamonds (82%). Therefore, the abundance of Type II diamonds of peridotitic and eclogitic parageneses may not be accurate and representative of the true value, with incorporation of more data this value could approach the global average.

Type I diamonds can be further classified based on the aggregation state of the N (i.e., the arrangement of N atoms in the diamond lattice). When diamonds form, they incorporate N as single substitutional impurities (called C-centers), at mantle temperatures, C-centers aggregate quickly into dimers or neighboring substitutional N atoms (A-centers). With time, A-centers further aggregate into groups of four N atoms surrounding a carbon vacancy in the lattice (B-centers). Mantle diamonds are classified based on the relative abundance of A- and B-centers (which can be measured by FTIR spectroscopy), usually expressed as %B (=100*B-centers/[A-centers + B-centers]). Diamonds with a %B <10% are called Type IaA, while if %B >90% they are called Type IaB, all diamonds with 10%< %B <90% are classified as Type IaAB (Banas et al., 2007).

Most Canadian diamonds (62%) have a IaAB aggregation state as expected since this group includes all diamonds with %B between 10 and 90. The IaA group comprises 30% of Canadian diamonds and the remaining 8% are in the IaB group. The proportions of Type IaA, IaB and IaAB diamonds have been calculated for the peridotitic and eclogitic suites. The peridotitic suite shows results similar to those obtained for the entire database, with 63% of the diamonds in the IaAB group, 33% in the IaA group and the remaining 4% in the IaB group. Eclogitic diamonds on the other hand exhibit major differences with respect to their N aggregation state compared to the peridotitic suite, with 62% of the diamonds in the IaA group, 35% in IaAB group and the remaining 3% in the IaB group. A possible explanation for the peculiar aggregation state of N observed in eclogitic diamonds will be discussed in section 3.6.3. Diamonds with peridotitic, eclogitic and undefined parageneses are plotted as a function N content and %B in Fig. 7. Interestingly, ~40 intense yellow diamonds containing unaggregated N (C-centers, single substitutional N) from the Q1–4 kimberlites (Rae Craton) was reported by North Arrow Minerals inc. in 2015 (also mentioned by Moore and Helmstaedt, 2023). This is, as of today, the only reported occurrence of Type Ib diamonds from Canada suggesting a relatively short mantle residence time and/or low mantle residence temperature compared to other Canadian diamonds. However, to the best of our knowledge, no further details on these diamonds have been published and thus we refrain from further interpretation of these diamonds.

Sub-lithospheric diamonds are typically Type II (Davies et al., 1998; Hutchinson et al., 1998; Kaminsky and Khachatryan, 2001; Stachel et al., 2002). Unfortunately, one cannot assume that a diamond with non-detectable N formed in the sub-lithospheric mantle, since lithospheric diamonds can also be Type II. For example, Type II Canadian diamonds with an assigned paragenesis (107 samples), are predominately (77%) lithospheric, the minority (23%) are sub-lithospheric diamonds.

Another feature related to N content that may indicate a sub-lithospheric origin is the coupling of high N aggregation states with low N concentrations. Since the process of N aggregation becomes increasingly slower as the N concentration decreases, a diamond with a low N content and a high %B must have resided at high (possibly sub-lithospheric) temperatures in the mantle. Otherwise, unreasonably long times (>4.6 Ga) would be required to attain high N aggregation states at temperatures in accord with a lithospheric origin. This criterion

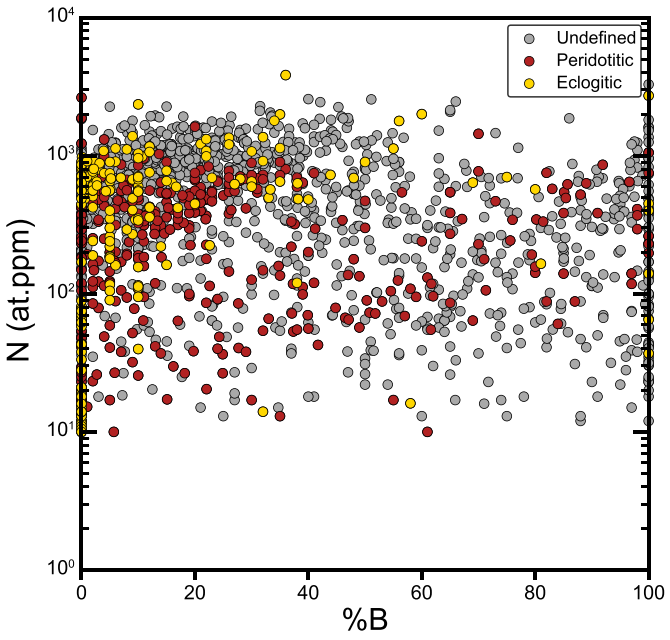

Fig. 7. Eclogitic, peridotitic and undefined Canadian diamonds plotted as a function of N content (at.ppm) and %B. Points indicated as "Undefined" refer to all the diamonds with unknown paragenesis. Type II diamonds are omitted here, as no %B can be calculated for these samples.

can be used to identify sub-lithospheric diamonds from cratonic areas where the temperature at the bottom of the lithosphere is low (e.g., Tappert et al., 2009). Canada, however, has a geotherm that approaches 1400 °C at the bottom of the lithosphere (Harris et al., 2018; Czas et al., 2020; Eeken et al., 2020; Timmerman et al., 2022), in this lithospheric environment, diamonds with low N and high %B could form in geologically reasonable times. For example, a diamond with 10 at.ppm N and %B = 99 can form at temperatures <1400 °C in <2 Ga, therefore this criterion cannot be used to identify sub-lithospheric diamonds in this dataset.

3.3. Carbon isotopic composition

Diamond, an allotrope of carbon, incorporates both ^{12}C and ^{13}C during formation. The C isotopic signature of diamonds provides information about the origin of the C required for diamond formation and about the reactions involved in the crystallization process.

Carbon isotopic data are expressed with the δ notation, $\delta^{13}C$ (in ‰) is the ratio of $^{13}C/^{12}C$ of the sample compared to that of a standard (the Pee Dee Belemnite; Craig, 1957). $\delta^{13}C$ is calculated as:

$$\delta^{13}C = \left(\frac{\left(\frac{^{13}C}{^{12}C}\right)_{sample}}{\left(\frac{^{13}C}{^{12}C}\right)_{standard}} - 1 \right) * 1000$$

A positive $\delta^{13}C$ indicates ^{13}C enrichment compared to the standard, and a negative value represents ^{13}C depletion.

C isotope data from 1881 Canadian diamonds were collected. The C isotopic composition of most diamonds in the database was measured by combustion of the entire diamond or a fragment of it. For measurements performed on multiple spots of a single diamond using SIMS, the isotopic composition of the diamond has been taken as the arithmetic mean of each $\delta^{13}C$ spot value.

Canadian diamonds have a $\delta^{13}C$ range from −41.4‰ (the most depleted $\delta^{13}C$ ever measured in a mantle diamond) to +1.6‰, with a mode at −4.6‰ (calculated from a kernel density). Both the upper and lower $\delta^{13}C$ boundary values of Canadian diamonds are from specimens with no assigned paragenesis. Considering all available data, 84% are in the main mantle range (from −8‰ to −2‰, Cartigny, 2005; Fig. 8) with an average $\delta^{13}C$ of −6.9‰ and a median of −4.8‰, in accord with the same value from the global database (Harris, 1987; Stachel and Harris, 2009; Shirey et al., 2013; Howell et al., 2020; Stachel et al., 2022a). Peridotitic diamonds fall in a narrow range of $\delta^{13}C$, from −22.8‰ to +1.3‰ (mode at −5.1‰), with 93% in the main mantle range, an average $\delta^{13}C = -4.8$‰ and a median of −5.0‰. Eclogitic diamonds, on the other hand, span a wider $\delta^{13}C$ range from −40.7‰ (the most depleted $\delta^{13}C$ ever measured in a natural eclogitic diamond) to −2.2‰, with a mode at −5.7‰, an average $\delta^{13}C$ of −16.0‰ and a median of −8.7‰. Of these eclogitic diamonds, 47% are in the main mantle range.

Peridotitic diamonds are almost entirely in the mantle range, a reflection of being formed purely from mantle material with little or no influx from fluids/melts with different carbon isotopic signatures (e.g., organic matter or recycled carbon).

Eclogitic diamonds from Canada have a peculiar distribution, in addition to the main peak, there is a second peak defined by $\delta^{13}C$ between −41‰ and − 35‰. This secondary peak is due to inclusion of diamonds from the Jericho kimberlite in the Slave Craton; these samples are the most ^{13}C-depleted mantle diamonds ever recorded. Two studies (De Stefano et al., 2009; Smart et al., 2011) investigated the C isotopic composition of 111 diamonds from the Jericho kimberlite. Some of the diamonds analyzed in these two studies do not have an assigned paragenesis but are most likely eclogitic given the very low number of non-eclogitic diamonds recovered at Jericho (only two websteritic and one peridotitic sample).

Among diamonds from Jericho, only 24 (22%) fall into the main mantle range, while the remaining 87 (78%) show a $\delta^{13}C < -24$‰.

It is expected that eclogitic diamonds are more depleted in ^{13}C with

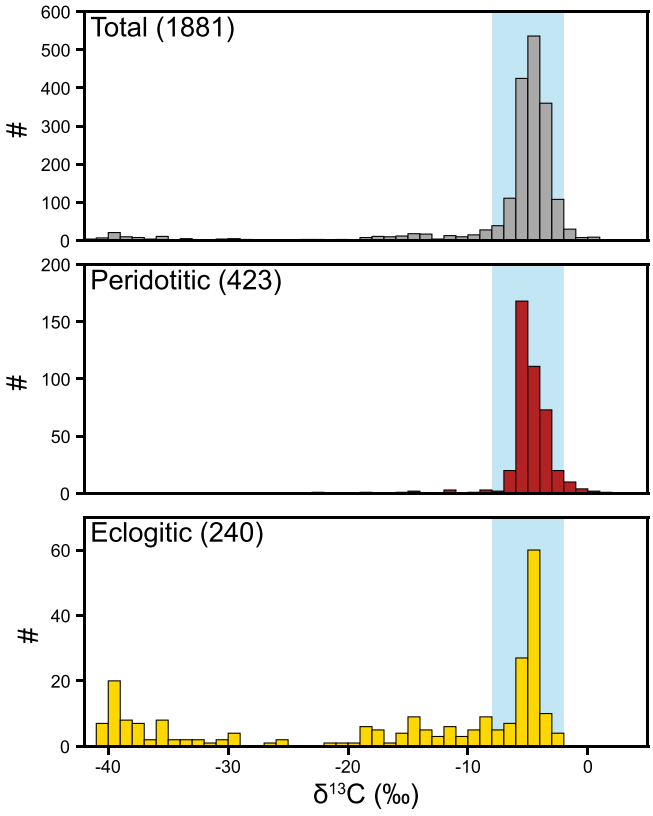

Fig. 8. Histogram showing the distribution of $\delta^{13}C$ for Canadian diamonds. The bin size is 1‰. The shaded, light-blue area between −8‰ and − 2‰ represents the main mantle range indicated by Cartigny (2005). (For interpretation of the references to colour in this figure legend, the reader is referred to the web version of this article.)

respect to peridotitic diamonds. The reasons for this depletion have been a matter of debate for decades, different models have been proposed and involve: (i) Mantle zones of primordial $\delta^{13}C$ heterogeneity (Deines et al., 1993), (ii) fractionation of C isotopes in an open system either before (Cartigny et al., 2001) or during (Deines, 1980) diamond formation and (iii) subduction of material that has a wide range of $\delta^{13}C$ due to fractionation processes (Milledge et al., 1983; Kirkley et al., 1991).

This debate has been addressed recently (Li et al., 2019; Stachel et al., 2022a) and the isotopic signature of diamonds has been recognized as the result of mixing (to different degrees) of five different reservoirs: (i) asthenospheric mantle fluids, (ii) shallow subducted oceanic crust, (iii) deep subducted oceanic crust, (iv) subducted marine carbonate sediment, and (v) subducted terrigenous sediment. This model can explain the observed variability of both the C and N isotopic composition of diamonds by involvement with mantle material and different parts of subducted oceanic crust.

The extremely ^{13}C-depleted composition of the diamonds from Jericho requires involvement of subducted sediments that must contain a certain amount of methanogenically-mediated organic carbon with strongly negative $\delta^{13}C$ values (Smart et al., 2011). Activity of methanotroph bacteria in a CH_4 substrate will produce organic carbon with a $\delta^{13}C$ range from −30 up to −60‰ (Schidlowski, 2001), in accord with the isotopic signature observed in diamonds from Jericho. However, this hypothesis seems unlikely, as the organic carbon would need to remain isolated (during subduction of the oceanic plate) from every other carbon reservoir until diamond crystallization to preserve its extremely depleted ^{13}C isotopic signature.

Fractionation has a small but noticeable effect on the isotopic composition of the crystallizing diamond, as is demonstrated by C isotopic studies of core-to-rim diamond profiles performed using SIMS. On the scale of a single growth zone, a progressive enrichment in ^{13}C towards the rim is observed (e.g., JDE B 25-S1, Smart et al., 2011) indicating crystallization of the diamond from oxidizing C phases (Cartigny et al., 2014). The opposite trend of rimward depletion in ^{13}C (indicative of crystallization from reduced C phases) has not been observed in Canadian diamonds. The effect of isotopic fractionation is not observed in all diamonds, some diamonds with uniform rimward $\delta^{13}C$ profiles are present (e.g., S1722, Petts et al., 2016). This may be due to diamonds forming from an isotopically homogenous fluid continuously supplied from a homogenous source, thus cancelling out the fractionating effect of diamond crystallization on the isotopic composition of the fluid (Cartigny et al., 2014).

Of the diamonds with measured C isotopic compositions, 1685 also have measured N contents, allowing examination of correlations between $\delta^{13}C$ and N content (Fig. 9). Diamonds of all paragenesis with mantle-like $\delta^{13}C$, show large variability in N content, covering the entire Canadian (and global) range of N contents (from 0 to 3833 at.ppm). This seems to suggest there is no coupling between N contents and the C isotopic signature of diamond.

On the other hand, almost all diamonds with light C isotopic signatures contain little to no N, only 10 diamonds with $\delta^{13}C < -20$‰ have N >100 at.ppm (Fig. 9). This was first noticed by Cartigny et al. (2001) and was expressed by the definition of a limit sector correlating the maximum N content of a diamond with its $\delta^{13}C$. This behavior is also exhibited by single diamonds in different growth zones (e.g., CH6–46, CH7–15, CH7–33 and CH7–35, Hogberg et al., 2016). These diamonds formed during discrete growth pulses, each involving fluids with extremely different isotopic and chemical compositions, one N-poor and ^{13}C-depleted and another N-rich and ^{13}C-enriched. This suggests that some form of coupling between the N content and the C isotopic composition of diamond-forming fluids may exist, however, it is not ubiquitous and the coupling mechanism is likely extremely complex and currently poorly understood (Hogberg et al., 2016).

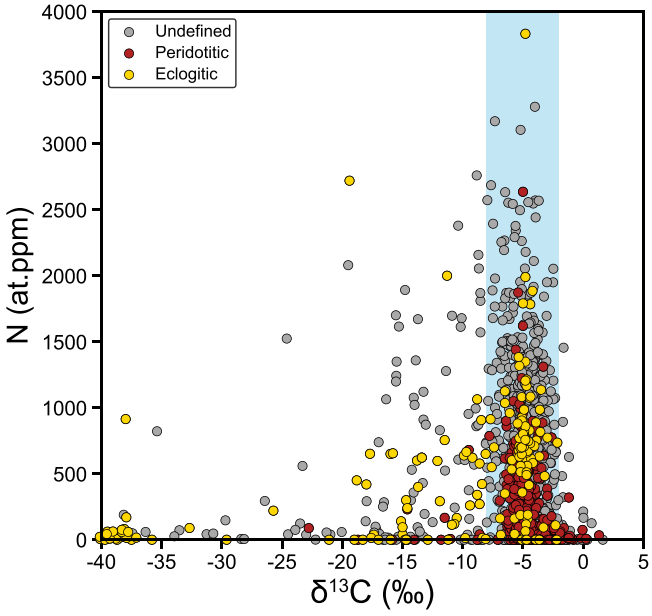

Fig. 9. Eclogitic, peridotitic and undefined Canadian diamonds plotted as a function of N content (at.ppm) and $\delta^{13}C$ (‰). Points indicated as "Undefined" refer to diamonds with unknown paragenesis. The shaded, light-blue area between −8‰ and − 2‰ represents the main mantle range indicated by Cartigny (2005). (For interpretation of the references to colour in this figure legend, the reader is referred to the web version of this article.)

3.4. Nitrogen isotopic composition

Nitrogen is the most common impurity in diamonds and the N isotopic composition of diamonds, especially when coupled with their $\delta^{13}C$, can provide information on the fluids from which diamonds crystallize.

Like C, N isotopic compositions are also expressed using the δ notation where the N isotopic composition of the atmosphere is used as the standard (Mariotti, 1984). $\delta^{15}N$ is calculated as:

$$\delta^{15}N = \left(\frac{\left(\frac{^{15}N}{^{14}N}\right)_{sample}}{\left(\frac{^{15}N}{^{14}N}\right)_{standard}} - 1 \right) * 1000$$

The N isotopic composition of more than half of the Canadian diamonds was measured using SIMS, where at least one measurement was performed on each diamond. For these samples, $\delta^{15}N$ was calculated as the arithmetic mean of all measured spots. Other diamonds were measured by combustion of the entire diamond or of a fragment of it, and therefore the measured $\delta^{15}N$ represents the bulk isotopic composition of these samples.

Unfortunately, only a small number (178, 5.8%) of the diamonds in this database were analyzed for $\delta^{15}N$. From this subset, the $\delta^{15}N$ spans a large range of values, from −17.2‰ to +15.4‰ (Fig. 10) with a mode at −2.3‰, an average $\delta^{15}N$ of −1.9‰, and a median of −2.3‰, in agreement with the global dataset of Stachel et al. (2022a). The $\delta^{15}N$ of diamonds in this database skew towards negative $\delta^{15}N$ values, 71% of diamonds have a light N isotopic signature ($\delta^{15}N$ <0‰) and 51% of the diamonds have $\delta^{15}N$ between −5‰ and 0‰. Based on the present data, Canadian diamonds appear to be enriched in ^{15}N with respect to the isotopic composition of the Earth's mantle (−5 ± 2‰, Cartigny and Marty, 2013; Fig. 10). The lowest $\delta^{15}N$ measured on a Canadian diamond is −17.2‰ (sample ON-DVK-276, Klein-BenDavid et al., 2007), this value was obtained as the mean of different SIMS measurements ranging from −2‰ to −35‰, the latter being the lowest $\delta^{15}N$ measured in a Canadian diamond. This sample also shows that variation among growth zones of $\delta^{15}N$ >30‰ can occur in a single diamond.

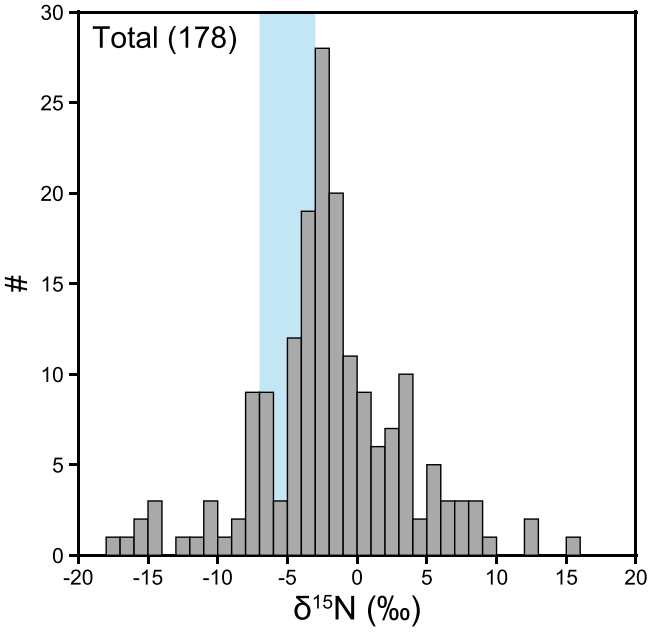

Fig. 10. Histogram showing $\delta^{15}N$ of Canadian diamonds. The bin size is 1‰. The shaded, light-blue area between −7‰ and − 3‰ represents the N isotopic composition of the Earth's mantle (Cartigny and Marty, 2013). (For interpretation of the references to colour in this figure legend, the reader is referred to the web version of this article.)

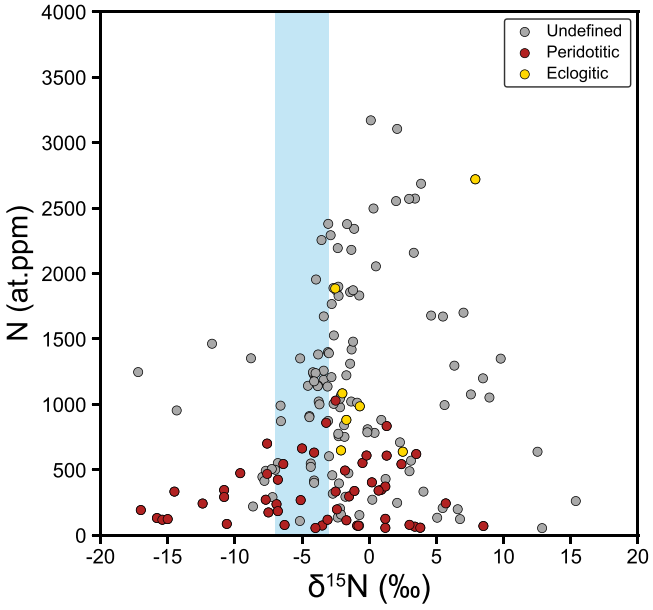

Fig. 11. Eclogitic, peridotitic and undefined Canadian diamonds plotted as a function of N content (at.ppm) and $\delta^{15}N$ (‰). Points indicated as "Undefined" refer to all the diamonds with unknown paragenesis. The shaded, light-blue area between −7‰ and − 3‰ represents the N isotopic composition of the Earth's mantle (Cartigny and Marty, 2013). (For interpretation of the references to colour in this figure legend, the reader is referred to the web version of this article.)

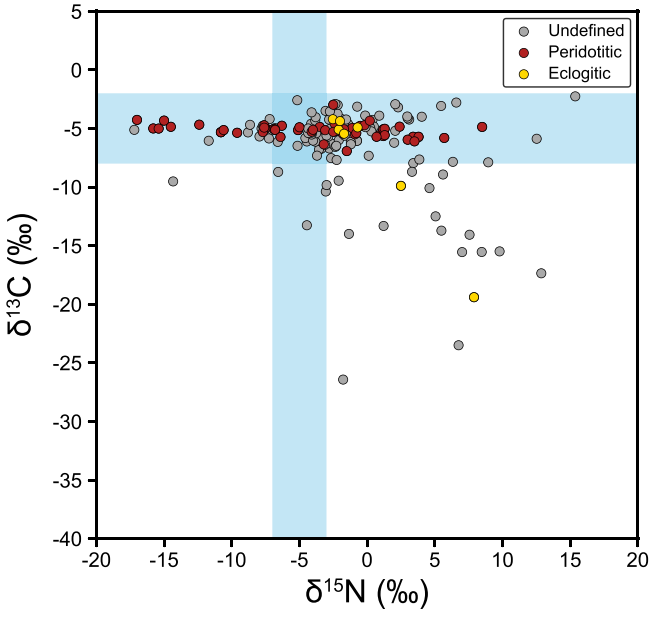

Fig. 12. Eclogitic, peridotitic and undefined Canadian diamonds plotted as a function of $\delta^{15}N$ (‰) and $\delta^{13}C$ (‰). Points indicated as "Undefined" refer to all diamonds with unknown paragenesis. The shaded light-blue areas refer to the mantle range ($\delta^{15}N = -7$ to −3‰ and $\delta^{13}C = -8$ to −2‰) indicated by Cartigny and Marty (2013) and Cartigny (2005). (For interpretation of the references to colour in this figure legend, the reader is referred to the web version of this article.)

Of the 656 peridotitic diamonds in this database, only 52 were analyzed for N isotopes, with $\delta^{15}N$ ranging from −17.2‰ to +8.5‰ with an average $\delta^{15}N$ of −3.9‰, a median of −2.8‰, and no clear mode, 71% of these diamonds have negative $\delta^{15}N$ values. Eclogitic diamonds, on the other hand, have $\delta^{15}N$ values that range from −2.5‰ to +7.9‰ and a mean of +0.2‰. However, in this database, only seven eclogitic diamonds have measured N isotopic compositions thus we could not conduct a statistically meaningful evaluation of any systematic differences in $\delta^{15}N$ between peridotitic and eclogitic Canadian diamonds.

By comparison of the $\delta^{15}N$ and N content of Canadian diamonds (Fig. 11) it can be shown that the entire range of N contents cluster in a narrow range of $\delta^{15}N$ values, and the other N isotopic compositions correspond to low N concentrations.

Analyses performed on different zones of a single diamond do not show significant coupling of $\delta^{15}N$ and N content. Several analyses performed on single diamonds show that N content increases, decreases and remains constant with increasing $\delta^{15}N$ (e.g., Petts et al., 2016). Hogberg et al. (2016), analyzed the N content and isotopic composition on an average of three different points per diamond from the Chidliak kimberlite field (Nain craton) and observed two subparallel trends of decreasing N content with increasing $\delta^{15}N$. These subparallel trends are observed in this database (on a log(N) vs. $\delta^{15}N$ plot) and can be associated to Rayleigh fractionation during diamond formation. Petts et al. (2015) also observed trends of decreasing N content with increasing $\delta^{15}N$ along profiles measured in individual growth zones of a diamond from the Jericho kimberlite (sample JDE-25, Petts et al., 2015; Smart et al., 2011). This confirms that Rayleigh fractionation may play an important role during diamond formation, but with respect to this dataset, appears to have minimal or no effect in most of the diamonds examined here.

No correlation is observed when considering C and N isotopic compositions (Fig. 12), samples with $\delta^{13}C$ in the mantle range have a wide range of $\delta^{15}N$, from −17.2 to +15.4‰ (the entire range observed in Canadian diamonds). However, diamonds with $\delta^{13}C < -8$‰ have, almost exclusively, $\delta^{15}N > -3$‰. This relationship is also observed in other works (see e.g., Stachel et al., 2022a for a global database and Chinn et al., 2018 for diamonds from Orapa), where it is attributed to a consequence of mixing of mantle and different altered oceanic crustal components. This mixing process explains the observed variations in isotopic composition of Canadian mantle diamonds.

3.5. Mineral inclusions

Mineral inclusions in diamonds play a fundamental role in the study of the Earth's interior as they represent the deepest samples from the otherwise inaccessible mantle that can be directly studied. Based on a set of one million diamonds from Africa, Stachel and Harris (2008) state that inclusion-bearing diamonds comprise only 1% of diamonds from global production. In the present work approximately 34% of the diamonds contain one or more inclusions. However, this is due to a strong selection bias and consequent overrepresentation of inclusion-bearing minerals which are targeted for scientific research.

The inclusions minerals observed in Canadian diamonds are: olivine, garnet, sulfides, magnesiochromite, clinopyroxene, orthopyroxene, ferropericlase, reverted bridgmanite (low-Ni enstatite), breyite, metallic Ni, SiO_2, rutile, carbonates, ilmenite, hematite, magnetite, diamond, kyanite, sillimanite, serpentines, feldspars, and micas. In this work, only those inclusions that are either abundant or provide information regarding the environment in which the diamonds form are considered, hereafter referred to as "major" inclusions. Other inclusions were not considered in the discussion.

The most abundant major inclusions observed in Canadian diamonds is olivine (446 inclusions, Fig. 13), which is observed in 309 specimens with up to 16 inclusions reported in a single diamond (Hunt et al., 2012). Garnet is the second most abundant major inclusion, 388 garnet inclusions are observed in 264 diamonds with up to 12 inclusions reported in a single diamond (Donnelly et al., 2007). The third most abundant major inclusion are sulfides, 340 sulfide inclusions are observed in 249 diamonds with up to six sulfide inclusions reported in a single diamond (Westerlund et al., 2006).

In order of decreasing abundance, magnesiochromite, clinopyroxene, orthopyroxene, ferropericlase, (former) bridgmanite, breyite and metallic Ni are also observed.

In this section, the inclusions observed in Canadian diamonds are discussed with respect to their major element composition. The minor and trace element compositions are also discussed where possible.

3.5.1. Garnet

Garnet inclusions exhibit different colors depending on their parageneses, peridotitic garnets are usually pale pink to purple and eclogitic garnets are typically orange (Stachel and Harris, 2008). The compositions of studied lithospheric garnet inclusions are summarized in Table 2. One harzburgitic garnet (sample SL_3–3), with an extremely high FeO concentration (21.2 wt%), was reported by Pokhilenko et al. (2004). However, this is likely a transcription error in the original manuscript as the exact same concentration was reported for MgO, and the calculated Mg# differs from the reported Mg#. Therefore, this garnet was excluded from the discussion below. Another garnet (sample Ash-106 A; Davies et al., 2004a) was excluded from all calculations and discussions as it was classified as possibly epigenetic; this sample exhibited extremely low SiO_2 (35.7 wt%) and MgO (3.9 wt%) and high FeO (32.0 wt%) and MnO (6.7 wt%) concentrations.

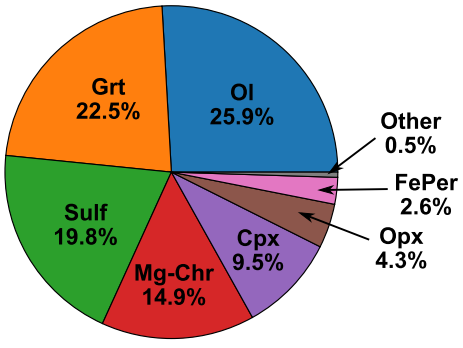

Fig. 13. Relative abundances of major mineral inclusions in this study. Majoritic garnets are grouped together with garnets, the "Other" group includes bridgmanite, breyite and metallic alloys.

Table 2 shows compositional trends for garnet inclusions related to their parageneses in this study. Eclogitic garnets appear poorer in Cr_2O_3 and MgO and richer in Al_2O_3, FeO, CaO, Na_2O and TiO_2 compared to peridotitic garnets.

Overall, eclogitic garnets show higher variability in chemical composition with respect to peridotitic garnets, specifically wider ranges of major element compositions. Websteritic garnets are typically transitional between peridotitic and eclogitic garnets in terms of major and minor element composition.

Among peridotitic garnets, wehrlitic garnet has the lowest SiO_2 and Al_2O_3 and the highest CaO contents. However, these observations are based on three wehrlitic samples and thus are not statistically significant. The MgO and Cr_2O_3 concentrations tend to increase from wehrlitic to lherzolitic to harzburgitic garnets. Lherzolitic garnets have a higher TiO_2 concentration compared to harzburgitic garnets, 1.4% (1 out of 72) of the lherzolitic garnets and 52.9% of the harzburgitic garnets have a TiO_2 content <0.04 wt%.

Based on the compositional differences of garnets from different parageneses, Sobolev et al. (1973) developed a classification scheme in which garnet paragenesis is determined based on the CaO and Cr_2O_3 concentration. Grütter et al. (2004) updated this classification scheme through examination of other major and minor elements in garnet. This classification diagram is still used today when studying garnets from the Earth's mantle. In Fig. 14, garnets inclusions from Canadian diamonds are plotted on this CaO vs Cr_2O_3 classification diagram.

Three garnet micro-inclusions in a single diamond (PAN 8, Tomlinson et al., 2006) were originally classified as lherzolitic but fall in the harzburgitic field, despite plotting very close to the boundary between the two fields. A fourth garnet inclusion in the same diamond plots in the lherzolitic field, but in a position very close to the boundary with the harzburgitic field. The small size of these inclusions led to poor analytical precision (with oxides summing to values as low as 66 wt%), requiring renormalization of the analyses to 100% total, thus modifying the CaO vs Cr_2O_3 proportions and leading to mistakes when plotting them in the classification diagram.

Even if the boundary between eclogitic and peridotitic garnets is fixed at $Cr_2O_3 = 1$ wt%, garnet inclusions in Canadian diamonds have a Cr_2O_3 concentration well below this threshold, as the highest Cr_2O_3 content observed in an eclogitic garnet is 0.38 wt% (two garnets included in diamond 344X from De Stefano et al., 2009). Websteritic garnets are treated as a transitional suite between peridotitic and the eclogitic and lack a precise compositional definition.

In Fig. 14, majoritic garnets are also plotted and are associated with a sub-lithospheric origin. At sub-lithospheric P-T conditions, clinopyroxene dissolves into the garnet, which causes an excess of Si^{4+} in the garnet ($Si^{4+} > 3$ *apfu*), as the capacity of the tetrahedral sites is 3 apfu, excess Si^{4+} must occupy the octahedrally coordinated sites. Majoritic and lithospheric garnets are both plotted in Fig. 14 as there is no difference in terms of CaO and Cr_2O_3 concentration between these two groups.

Principal component analysis (PCA) was performed using the major and some minor elements for the available samples, including SiO_2, Al_2O_3, MgO, FeO, CaO, Na_2O, Cr_2O_3, and TiO_2. The epigenetic garnet mentioned above and all majoritic garnet were excluded, as their high SiO_2 content may obscure correlations between the oxides and the parageneses. Inspection of Fig. 15a shows a clear distinction between peridotitic and eclogitic parageneses, as they plot as two separated clusters of points. Figs. 15a-b show that peridotitic garnets tend to be richer in Cr_2O_3 and MgO. On the other hand, eclogitic garnets are richer in FeO, TiO_2 and Na_2O, and show a higher degree of compositional variability, with some of the samples being CaO-rich and others Al_2O_3-rich. Figs. 15c-d show PCA performed on a dataset composed of only peridotitic garnets; from these plots it appears that the CaO, FeO, TiO_2 and Na_2O contents progressively increase from harzburgitic to lherzolitic to wehrlitic parageneses. Harzburgitic garnets tend to be richer in

Table 2
Average, maximum and minimum concentrations of major and minor elements (measured with EMPA) for garnet inclusions in Canadian diamonds (expressed in oxide wt%). BD = below detection.

	Average	Max	Min	# Analyses		Average	Max	Min	# Analyses
Lherzolitic					**Websteritic**				
SiO_2	41.29	42.82	39.83	88	SiO_2	41.66	42.13	40.84	8
Al_2O_3	17.69	21.88	15.89	88	Al_2O_3	23.25	23.73	22.75	8
FeO	7.30	8.03	5.86	88	FeO	8.75	10.03	8.41	8
MgO	19.56	21.47	17.28	88	MgO	20.43	20.68	19.54	8
MnO	0.36	0.43	0.17	78	MnO	0.30	0.32	0.27	8
CaO	6.03	6.63	4.46	88	CaO	4.20	4.29	4.09	8
Na_2O	0.05	0.41	0.01	88	Na_2O	0.06	0.07	0.05	8
K_2O	0.04	0.81	BD	83	K_2O				0
TiO_2	0.16	0.36	0.02	82	TiO_2	0.48	0.54	0.29	8
NiO	0.01	0.25	BD	79	NiO				0
Cr_2O_3	7.37	9.08	2.68	88	Cr_2O_3	0.61	0.81	0.28	8
V_2O_3	0.07	0.09	0.03	68	V_2O_3				0
P_2O_5	0.05	0.13	BD	74	P_2O_5				0
Mg#	82.69	86.72	80.56		Mg#	80.62	81.31	77.65	
Harzburgitic					**Eclogitic**				
SiO_2	41.46	42.33	40.26	69	SiO_2	40.21	41.99	38.65	133
Al_2O_3	15.68	19.16	11.53	69	Al_2O_3	21.80	23.36	20.07	133
FeO	6.28	7.11	5.50	69	FeO	15.44	21.38	8.34	133
MgO	21.35	23.44	19.20	69	MgO	12.06	19.77	5.74	133
MnO	0.29	0.37	0.13	69	MnO	0.35	0.52	0.18	133
CaO	4.26	6.14	2.64	69	CaO	9.10	20.32	3.04	133
Na_2O	0.04	0.31	BD	69	Na_2O	0.17	0.51	0.05	133
K_2O	<0.01	0.04	BD	40	K_2O	0.03	0.06	<0.01	91
TiO_2	0.05	0.18	BD	69	TiO_2	0.65	1.24	0.27	133
NiO	0.01	0.02	BD	49	NiO	BD	0.01	BD	27
Cr_2O_3	10.09	15.68	6.75	69	Cr_2O_3	0.09	0.38	0.01	128
V_2O_3	0.05	0.06	0.04	10	V_2O_3	0.02	0.03	0.00	14
P_2O_5	0.02	0.04	0.01	34	P_2O_5	0.06	0.20	0.02	22
Mg#	85.81	88.04	83.38		Mg#	57.26	77.00	36.68	
Wehrlitic									
SiO_2	39.80	40.65	39.27	3					
Al_2O_3	13.86	18.81	11.09	3					
FeO	7.49	8.11	7.16	3					
MgO	15.89	18.25	14.54	3					
MnO	0.42	0.47	0.36	3					
CaO	9.94	11.46	7.06	3					
Na_2O	0.04	0.05	0.02	3					
K_2O	BD	BD	BD	3					
TiO_2	0.25	0.45	0.14	3					
NiO	0.01	0.01	0.01	2					
Cr_2O_3	11.94	15.59	5.37	3					
V_2O_3	0.07	0.07	0.06	2					
P_2O_5	0.12	0.14	0.11	2					
Mg#	79.02	80.04	78.37						

MgO and Cr_2O_3; this is due to the depleted nature of harzburgites, which undergo high degrees of melt extraction. Interestingly, the inclusions from Tomlinson et al. (2006) that plotted in the harzburgitic field in the CaO vs Cr_2O_3 diagram, overlap here with the lherzolitic samples, suggesting that they are indeed part of this latter paragenesis. Therefore, their classification as harzburgitic (based on CaO-Cr_2O_3 content) was a consequence of the normalization to 100% of their composition. Finally, Figs. 15e-f show PCA performed on the eclogitic + websteritic garnets. Here, all websteritic garnets plot close together and do not overlap with the eclogitic garnets, suggesting that no eclogitic diamonds have been misclassified as websteritic. However, due to the small number of websteritic samples, the possibility that some websteritic samples have been erroneously classified as eclogitic cannot be dismissed, as no clear separation between the two clusters of points can be observed in Fig. 15e.

As shown in Table 2, the Mg# of garnet inclusions shows systematic variations as a function of paragenesis (Fig. 16). Eclogitic garnets exhibit a broad range of Mg# (from 36.7 to 77.0) caused by their variable FeO and MgO content, which ranges from 8.3 to 21.4 wt% and from 5.7 to 19.8 wt%, respectively. Peridotitic garnets on the other hand exhibit a narrower Mg# range but always plot at higher values (from 78.4 to 88.0) compared to eclogitic garnets. Websteritic garnets are located in between the peridotitic and eclogitic suites with Mg# ranging from 77.6 to 81.3, with only one websteritic garnet showing a Mg# <80. This is however just the result of the small amount of websteritic garnets in this study, as Mg# as low as 51.8 have been recorded in websteritic garnet inclusions from other localities (Stachel and Harris, 2008).

Among peridotitic garnet inclusions, the harzburgitic type exhibit the highest Mg#, with 82.4% showing a Mg# >85. Lherzolitic garnets on the other hand, generally have lower Mg#, with only 6.4% of them having Mg# >85. In Fig. 16, all the sub-lithospheric garnets (as no differences in the Mg# are observed between lithospheric and sub-lithospheric samples) are also plotted.

Some of the garnets present in this work were also analyzed for their trace elements contents (Davies et al., 2004a, 2004b; Tappert et al., 2005; Tomlinson et al., 2006; Donnelly et al., 2007; De Stefano et al., 2009; Smart et al., 2012; Stachel et al., 2018). In Fig. 17, the Rare Earth Elements (REE) concentrations of garnets normalized to the C1-chondrite of McDonough and Sun (1995) are shown. Harzburgitic garnets show a sinusoidal REE_N pattern, with a positive slope in the $LREE_N$, a negative slope in the heavier $LREE_N$ and the $MREE_N$ and a positive slope in the $HREE_N$. These data agree with the pattern recently observed by Stachel et al. (2022b) in worldwide diamond database. Lherzolitic garnets, on the other hand, exhibit a sinusoidal pattern different from the one observed in harzburgitic garnets with a positive slope over the entire range of the $LREE_N$ with the highest concentration (~10–20 times

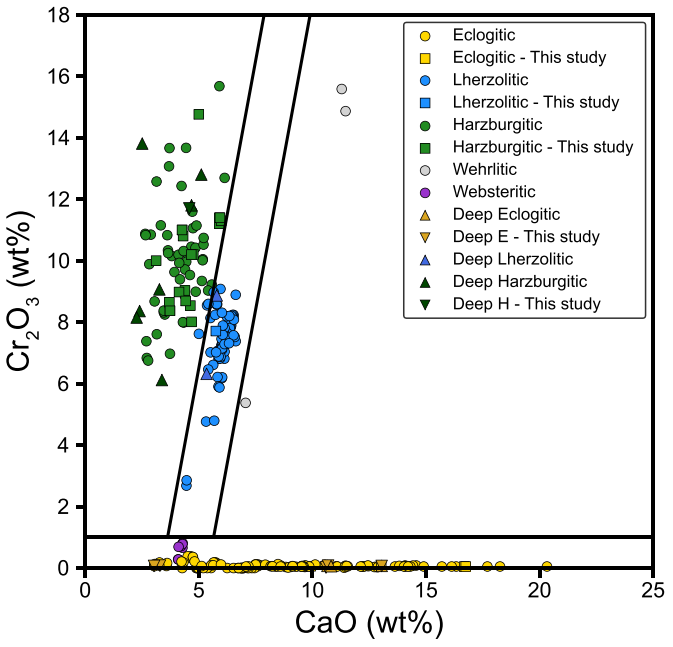

Fig. 14. Garnet inclusions from Canadian diamonds plotted as a function of Cr_2O_3 and CaO contents (wt%). The lines separating the fields are based on Grütter et al. (2004). "Deep" indicates majoritic garnets. "This study" indicates garnets that had a paragenesis assigned in this work.

the chondritic values) observed for Sm, a negative slope over the entire range of $MREE_N$ and a positive slope in the $HREE_N$. These patterns agree with those observed by Stachel et al. (2022b) and arise from garnets included in diamonds from the Victor Mine (Stachel et al., 2018). These sinusoidal patterns in lherzolitic garnets were attributed to metasomatism by a C-O-H fluid with a steep negative $LREE_N$-$HREE_N$ slope. If we do not consider the samples from the Victor Mine, the REE_N signature of lherzolitic garnet inclusions in Canadian diamonds show the so-called "normal pattern" (a positive slope in the $LREE_N$ and a plateau in the $MREE_N$ and $HREE_N$) defined by Stachel et al. (2022b) which is also exhibited by lherzolitic garnets from xenoliths. Stachel et al. (2004) explained the REE_N pattern of peridotitic garnets by metasomatic interaction with a highly differentiated fluid/melt extremely enriched in $LREE_N$. The lower LREE content in lherzolitic garnets reflects equilibration with clinopyroxene and a metasomatizing agent depleted in LREE. This becomes more obvious by normalizing the composition of harzburgitic and lherzolitic garnets to a primitive garnet instead of a C1-chondrite (Stachel et al., 2004).

Eclogitic garnets display a steep slope in $LREE_N$ that tends to flatten in the $MREE_N$ and $HREE_N$, reaching concentrations >100 times those observed in chondrites. This pattern agrees with the observations of Stachel et al. (2022b). Five garnets from Davies et al. (2004a), however, show a peculiar enrichment in La and Ce with respect to the other eclogitic garnets, which could be the result of a complex history involving metasomatic enrichment of these samples. The reason for the REE_N pattern observed in eclogitic garnets is discussed in the next section (3.5.2).

3.5.2. *Clinopyroxene*

In total, 163 clinopyroxene inclusions are recorded in Canadian diamonds. Canadian clinopyroxene compositions are summarized in Table 3. A single sample reported as lherzolitic in the original paper (sample 13544, Hunt et al., 2012) was not included in the calculations due to its unusually low Cr_2O_3 content and Cr#. This was in fact a transcription error as this clinopyroxene was classified as epigenetic in the supplementary materials of the article.

Based on the present data peridotitic clinopyroxenes have the highest average SiO_2, MgO and Cr_2O_3 contents. Eclogitic samples show the highest Na_2O and K_2O concentrations and a wider range of FeO concentrations that, like garnets, corresponds to a larger range of Mg# for eclogitic samples with respect to peridotitic. Eclogitic clinopyroxenes also show high TiO_2 contents, up to 2.8 wt%, with 97.4% of the samples having TiO_2 >0.1 wt%. In contrast, peridotitic samples are relatively depleted in TiO_2, with 71.4% of all clinopyroxenes having TiO_2 <0.1 wt %. As is the case for garnets, websteritic clinopyroxenes lack a rigorous compositional definition and are transitional between the peridotitic and eclogitic compositions. In this dataset, websteritic clinopyroxenes have the lowest average SiO_2 concentrations which could simply be a consequence of the low number of websteritic clinopyroxenes included in this work.

Clinopyroxene inclusions can be used to assign parageneses to the diamonds in which they occur. The distinction between peridotitic and eclogitic is based on the Cr# (100*Cr/[Cr + Al]). Due to their high Cr_2O_3 and low Al_2O_3 contents peridotitic clinopyroxenes have Cr# >7–10 while the eclogitic samples, exhibit Cr# <7. Websteritic clinopyroxenes have Cr# above and below this threshold separating peridotitic and eclogitic samples. The Cr# plotted as a function of Mg# for clinopyroxenes is shown in Fig. 18.

In the literature, all peridotitic clinopyroxenes are usually classified as lherzolitic due to the clinopyroxene-free nature of the harzburgitic paragenesis (Richardson et al., 1993; Stachel et al., 2004). However, a very small number of wehrlitic clinopyroxene inclusions in diamonds have been recorded in the literature (Stachel and Harris, 2008), and the presence of the wehrlitic paragenesis can hamper the classification of peridotitic clinopyroxenes that do not coexist with garnet inclusion in the same diamond. In this study, a conservative approach is adopted and all newly recognized peridotitic clinopyroxenes are not assigned a lherzolitic paragenesis but simply classified as peridotitic, unless they coexist in the same diamond with a garnet. In Fig. 18, the broad range of Mg# for eclogitic clinopyroxenes, with the lowest value at 66.48 and the highest at 90.54, is clearly visible. However, most eclogitic clinopyroxenes (64.9%) have Mg# values between 70 and 80. The transitional nature of the websteritic samples, both in terms of Mg# and Cr#, can also be seen in Fig. 18.

Stachel and Harris (2008) observed a positive correlation among different element concentrations in clinopyroxenes inclusions. For eclogitic clinopyroxenes, these authors observed a positive, close to 1:1, correlation between Na^+ and Al^{3+}, indicative of the presence of a jadeite component in the omphacites. For peridotitic clinopyroxenes, a positive correlation between Na^+ and Cr^{3+}, indicative of the presence of a kosmochlor component, was observed. For Canadian samples in this study the same correlations are observed.

Trace elements concentrations of clinopyroxene inclusions in Canadian diamonds are available for 18 eclogitic specimens (Davies et al., 2004b; Promprated et al., 2004; De Stefano et al., 2009; Smart et al., 2012). The concentrations of trace elements normalized to the C1-chondrite (McDonough and Sun, 1995) are plotted in Fig. 19.

Most Canadian eclogitic clinopyroxenes show a positive slope in the $LREE_N$ peaking at Nd, with concentrations up to almost 50 times chondritic values. A negative slope towards Lu, with concentrations approaching chondritic values (0.4 to 4 times), is also observed. These patterns agree with those observed by Stachel et al. (2022b) for a global dataset. However, two clinopyroxenes (SL3–32/00 and SL5–6/00; Promprated et al., 2004) show flat REE_N patterns with slightly negative slopes in the $HREE_N$. The authors reporting these data associated these patterns to the low K_2O content of the clinopyroxenes. However, trace element concentrations have been measured for other K_2O-poor clinopyroxenes present in this study and no such pattern was observed, ruling out a possible relationship between the K_2O and REE_N signature for Canadian clinopyroxenes. A single sample (377X6, De Stefano et al., 2009) has been excluded from Fig. 18 as it exhibited a highly unusual REE_N pattern with a positive slope from the $LREE_N$ to the $HREE_N$, indistinguishable from the REE_N pattern of an eclogitic garnet. This is

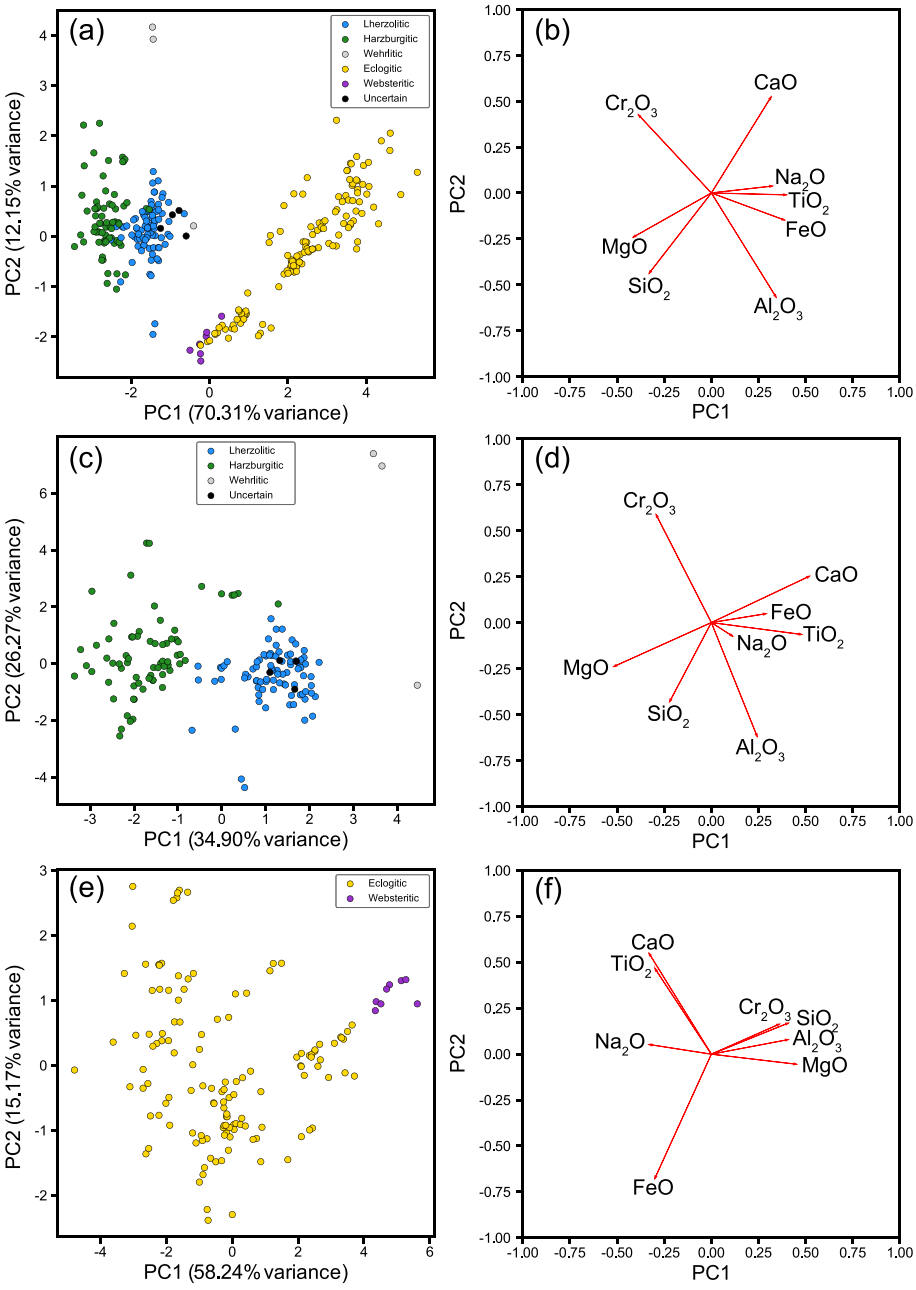

Fig. 15. Plots of the scores (left) and loadings (right) obtained from the principal component analysis of garnet inclusions in Canadian diamonds. (a-b) all garnets, (c-d) peridotitic garnets, (e-f) eclogitic and websteritic garnets. The arrows in the loadings plots inform on correlations between variables: if two variables are plotted at a close angle from each other, then there is a correlation between them, if instead they are at 180° from each other it is a sign of complete anti-correlation between the two. The scores plots on the other hand help us to see possible groupings among the samples. By looking at the scores and the loadings together it is possible to retrieve information about the composition of the samples, since the closer a point is to the direction an arrow points to, the higher its value for that variable. The "Uncertain" class represents the garnet inclusions from diamond PAN 8 from Tomlinson et al. (2006).

likely a transcription error in the original paper as this pattern is not plotted by the authors.

Knowledge of trace element concentrations in both eclogitic clinopyroxenes and garnets allows one to calculate a REE_N pattern for a bulk Canadian eclogitic diamond source. This exercise can be done by simply averaging the REE_N patterns observed in garnets and clinopyroxenes, as displayed in Fig. 20.

Assuming a modal ratio of 55% garnet and 45% clinopyroxene (Aulbach et al., 2020a), the calculated bulk rock pattern is almost flat with a slight positive slope from La (~8–9 times the chondritic concentration) to Lu (~20–30 times the chondritic values). The REE_N pattern for the reconstructed bulk rock shows lower concentrations of $LREE_N$ and $MREE_N$ with respect to N-MORBs, but also shows a step at Dy that brings the concentrations of $HREE_N$ very close to those of N-MORBs. This stepped patten was already observed in reconstructed eclogitic xenoliths and attributed to interaction with deserpentinization fluids from subducted slabs (Aulbach et al., 2020b). Here, the strongly incompatible LREE are removed from garnet by fluids, generating the observed low LREE concentrations and the stepped pattern in the reconstructed bulk rock pattern.

3.5.3. *Olivine*

Olivine is the most common inclusion in Canadian diamonds. Usually, olivine included in diamonds appear colorless and have a high

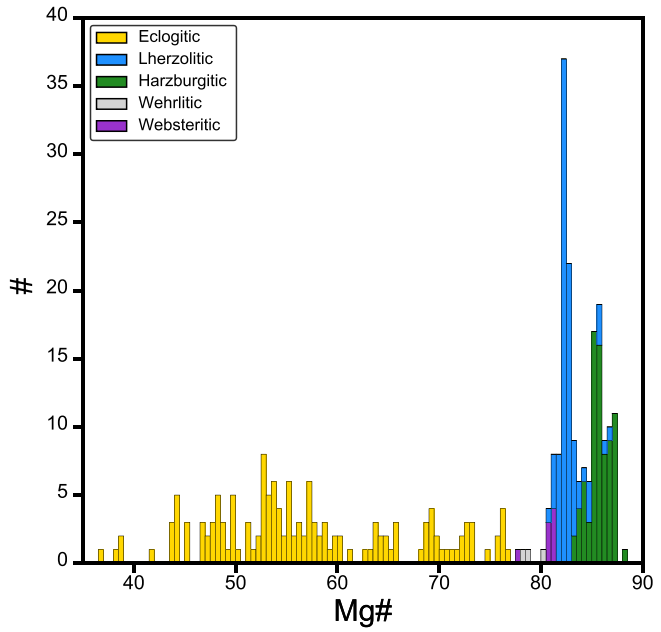

Fig. 16. Mg# distribution of garnets inclusions in Canadian diamonds. Both the lithospheric and sub-lithospheric samples are included and colored based on parageneses. The bin size is 0.5.

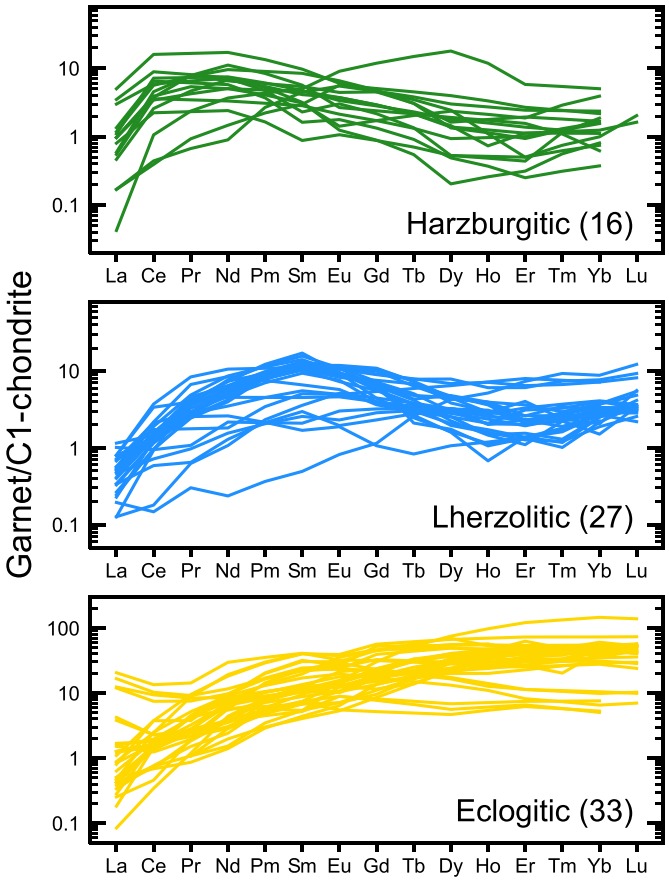

Fig. 17. REE concentrations of harzburgitic, lherzolitic and eclogitic garnet inclusions in Canadian diamonds, normalized to the composition of the C1-chondrite (McDonough and Sun, 1995).

Table 3
Average, maximum and minimum concentrations of major and minor elements (measured with EMPA) for clinopyroxene included in Canadian diamonds (expressed in wt%). BD = below detection.

	Average	Max	Min	# Analyses
Peridotitic				
SiO_2	55.18	57.23	53.57	53
Al_2O_3	1.38	3.34	0.05	53
FeO	2.44	4.36	1.38	53
MgO	17.63	29.92	15.04	53
MnO	0.10	0.14	BD	40
CaO	19.54	26.22	6.60	53
Na_2O	1.32	2.88	0.18	53
K_2O	0.11	0.71	0.02	44
TiO_2	0.10	0.51	BD	49
NiO	0.06	0.19	0.01	36
Cr_2O_3	1.55	2.86	0.18	53
V_2O_3	0.03	0.03	0.02	8
P_2O_5	0.01	0.02	BD	17
Mg#	92.81	95.45	89.42	
Cr#	44.22	73.27	13.65	
Websteritic				
SiO_2	52.84	54.70	48.40	6
Al_2O_3	3.31	4.91	0.77	6
FeO	5.86	7.38	3.57	6
MgO	13.92	16.69	11.91	6
MnO	0.09	0.12	0.06	6
CaO	19.63	22.98	16.51	6
Na_2O	1.94	3.38	0.40	6
K_2O	0.12	0.14	BD	5
TiO_2	0.88	1.85	0.20	6
NiO	BD	BD	BD	5
Cr_2O_3	0.43	1.23	0.13	6
V_2O_3				0
P_2O_5				0
Mg#	80.73	87.42	74.31	
Cr#	10.89	29.22	2.72	
Eclogitic				
SiO_2	54.22	56.40	50.01	77
Al_2O_3	6.89	17.71	1.57	77
FeO	5.76	12.15	1.18	77
MgO	11.48	17.78	6.03	77
MnO	0.09	0.36	0.03	76
CaO	16.82	23.72	9.20	77
Na_2O	3.24	6.09	0.28	77
K_2O	0.50	1.61	0.01	76
TiO_2	0.43	2.77	0.07	77
NiO	0.08	0.41	BD	29
Cr_2O_3	0.07	0.27	0.02	72
V_2O_3	0.03	0.04	BD	5
P_2O_5	0.02	0.04	BD	6
Mg#	77.95	90.54	66.48	
Cr#	0.46	2.82	0.00	

forsterite content (Stachel and Harris, 2008). The composition of olivine inclusions in Canadian diamonds is reported in Table 4.

Only a small number of olivine inclusions (66 inclusions, 15%) examined in this work coexist with a garnet inclusion allowing assignment of a harzburgitic or lherzolitic paragenesis. The Na_2O content of olivine inclusions is very low with 77.7% containing <0.03 wt% Na_2O. Nevertheless, some high Na_2O olivines are observed, with 17 samples showing Na_2O concentration >0.2 wt%. These 17 olivine inclusions are from the Panda kimberlite (Stachel et al., 2003; Tomlinson et al., 2006) 16 of which are found in three diamonds studied by Tomlinson et al. (2006) and are very small in size (2–20 μm).

Based on the available data, the Mg# of olivine inclusions in Canadian diamonds ranges from 87.2 to 96.5 with a mean at 92.5 and a mode between 93 and 93.5, with only 1.1% of the specimens having Mg# <90 (Fig. 21), similar to values reported by Stachel and Harris (2008). The highest Mg# (96.5) is observed in one inclusion reported by Davies et al. (2004b; sample DO27300) , where olivine coexists in the same diamond with inclusions of ferropericlase and low-Ni enstatite (former bridgmanite). The occurrence of these phases together suggests that this

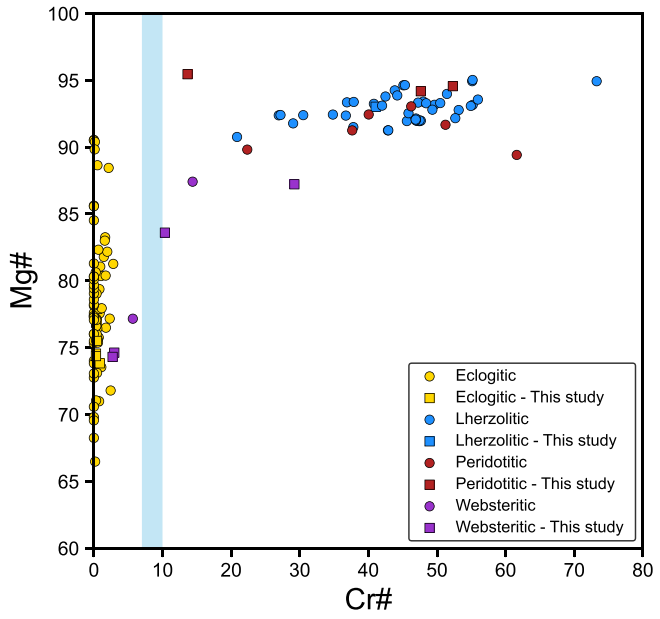

Fig. 18. Cr# vs Mg# plot for clinopyroxene inclusions in Canadian diamonds. The shaded area at Cr# = 7–10 indicates the boundary between the eclogitic and peridotitic clinopyroxenes (See text). Symbols indicated as "This study" represent clinopyroxenes with paragenesis assigned in this study.

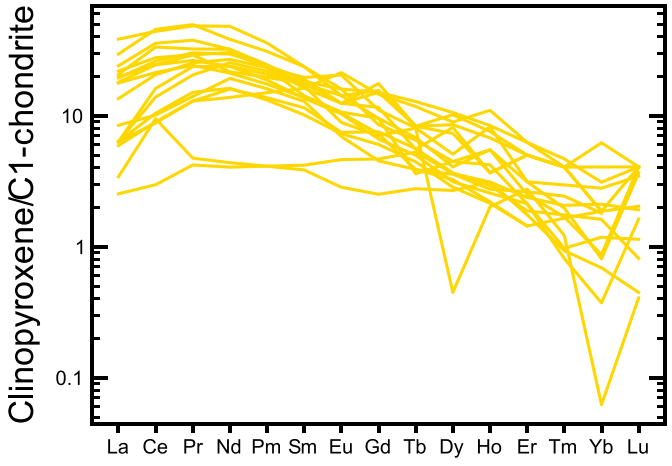

Fig. 19. REE concentrations of 18 eclogitic clinopyroxene included in Canadian diamonds, normalized to the C1-chondrite of McDonough and Sun (1995).

diamond formed at the boundary between the transition zone and the lower mantle (~660 km) where an assemblage of ringwoodite + majoritic garnet + ferropericlase + bridgmanite + Ca-perovskite is stable (Harte, 2010).

This suggests that this particular inclusion, with olivine stoichiometry, may be ringwoodite, or at least was ringwoodite when the diamond formed, and subsequently transformed to the low-pressure polymorph (olivine) upon ascent towards the surface.

A difference in the Mg# of harzburgitic and lherzolitic olivine can be observed in Fig. 21: lherzolitic olivine tends to have a lower Mg# than harzburgitic olivine, however, the degree of overlap between these two parageneses is too high to allow a rigorous classification to be performed based on Mg#. Stachel et al. (2022b) studied a larger set of olivine inclusions with known paragenesis (232 harzburgitic and 76 lherzolitic) from a global database, and from their statistics it is possible to make hypotheses about the parageneses of the unclassified olivine inclusions. Canadian olivine inclusions exhibit a unimodal distribution with an

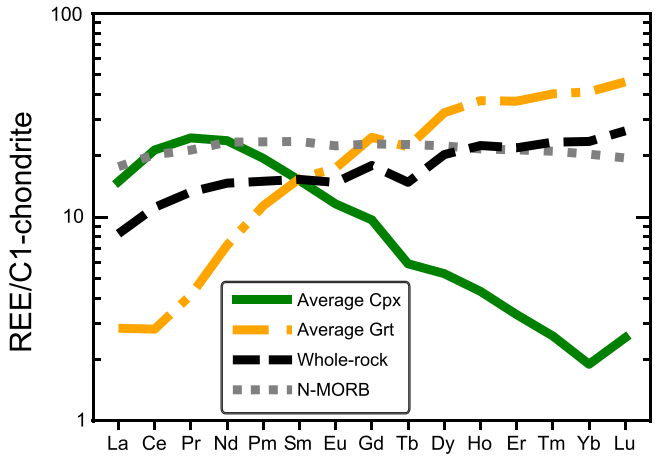

Fig. 20. Averages of REE_N contents in eclogitic clinopyroxenes and garnets from inclusions in Canadian diamonds and whole-rock REE_N content calculated for a modal ratio of 55% garnet and 45% clinopyroxene in eclogite. The "N-MORB" line is the average REE_N content of N-MORBs reported by Gale et al. (2013).

Table 4
Average, maximum and minimum concentrations of major and minor elements (measured with EMPA) for olivine inclusions in Canadian diamonds (in wt%). BD = below detection.

	Average	Max	Min	# Analyses
SiO_2	41.03	45.17	38.71	390
Al_2O_3	0.02	0.40	BD	353
FeO	7.33	12.13	3.52	390
MgO	50.77	54.76	46.27	390
MnO	0.10	0.18	0.04	374
CaO	0.04	0.41	BD	367
Na_2O	0.04	0.30	BD	217
K_2O	0.00	0.06	BD	222
TiO_2	0.00	0.04	BD	266
NiO	0.35	0.50	0.03	385
Cr_2O_3	0.05	0.27	BD	376
V_2O_3	0.00	0.01	BD	87
P_2O_5	0.01	0.04	BD	117
Mg#	92.50	96.47	87.22	

average Mg# = 92.5, in accord with a calculated Mg# using 55% harzburgitic and 45% lherzolitic olivine and the average Mg#s calculated by Stachel et al. (2022b). This suggests a higher-than-expected number of unrecognized lherzolitic diamonds (compared to the abundances calculated by Stachel and Harris, 2008, 75% harzburgitic and 25% lherzolitic), suggesting that the high abundance of lherzolitic diamonds may be a characteristic of the entire Canadian lithosphere, and not only of the lithosphere below the Victor Mine. However, it is important to notice that the calculated average Mg#, using a relatively small number of olivine inclusions in this study, are different from those reported by Stachel et al. (2022b). Canadian harzburgitic olivine inclusions have an average Mg# = 92.4 and Canadian lherzolitic olivine inclusions exhibit an average Mg# = 91.5. This may simply be the result of the small number of classified olivine inclusions and non-representative statistics. However, if this is not the case and the data are representative for all Canadian olivine inclusions, then it would mean that a higher abundance of harzburgitic olivine need to be present to obtain the average (Mg# = 92.5) calculated for all the available Canadian olivine inclusions.

In an attempt to separate harzburgitic from lherzolitic olivine inclusions, PCA was performed for the major and minor elements (SiO_2, Al_2O_3, FeO, MgO, MnO, CaO, NiO, Cr_2O_3) for olivine inclusions in Canadian diamonds. As shown in Fig. 22, a distinction between the two parageneses is not observed based on the major elements

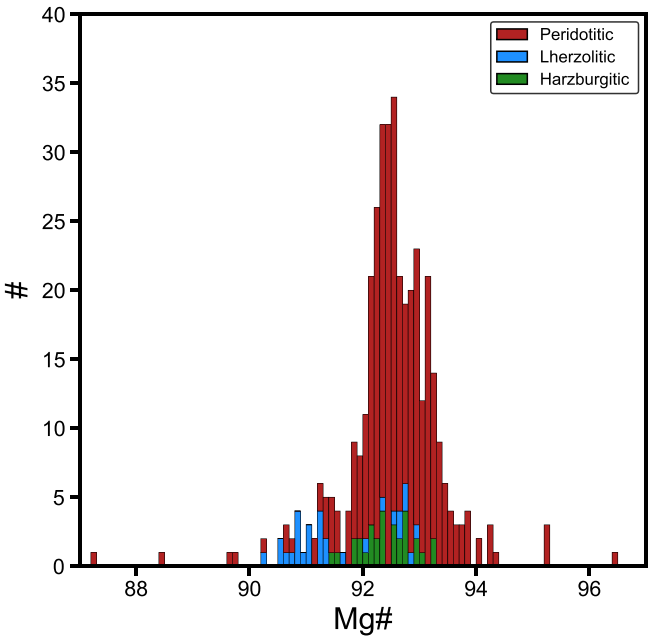

Fig. 21. Mg# distribution of olivine inclusions in Canadian diamonds. The term "peridotitic" refers to samples that do not coexist with garnet and thus could not be assigned a lherzolitic or harzburgitic paragenesis. The bin size is 0.1.

concentrations, which are similar regardless of paragenesis (Fig. 22).

3.5.4. Orthopyroxene

Orthopyroxenes are very rare in Canadian diamonds with only 74 inclusions found thus far. In total, 16 of these inclusions coexist with garnet and are assigned a harzburgitic, lherzolitic or websteritic paragenesis. Another websteritic orthopyroxene has been identified using the criterion proposed by Stachel and Harris (2008) where an orthopyroxene can be considered websteritic if Mg# <86, or Na_2O >0.25 wt% or TiO_2 >0.12 wt%. This criterion however is not absolute, as the authors pointed out, and in this work, a websteritic orthopyroxene coexisting with garnet does not meet the requirements described above. The average composition for the available peridotitic orthopyroxenes is reported in Table 5.

Four lherzolitic orthopyroxenes (from Tomlinson et al., 2006) have been excluded from the calculation of the average composition as they are very small (2 to 20 μm) which made elemental analyses challenging and consequently the oxide wt% totals did not sum to 100% and required normalization that may have introduced errors. These four orthopyroxenes have a reported SiO_2 concentration >60 wt%, which is significantly higher than what is expected for orthopyroxenes.

Based on the available data, orthopyroxenes included in Canadian diamonds have a relatively high Mg#, ranging from 89.5 to 96.5, with only 6.8% of the samples having a Mg# <92, in accord with data reported by Stachel and Harris (2008).

One lherzolitic orthopyroxene (sample AB10, Van Rythoven and Schulze, 2009) has a very low CaO content (0.05 wt%) likely due to this inclusion being in contact with a diopside inclusion.

3.5.5. Magnesiochromite

Magnesiochromite is observed in 257 samples and is the fourth most abundant inclusion found in Canadian diamonds. The average composition of magnesiochromite inclusions is reported in Table 6.

At the pressure-temperature conditions of diamond formation, garnet is stable over spinel in mantle peridotites (O'Hara et al., 1971), however, a high Cr/Al ratio in the system expands the stability of spinel to higher pressures (O'Neill, 1981; Webb and Wood, 1986; Klemme, 2004). Experiments (Doroshev et al., 1997) predict that to have spinel coexisting with garnet at depths into the diamond stability field, a Cr#

Table 5
Average, maximum and minimum concentrations of major and minor elements (measured with EMPA) for orthopyroxene inclusions in Canadian diamonds (in oxide wt%). BD = below detection.

	Average	Max	Min	# Analyses
SiO_2	57.44	58.83	49.59	59
Al_2O_3	0.48	1.30	0.03	59
FeO	4.49	7.17	2.46	59
MgO	35.81	42.45	23.98	59
MnO	0.12	0.75	BD	59
CaO	0.40	0.81	0.05	59
Na_2O	0.07	0.51	BD	58
K_2O	0.01	0.17	BD	43
TiO_2	0.02	0.10	BD	58
NiO	0.10	0.16	0.02	43
Cr_2O_3	0.33	0.60	BD	58
V_2O_3	0.01	0.01	BD	12
P_2O_5	0.01	0.02	BD	15
Mg#	93.40	96.48	89.52	

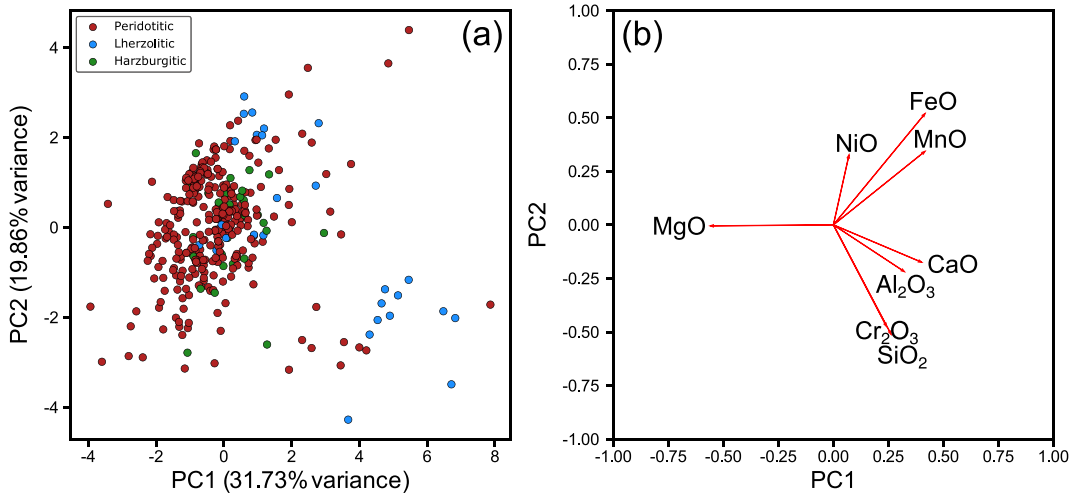

Fig. 22. Scores (a) and loadings (b) plot for the Principal Components of the total dataset of olivine inclusions in Canadian diamonds. The percentages in the axes title represent the variance explained by every Principal Component. The "Peridotitic" class refers to all the olivine inclusions that do not coexist with garnet in the same diamond.

Table 6
Average, maximum and minimum concentrations of major and minor elements (measured with EMPA) for magnesiochromite inclusions in Canadian diamonds (in wt%). BD = below detection. The Fe_2O_3 content, if not already indicated in the original paper, has been calculated using the formula by Droop (1987).

	Average	Max	Min	# Analyses
SiO_2	0.23	0.61	0.05	211
Al_2O_3	6.76	15.44	3.36	211
FeO	11.68	15.82	9.05	211
Fe_2O_3	3.11	7.37	1.13	211
MgO	14.05	16.49	10.96	211
MnO	0.13	0.41	BD	211
CaO	0.01	0.10	BD	146
Na_2O	0.02	0.11	BD	52
K_2O	0.00	0.08	BD	46
TiO_2	0.14	2.43	BD	211
NiO	0.10	0.80	BD	207
Cr_2O_3	63.74	68.77	52.40	211
ZnO	0.07	0.14	0.02	136
V_2O_3	0.25	0.31	0.16	77
P_2O_5	0.00	0.01	BD	18
Mg#	68.17	76.23	55.25	
Cr#	86.39	92.88	69.93	
Fe^{3+}#	19.27	31.90	8.31	

>80 is required. Fig. 23 shows how almost all magnesiochromite inclusions (96.2%) in Canadian diamonds have Cr# >80. The samples with Cr# <80 could not have been in equilibrium with garnet and they must have formed in dunitic substrates as indicated by Stachel and Harris (2008).

Based on the present data, Canadian magnesiochromite inclusions have Mg# that range from 55.3 to 76.2, with 74.9% of them ranging between Mg# of 65 and 71. The Fe^{3+}# ranges from 8.3 to 31.9, where most of the samples (54.0%) have a Fe^{3+}# between 10 and 20.

ZnO in magnesiochromite inclusions from Canadian diamonds is present in unusually high concentrations (Fig. 24), up to 0.14 wt%. Usually, high Zn^{2+} contents are linked to low formation temperatures (Ryan et al., 1996). However, most of the samples exhibiting high ZnO concentrations come from the A-154 South pipe in the Diavik Mine (Slave craton), where high ZnO contents have also been measured for olivine inclusions in diamonds and an overall higher-than-usual Zn concentration in the diamond formation environment has been proposed (Donnelly et al., 2007).

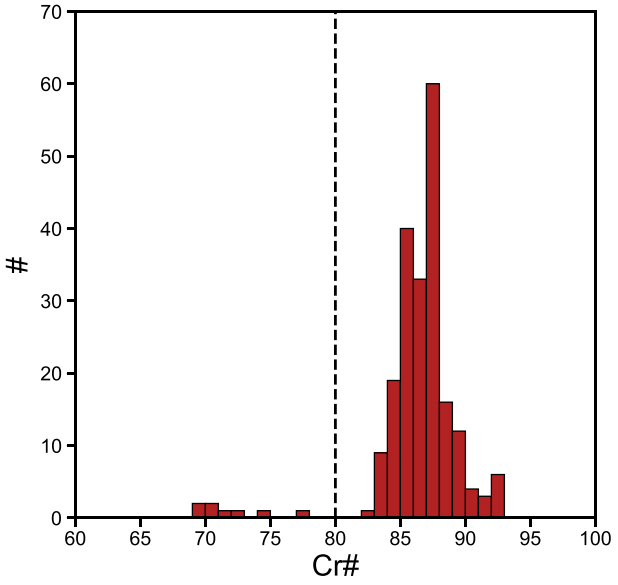

Fig. 23. Cr# distribution for magnesiochromite inclusions in Canadian diamonds. The dashed line separates magnesiochromite inclusions with Cr# >80 from those with Cr# <80.

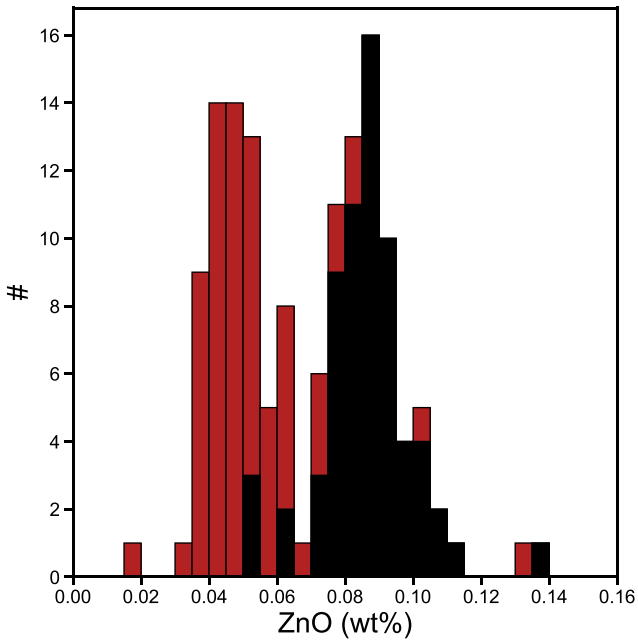

Fig. 24. Distribution of ZnO concentration for magnesiochromite inclusions in Canadian diamonds. Data from the A-154 South pipe (Diavik Mine, Slave craton) are shown in black.

3.5.6. *Sulfides*

Sulfides are the third most abundant inclusion mineral in Canadian diamonds. Sulfide inclusions are opaque with a metallic luster and are often surrounded by fractures caused by the difference in thermal expansion coefficients of diamonds and sulfides (Taylor and Liu, 2009). Sulfide inclusions are often used to assign a peridotitic or eclogitic paragenesis to their host diamonds based on their Ni concentration (Bulanova et al., 1996), with Ni-rich (Ni >22 wt%) sulfides belonging to the peridotitic suite and Ni-poor (Ni <12 wt%) sulfides belonging to the eclogitic suite. However, this classification scheme has two important limitations: (1) at the temperatures of diamond formation sulfides are present in the form of a monosulfide solid solution (mss), during ascent the mss destabilizes and exsolves into various sulfides (mainly pyrrhotite, pentlandite and chalcopyrite; Richardson et al., 2001) and some Ni-rich and Ni-poor zones can form in the inclusion. Thus, accurate assignment of sulfide inclusions to peridotitic and eclogitic parageneses requires reconstructing the Ni concentration of the original mss. This can be achieved by chemical analysis and X-ray imaging of all the exsolved phases (Stachel and Harris, 2008), or by Rietveld refinement of X-ray diffraction data (Pamato et al., 2021). (2) Some authors (Deines and Harris, 1995; Bulanova et al., 1996; Pearson et al., 1998) have observed a continuum of Ni concentrations in sulfide inclusions, making it difficult to place a meaningful boundary between the Ni content of peridotitic and eclogitic sulfides.

Other methods have been proposed to aid in the distinction of sulfide parageneses together with the Ni concentration. Deines and Harris (1995) calculated the Ni/Fe ratio of sulfides in equilibrium with olivine with different Mg# and observed that as the Mg# of olivine increases from ~88 to ~96, the Ni/Fe ratio of coexisting sulfides increases from ~0.2 to ~0.6, suggesting that a sulfide with a low Ni/Fe ratio (<0.2) could not have coexisted in equilibrium with mantle olivine, and therefore probably formed in an olivine-free environment and thus must be eclogitic. It has also been shown that the Os concentration varies, at orders of magnitude, between peridotitic (Os-rich) and eclogitic (Os-poor) sulfides (Pearson et al., 1998; Pearson et al., 1999; Pearson and Shirey, 1999). Stachel and Harris (2008) suggest that one check the Cr

and Ni concentration of sulfide inclusions as eclogitic sulfides are expected to show very low Cr concentrations (<0.02 wt%). Unfortunately, Cr content is rarely analyzed for, and therefore there is a limited amount of data regarding the Cr concentration in sulfide inclusions in diamond.

Here, all of the above criteria were considered when determining paragenesis of sulfide inclusions. First of all, the Ni concentration of all the inclusions was checked and a bimodal distribution was identified (Fig. 25a) with a main peak at Ni <7 wt% (low-Ni group) and a secondary peak at Ni >19 wt% (high-Ni group). A small number of sulfide inclusions (8%) exhibited a Ni concentration transitional between these two groups. Then, as a first step, all the sulfides with Ni <7 wt% were assumed to be eclogitic and those with Ni >19 wt% were assumed to be peridotitic, the paragenesis of the transitional group was not defined. Together with the Ni concentration, the Ni/Fe ratio for the inclusions was checked, and all the sulfides belonging to the high-Ni group have a Ni/Fe >0.4, while those in the low-Ni group have a Ni/Fe <0.2 (most of which lower than 0.1), in accord with the results based on purely the Ni concentration, as described above.

The parageneses of sulfide inclusions determined in this way were compared to those inferred from the composition of coexisting silicate and oxide inclusions and they show perfect agreement between each other. A sulfide inclusion with a Ni content of 13.02 wt% was determined to be peridotitic as it coexists in the same diamond with a magnesiochromite inclusion. Finally, the concentration of Cr (Fig. 25b) and Os (Fig. 25c) were checked where available to further confirm the paragenetic assignments. Following the classification procedure outlined above we determined 63.6% of the sulfide inclusions are eclogitic, and the remaining 36.4% are peridotitic. A possible explanation for these abundances is that sulfides may be more common in eclogitic lithologies than in peridotitic lithologies. The composition of sulfide inclusions in Canadian diamonds of the peridotitic, eclogitic and undefined paragenesis is expressed in terms of normalized S, Ni and Fe content in Fig. 26.

3.5.7. *Sub-lithospheric inclusions*

A total of 71 sub-lithospheric inclusions has been recognized in 49 Canadian diamonds and include: 44 ferropericlases, 18 majoritic garnets, 4 low-Ni enstatites (retrogressed bridgmanite), 3 breyites, 1 metallic Ni and 1 inclusion indicated as Mg_2SiO_4 (possibly former ringwoodite based on the phase assemblage, see section 3.5.3). Majoritic garnets have already been described in the garnet section (section 3.5.1) as the same information regarding garnet paragenesis can be retrieved from majoritic and non-majoritic garnet.

Based on the present data, most of Canadian ferropericlase inclusions

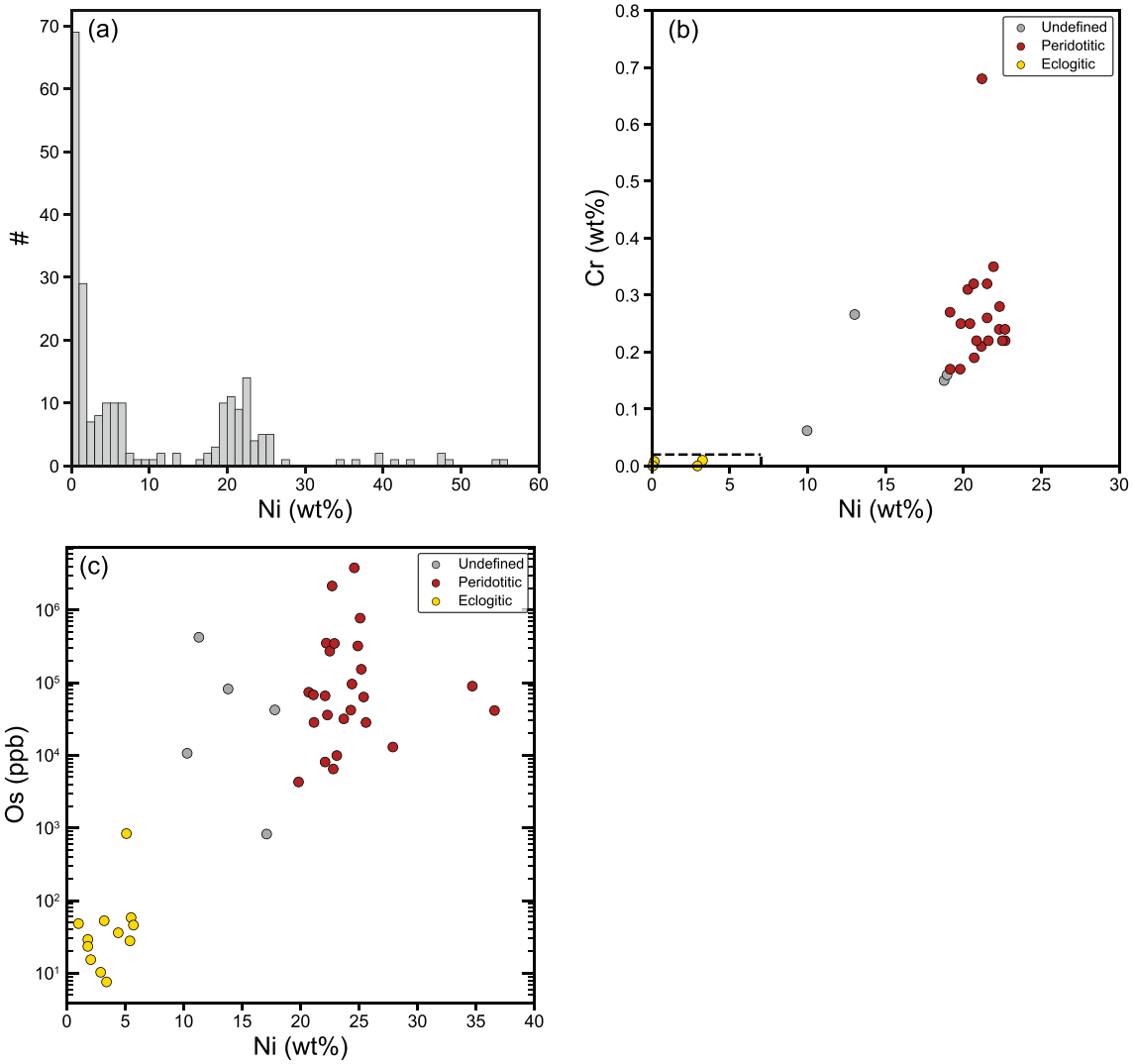

Fig. 25. (a) Ni (wt%) histogram for sulfide inclusions in Canadian diamonds. (b) Ni (wt%) vs Cr (wt%) scatter plot for sulfide inclusions in Canadian diamonds. The dashed line separates the eclogitic and peridotitic fields (Ni (wt%) limit for the eclogitic field is 7 wt%). (c) Ni (wt%) vs Os (ppb) scatter plot for sulfide inclusions in Canadian diamonds.

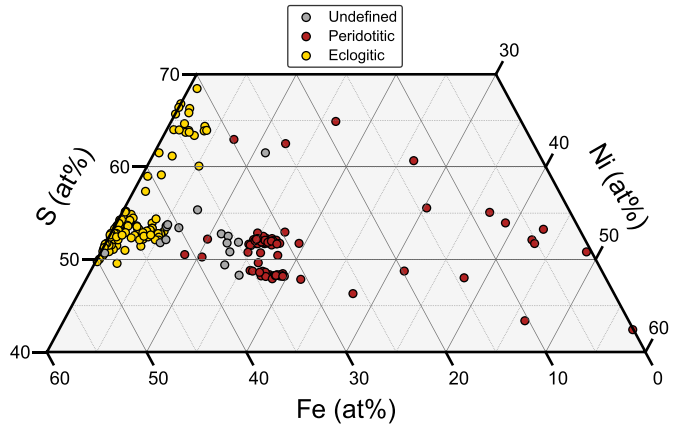

Fig. 26. Sulfide quadrilateral showing the composition of sulfide inclusions in Canadian diamonds in terms of Ni, Fe and S expressed in atomic %.

do not coexist with other phases in the same diamond, however, ferropericlase together with breyite, bridgmanite, SiO_2, and metallic Ni has been observed in some diamonds. The Mg# for Canadian ferropericlase inclusions ranges from 80.1 to 89.7 with an average of 85.1, a median of 85.8 and 64% of the samples have Mg# that range from 85 and 88, without a single Fe-rich ferropericlase like those observed in other locations (e.g. Juina, Brazil; see Hayman et al., 2005, Stachel et al., 2005). The high Mg# character of ferropericlase inclusions in Canadian diamonds is compatible with equilibration with bridgmanite in meta-peridotitic assemblages (see Walter et al., 2022) and such inclusions may therefore represent protogenetic minerals included during formation of the diamond in the lower mantle (Lorenzon et al., 2023). All Canadian ferropericlase inclusions are almost pure MgO + FeO, with all other elements present at very low concentrations, except for NiO, which is the only element that consistently occurs at concentrations >1 wt% (only 3 samples have NiO <1 wt%).

The three breyite inclusions are reported by Davies et al. (2004b) and Tappert et al. (2005). According to Walter et al. (2022), $CaSiO_3$-rich inclusions can be divided into a high-TiO_2 (>2 wt%) and low-TiO_2 (<0.7 wt%) group, the former can be associated with meta-peridotitic assemblages, while the latter is linked to meta-basaltic assemblages. In this database all three inclusions belong in the low-TiO_2 group, and therefore are associated with a meta-basaltic origin.

The four (former) bridgmanite inclusions are reported by Davies et al. (2004b). Like the $CaSiO_3$-rich inclusions, these can also be assigned to a meta-peridotitic or meta-basaltic association, the first having Al_2O_3 <3.5 wt% and the second with Al_2O_3 >7 wt% (Walter et al., 2022). Canadian bridgmanites always show an Al_2O_3 concentration <3.5 wt%, and therefore belong to the meta-basaltic association.

The single metallic alloy found inside a Canadian diamond from the DO27 kimberlite (Slave craton) is almost pure Ni.

3.6. Geothermobarometry

The chemical composition of single inclusions or inclusion pairs inside diamonds can be used to determine the pressure and temperature conditions of diamond formation. The diamonds N content and its aggregation state can also be used to calculate the average residence temperature of diamond in the mantle. Here, both single mineral and inclusion pairs geothermobarometers have been applied to the compositions of mineral inclusions in Canadian diamonds.

3.6.1. Single mineral geothermobarometry

The Al-in-olivine ($T_{Al\text{-}in\text{-}Ol}$, Bussweiler et al., 2017), Ni-in-garnet ($T_{Ni\text{-}in\text{-}Grt}$, Sudholz et al., 2021) and Zn-in-chromite ($T_{Zn\text{-}in\text{-}Chr}$, Ryan et al., 1996) thermometers have been applied to inclusions in this work. The Ni-in-garnet and Zn-in-chromite thermometers are pressure-independent, and the Al-in-olivine thermometer requires knowledge of the formation pressure of the inclusions. A pressure of 6 GPa has been used for such calculations as it represents the pressure mode for diamond formation (Nimis et al., 2020; Nimis, 2022). When divergence of >150 °C was observed in the temperatures determined by the different thermometers or in different inclusions in the same diamond the data were discarded, as such discrepancies likely result from disequilibrium in the system or poor analytical precision during measurement of minor element concentrations. Moreover, calculated temperatures <900 °C and >1400 °C (the temperature window for lithospheric diamonds) were also discarded since they are assumed to reflect disequilibrium (Stachel and Harris, 2008). The calculations result in average temperatures of 1222 °C for olivine, 1186 °C for garnet and 1215 °C for magnesiochromite (Fig. 27) and are in accord with previous calculations for a global dataset from Nimis (2022).

The relatively high formation temperature of magnesiochromite inclusions is due to a set of inclusions from Wawa (Miller et al., 2012) with average formation temperatures of 1281 °C. Interestingly a set of olivine inclusions from Wawa (Stachel et al., 2006; Miller et al., 2012) also shows formation temperatures >1300 °C, suggesting diamond formation at a particularly high temperature in this area.

The Cr-in-diopside barometer (P_{NT00}) and the enstatite-in-clinopyroxene thermometer (T_{NT00}) of Nimis and Taylor (2000) have been applied to 26 clinopyroxenes selected using the criteria proposed by Ziberna et al. (2016) to obtain accurate formation pressure and temperature estimates. The calculated pressures have been subsequently corrected using the formula proposed by Nimis et al. (2020) and the results are summarized in Fig. 28.

P_{NT00} and T_{NT00} have been calculated using an iterative approach: first, a T_{NT00} was calculated starting from an initial pressure of 5 GPa; second, with the obtained T_{NT00}, P_{NT00} was calculated. The newly calculated P_{NT00} was then used in the T_{NT00} formula, and the process was repeated until convergence was reached. The calculations show a formation pressure and temperature windows from 4.8 to 7.3 GPa and from 928 to 1276 °C, respectively, with the majority of data plotting between the 35 and 40 mW/m^2 geotherms of Hasterok and Chapman (2011) and no samples plot outside of the diamond stability field. The temperature window is in good agreement with the temperatures calculated from olivine, garnet and chromite inclusions.

Finally, the geobarometer from Thomson et al. (2021, P_{Th21}) was also employed to estimate the formation pressure of diamonds hosting majoritic garnet inclusions. This barometer uses machine learning to calculate pressure from two different majoritic components, the majoritic substitution ($2B^{3+} = M^{2+} + Si^{4+}$) and the Na-majorite substitution ($B^{3+} + M^{2+} = X^{+} + Si^{4+}$). In this work, P_{Th21} was applied on 18 garnets with Si >3.06 apfu, 11 of which were already recognized as majoritic in the literature (Davies et al., 2004b; Pokhilenko et al., 2004; Stachel et al., 2006; Banas et al., 2007) while the other 7 were identified in this study. This geobarometer provides pressures of formation between 8.6 and 18.5 GPa corresponding to depths from the upper mantle into the transition zone.

The presence of clinopyroxene exsolutions in majoritic garnet inclusions has been observed and suggested for most, if not all, crystals (Thomson et al., 2021; Walter et al., 2022). Ideally such exsolutions should be reintegrated into the garnet composition before using the geobarometer, otherwise pressures of formation will be underestimated. This, however, is usually not possible since these exsolutions are not described in most studies. Therefore, it is important to note that the formation pressures calculated for majoritic garnets in this study are most likely minimum pressure estimates.

3.6.2. Inclusion pairs geothermobarometry

The compositions of some non-touching inclusion pairs hosted in Canadian diamonds have been used to estimate pressure and temperature of formation using different geothermobarometers.

In this work, few inclusion pairs are suitable for

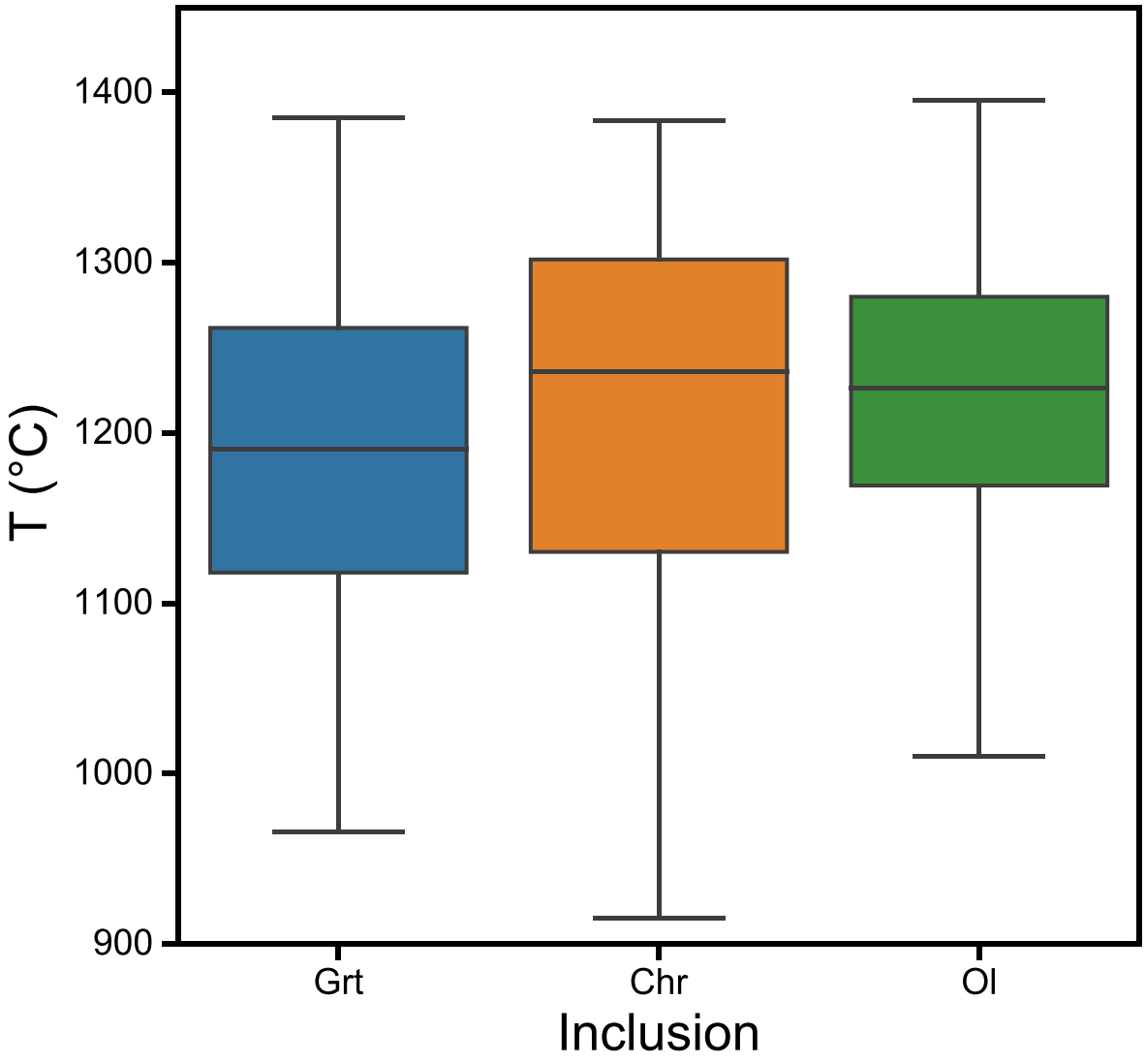

Fig. 27. Boxplot of the temperatures calculated with the Al-in-olivine, Ni-in-garnet and Zn-in-chromite geothermometers for inclusions in Canadian diamonds with an assumed pressure of 6 GPa for the olivine thermometer. The horizontal line inside the boxes represents the median of the data.

geothermobarometry analysis. If a diamond contained more than a single inclusion pair (e.g., sample SL5–75, Promprated et al., 2004, with 3 orthopyroxenes and 2 clinopyroxenes) the calculations were performed for all possible unique inclusion pair combinations. As for single mineral geothermometers, temperatures outside the lithospheric diamonds window were discarded as they are likely the result of disequilibrium.

For clinopyroxene-orthopyroxene pairs, the T_{BK90} (Brey and Köhler, 1990) and T_{Ta98} (Taylor, 1998) thermometers were used with an assumed pressure of 6 GPa. A total of 10 possible inclusion pairs in 4 diamonds result in an average T_{BK90} and T_{Ta98} of 1200 °C and 1229 °C respectively, showing good agreement between the thermometers and with the single mineral geothermometers.

For garnet-orthopyroxene pairs, the T_{NG09} (Nimis and Grütter, 2010) thermometer and the P_{BK90} (Brey and Köhler, 1990) were applied together using an iterative approach identical to the one used for the single clinopyroxene geothermobarometer. For a total of 9 inclusion pairs in 7 diamonds, a formation pressure between 4.4 and 7.1 GPa and a formation temperature from 1007 to 1301 °C were determined and plotted together with the results from the single clinopyroxene geothermobarometer (with which they show perfect agreement) in Fig. 28. For the same set of garnet-orthopyroxene inclusion pairs, the geobarometer P_{NG85} (Nickel and Green, 1985) was used with the T_{NG09} determined from the previous calculation. The resulting pressures range from 5.2 to 7 GPa, and are in good agreement with P_{BK90}, with the maximum mismatch of 0.8 GPa (P_{BK90} = 4.4 GPa, P_{NG85} = 5.2 GPa, sample Wsc13, Miller et al., 2012).

The geothermometer of Krogh, (1988, T_{Kr88}) was applied to 26 garnet-clinopyroxene inclusion pairs hosted in 11 diamonds. An assumed pressure of 6 GPa was used, and the resulting temperatures range from 1075 to 1386 °C with an average temperature of 1234 °C. Importantly, this is the only thermometer that could also be applied to inclusions of eclogitic paragenesis, in fact, most of the inclusion pairs (22 out of 26) were eclogitic. Eclogitic inclusions show formation temperatures matching those from peridotitic inclusions, suggesting that peridotitic and eclogitic diamonds form in similar temperature conditions, at least in the lithospheric settings.

3.6.3. *Nitrogen aggregation geothermometry*

Nitrogen impurities in diamonds tend to aggregate to form B-centers (see section 3.2). The aggregation from C-centers to A-centers occurs over very short geologic times (Nimis, 2022), but the aggregation of A-centers to B-centers occurs much slower and is a function of the N content, the average mantle residence temperature of the diamond, and the diamond residence time (Taylor et al., 1990). Ideally, calculation of the mantle residence temperature of a diamond requires knowledge of

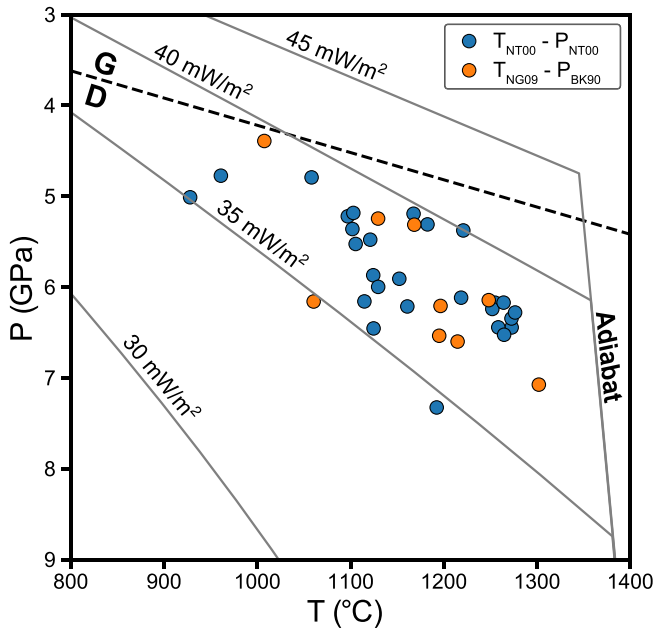

Fig. 28. Pressures and temperatures calculated with the Cr-in-diopside barometer + enstatite-in-clinopyroxene thermometer (Nimis and Taylor, 2000; blue dots) and the garnet-orthopyroxene barometer (Brey and Köhler, 1990) + thermometer (Nimis and Grütter, 2010; orange dots). The dashed black line separates the graphite (G) and diamond (D) stability field (Day, 2012), the solid grey lines are the 30, 35, 40 and 45 mW/m^2 surface heat flux geotherm intersecting an adiabat with a potential temperature of 1300 °C and a gradient of 0.3 °C/km (Hasterok and Chapman, 2011). (For interpretation of the references to colour in this figure legend, the reader is referred to the web version of this article.)

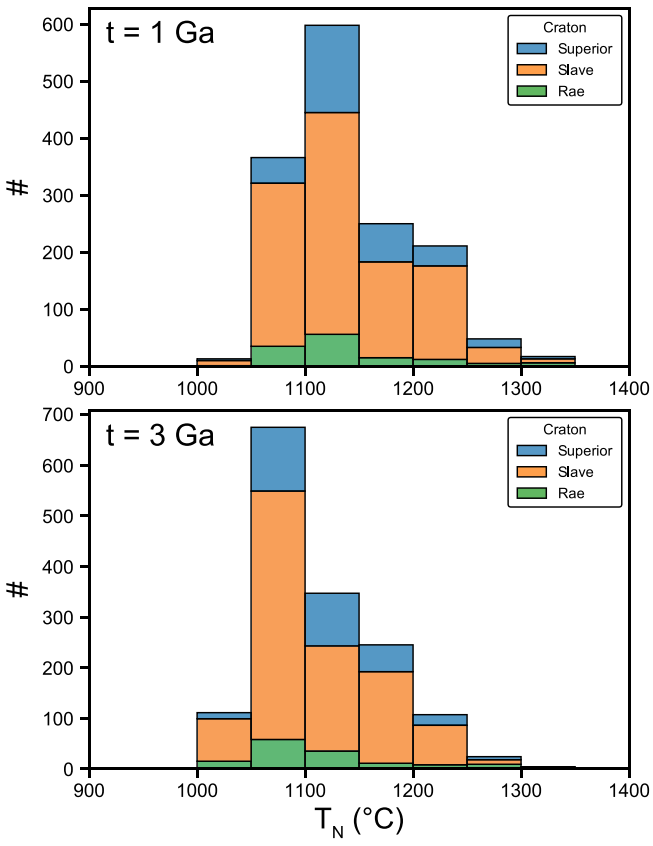

Fig. 29. Distribution of residence temperatures calculated with the geothermometer of Taylor et al. (1990) for 1538 Canadian diamonds for a residence time of 1 Ga (top) and 3 Ga (bottom). The different colors are related to the craton of origin of the diamonds as indicated in the legend.

the residence time, but since the time-dependence of conversion of A-centers to B-centers is minimal, a good estimate of the residence temperature can be determined using only the N concentration and the abundance of B-centers. Thus, this geothermometer (T_N; Evans and Harris, 1986; Taylor et al., 1990) has been used to estimate the average residence temperature of Canadian diamonds in the mantle.

In Fig. 29, the calculated average residence temperatures for 1552 Canadian diamonds are plotted for assumed residence times of 1 and 3 Ga. The calculations have been performed also for residence times of 0.5 and 2 Ga but given the weak time dependence of this geothermometer, the results from these calculations are not reported as they do not show discernable difference with respect to the 1 Ga and 3 Ga calculations.

The average mantle residence temperature calculated for a residence time of 1 Ga is 1141 °C with a mode at 1110 °C, and 1114 °C with the mode at 1084 °C if one assumes the mantle residence time is 3 Ga. Peridotitic diamonds show an average residence temperature of 1148 and 1121 °C for 1 and 3 Ga residence times, respectively. Eclogitic diamonds show similar residence temperatures of 1099 and 1074 °C for 1 and 3 Ga residence times, respectively. It is important to consider that, based on the ages of Canadian diamonds given by dating of sulfide inclusions, (see section 3.7) the peridotitic suite appear to be generally older than the eclogitic suite (peridotitic diamonds from the Slave craton are >1 Ga older than eclogitic diamonds from the same area).

This is in accord with data from the global database (Smit et al., 2022a) indicating that only peridotitic diamonds formed prior to 3 Ga. It is generally accepted that eclogitic diamonds are on average younger than peridotitic diamonds, in fact, some eclogitic diamonds are coeval with the age of kimberlite eruption (e.g., Orapa and Cullinan, see Gress et al., 2021 and Navon, 1999, respectively). This could explain the lower N aggregation state observed in eclogitic Canadian diamonds with respect to peridotitic Canadian diamonds (see section 3.2).

Diamonds from different cratonic areas show almost the same residence temperature distribution (Fig. 29), suggesting there are minimal differences in the average mantle temperature among Canadian cratons. In fact, the average residence temperature calculated for the Slave, Superior and Rae craton (for a residence time of 2 Ga) is 1121 °C, 1129 °C and 1127 °C respectively.

Fig. 30 shows a plot of all diamonds on which both inclusion thermometry and N aggregation thermometry (for calculation using a residence time of 2 Ga) have been performed. It appears that inclusions typically record a higher temperature with respect to N aggregation thermometry. Despite uncertainties and error in the associated calculations caused by (i) the arbitrary choice of a 2 Ga residence time, (ii) the choice of 6 GPa formation pressures for all thermometers that required known pressure, and (iii) the use of different inclusion geothermometers for the comparison with the residence temperature, the lack of agreement is still significant. This disagreement is due to the fact that N aggregation thermometry records only the average residence temperature of the diamond, and therefore the effect of short thermal anomalies or decreases in ambient temperature due to upwelling will be averaged with geological times (Nimis, 2022). The inclusions on the other hand record the temperature at which they were entrapped by the diamond (i.e., the temperature of diamond formation), implying that Canadian diamonds formed mostly at temperature higher than the ambient mantle in which they resided, as previously proposed for different works (see Nimis et al., 2020; Nimis, 2022).

3.7. *Isotopic dating of diamonds*

The age of diamond formation can be obtained by dating their mineral inclusions (e.g., Smit et al., 2022b; Richardson et al., 1984). Depending on the size of a mineral inclusion and the temperatures at

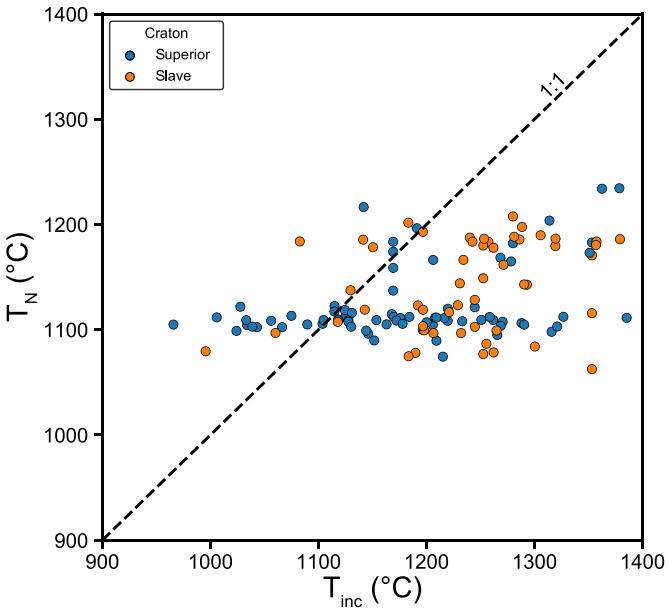

Fig. 30. Diamond formation temperatures calculated from inclusion thermometry plotted as a function of diamond residence temperature calculated from N aggregation thermometry. For thermometers that required it, the P of formation was assumed to be 6 GPa. The N aggregation temperatures are calculated using a residence time of 2 Ga. The different colors are related to the craton of origin of the diamonds as indicated in the legend.

which it formed, even protogenetic mineral inclusions can be used to date diamond formation (see Pamato et al., 2021 for sulphides; Nestola et al., 2019 for garnets; Pasqualetto et al., 2022 and Nestola et al., 2017 for clinopyroxenes). Several isotope systematics are used to date mineral inclusions, most commonly *Re*—Os for sulfides and Sm—Nd for garnets and clinopyroxenes (e.g., Pearson and Shirey, 1999; Shirey et al., 2013; Smit et al., 2022a). Only three studies dating inclusions in Canadian diamonds have been published (Westerlund et al., 2006; Aulbach et al., 2009; Aulbach et al., 2018), where sulfide inclusions in eclogitic and peridotitic diamonds from the Slave and Superior craton are dated using the Re—Os isochron method. Diamond ages obtained for peridotitic diamonds from the Slave craton are 3.2–3.5 ± 0.17 Ga (Westerlund et al., 2006; Aulbach et al., 2009) and 1.86 ± 0.19 Ga (Aulbach et al., 2009) for eclogitic diamonds. Regarding diamonds from the Superior craton, only peridotitic sulfides were dated, providing a younger age of 718 ± 49 Ma.

The age of a diamond deposit can constitute indirect evidence for the age of diamonds (Smit et al., 2022a). Two sedimentary deposits hosting diamonds are known in Canada, the Wawa-Abitibi terrane in the Superior craton and the newly discovered Tree River deposit in the Slave craton. These two deposits have an age of ~2.7 (Wyman and Kerrich, 1993) and ~2.9 Ga (Timmerman et al., 2022), respectively, indicating that the diamonds they host are at least as old.

However, it is clear that, in order to have more reliable and extensive information about the age of Canadian diamonds, more data would be necessary.

3.8. Comparison among cratons

The diamonds reported in this database were collected from four Canadian cratons, the Slave, Rae, Superior and Nain cratons (see Fig. 2). In this section, the most important petrological and geochemical aspects of Canadian diamonds are presented to highlight possible differences in the diamond forming environments associated with each craton (Table 7).

3.8.1. Slave

The Slave province is one of the most studied cratonic areas in the world, and a summary of its geology and evolution can be found in Helmstaedt et al. (2021). Of the diamonds investigated in this work, 1924 (63%) are from the Slave craton. Nitrogen contents were determined for 81.2% (1563) of these specimens, that were classified as Type I (87.7%) and Type II (12.3%) diamonds. As the majority of diamonds in this database are from Slave craton, it is no surprise that these abundances are similar to those calculated for the entire dataset of Canadian diamonds (82.4% Type I and 17.6% Type II). The highest N content in a Canadian diamond (3833 at.ppm) is observed for a sample from the Slave craton. The median N content for diamonds from the Slave craton is 524 at.ppm, which is ~1.5 times the median observed for all Canadian diamonds in this work (380 at.ppm). Regarding the N aggregation state, diamonds from the Slave craton exhibit values similar to those for the entire Canadian database, with 60% of diamonds being Type IaAB, 35% Type IaA and 5% Type IaB.

A paragenesis was assigned to 41% (789) of the diamonds from the Slave craton. As reported above, 40 sub-lithospheric diamonds are from the Slave province and their relative abundance compared to lithospheric diamonds from this craton is 5.1%, higher than the Canadian average. However, this may be the result of overrepresentation of sub-lithospheric diamonds due to the relatively small number of diamonds studied and sampling bias.

The ratio of peridotitic to eclogitic diamonds is almost 6:4 (58% peridotitic and 42% eclogitic diamonds). The higher abundance of eclogitic diamonds in the Slave craton compared to the entire Canadian dataset may explain the high median N content observed in diamonds from Slave craton as eclogitic diamonds tend to have a higher median N content than peridotitic diamonds (see section 3.2, and Stachel et al., 2022b). If only parageneses determined from garnet inclusions are considered, the Slave Craton shows a ratio of harzburgitic and lherzolitic diamonds (83% and 17%, respectively), in agreement with that

Table 7
Summary of the main geochemical and petrological characteristics of diamonds from three global datasets and the Canadian dataset grouped by craton.

		Global*	Canada	Slave	Superior	Rae	Nain
Nitrogen	#	5115	2567	1563	606	255	143
	Type II (%)	17.8	17.5	12.3	33.0	15.3	4.2
	Max (at.ppm)	3833	3833	3833	1662	3280	3171
	Median (at.ppm)	160	380	524	80	326	1295
Carbon	#	4307	1881	1195	373	185	128
	Min (‰)	−41.4	−41.4	−41.4	−15.0	−29.7	−28.4
	Max (‰)	2.5	1.6	1.6	1.3	−1.7	−1.9
	Mode (‰)	−5.1	−4.6	−4.6	−5.2	−5.1	−5.7
Paragenesis	#	2844	1069	789	244	36	0
	Sub-lithospheric (%)	2.0	4.6	5.1	2.0	11.1	–
	Peridotitic (%)	65.0	64.3	57.0	87.2	50.0	–
	Eclogitic (%)	32.8	34.8	42.1	10.8	43.8	–
	Websteritic (%)	2.3	0.9	0.9	0	6.2	–

* Data from Stachel and Harris (2008) and Stachel et al. (2022a, 2022b)

observed by Stachel et al. (2022b) for a global database.

Diamonds from the Slave craton cover the entire range of $\delta^{13}C$ values of Canadian diamonds from this database, from −41.4‰ to +1.6‰ (Fig. 31). The average $\delta^{13}C$ is −7.4‰, the mode is −4.6‰, the median is −4.7‰ and 83.9% of the diamonds overlap with the mantle range of $\delta^{13}C$ (from −8 to −2‰; Cartigny, 2005).

Two studies have been completed using the *Re*—Os isotopic system applied to sulfide inclusions from the Slave craton (Westerlund et al., 2006; Aulbach et al., 2009). These authors calculated an age of 3.52 ± 0.17 Ga for a set of peridotitic sulfides in the Panda kimberlite and ages of 3.2–3.5 Ga and 1.86 ± 0.19 Ga for peridotitic and eclogitic sulfides included in diamonds from Diavik, respectively.

Thermobarometric data on mineral inclusions in diamonds from the Slave Craton show average pressures and temperatures of formation of 5.6 GPa and 1185 °C respectively.

3.8.2. *Superior*

Of the diamonds included in this study, 24% (734) are from the Superior craton. Of the diamonds from the Superior craton, 82.6% (606) were analyzed for N content, many of which are Type II diamonds (33%) with respect to the total database and have a median N content of 80 at. ppm. This high percentage of Type II diamonds in the Superior province is mainly attributed to the work of Smit et al. (2014) on the T1 and U2 kimberlites where 93% and 75% of the studied diamonds, respectively, were classified as Type II and no clear explanation is given for this particular abundance of Type II diamonds yet.

Superior diamonds also show a low degree of N aggregation, with 56% of the samples classified as Type IaA, 41% as Type IaAB and 3% as Type IaB. This is most likely associated with the young age of some of the diamonds (see Smit et al., 2014; Aulbach et al., 2018).

A paragenesis was assigned to 244 diamonds (33%) from the Superior province, and 5 (2.0%) sub-lithospheric diamonds have been described from the Superior craton. The small number of samples from this area, however, limits the statistical significance of this data, as it would most likely change as new diamonds are studied. Regarding lithospheric diamonds, a very low abundance of eclogitic samples is observed, only 10.8% of diamonds from the Superior craton are eclogitic. This 9:1, peridotitic:eclogitic ratio may be due to either a low amount of eclogites in the lithosphere of the Superior craton or, by a preferential sampling of peridotites. Among peridotitic diamonds, 83% are lherzolitic, 14% are harzburgitic and 3% are wehrlitic diamonds (according to the parageneses retrieved from garnet inclusions) however, the dominance of lherzolitic diamonds is likely associated with diamond production from the Victor Mine.

Diamonds from the Superior craton have a narrow $\delta^{13}C$ range, from −15.0‰ to +1.3‰, with 92.8% of the diamonds falling in the main

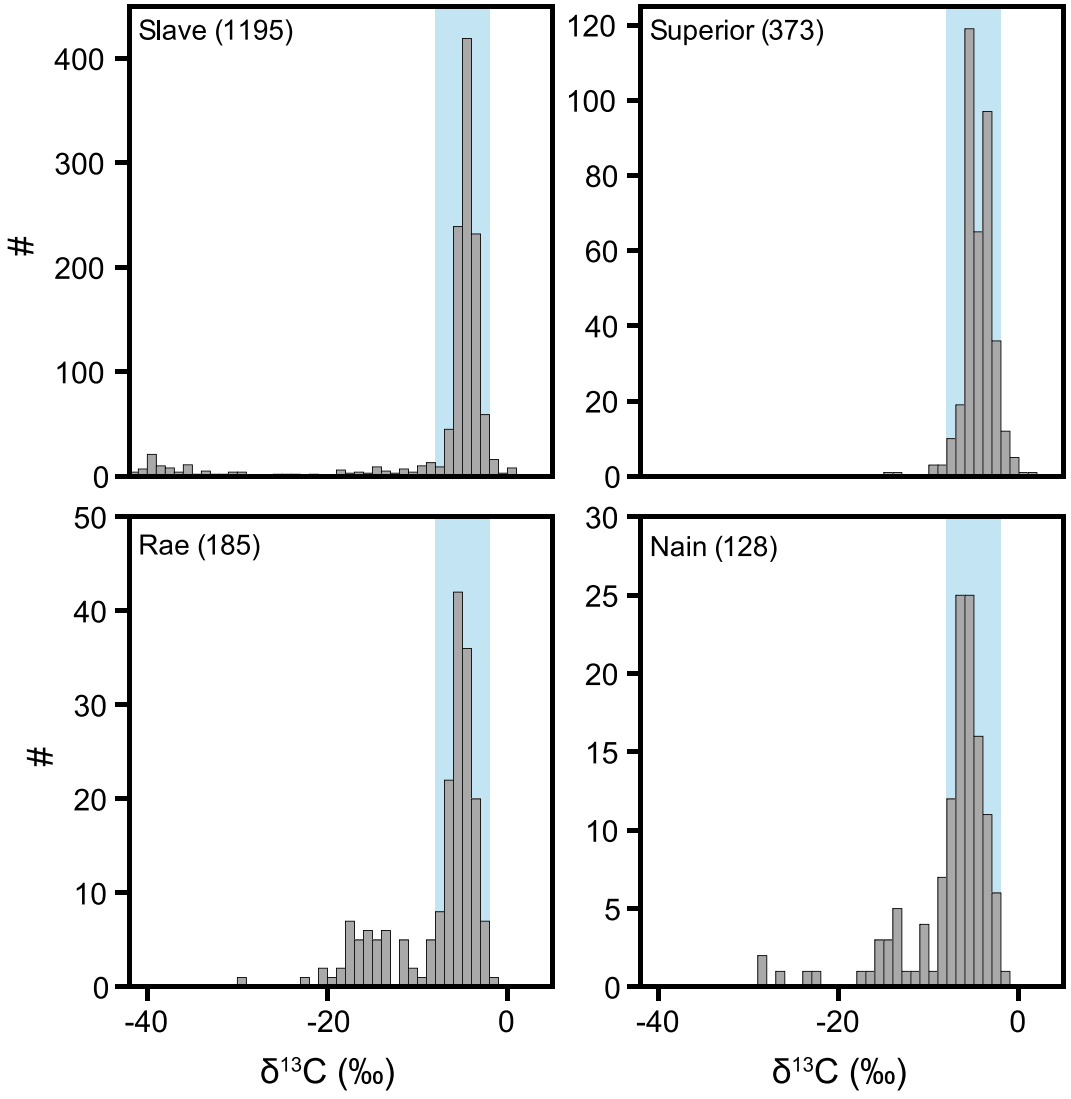

Fig. 31. $\delta^{13}C$ distribution for diamonds from the Slave, Superior, Rae and Nain cratons. The bin size is 1‰. The shaded, light-blue area between −8‰ and − 2‰ represents the main mantle range indicated by Cartigny (2005).

mantle range (Fig. 31). This is due to the predominance of peridotitic diamonds from the Superior craton that typically show narrow $\delta^{13}C$ ranges around the mantle average (Stachel et al., 2022b). The average $\delta^{13}C$ for Superior diamonds is −4.5‰, the mode is at −5.2‰ and the median is at −4.7‰, in good agreement with an almost pure peridotitic suite (Stachel et al., 2022a).

Aulbach et al. (2018) used Re—Os geochronology applied to peridotitic sulfide inclusions from the Victor Mine to calculate a very young diamond formation age of 718 ± 49 Ma. Moreover, Smit et al. (2014) inferred a young age for diamonds from the U2 kimberlite based on consideration of N thermochronometric data and knowledge of the paleogeotherm of the area.

Thermobarometric calculations performed on mineral inclusions in diamonds from the Superior Craton show average pressures and temperatures of formation of 6.3 GPa and 1190 °C, respectively.

3.8.3. Rae

Only 9% (270) of the diamonds in this database are from the Rae craton, and 255 of these have been analyzed for their N content. The abundances of Type I (84.7%) and Type II (15.3%) diamonds are consistent with the entire Canadian database. The median N content is 326 at.ppm, in good agreement with the total database, 33% of diamonds are Type IaA, 40% are Type IaAB and 27% are Type IaB. The high abundance of Type IaB diamonds could be due to residence in the mantle either at a high temperature or for a long time.

No data regarding the N isotopic composition of diamonds from Rae is reported in the literature.

Very few diamonds from the Rae craton (only 36) have mineral inclusions upon which a paragenesis can be determined. Among diamonds from the Rae craton, 4 (11.1%) are from a sub-lithospheric environment. However, this relatively high proportion of sub-lithospheric diamonds compared to lithospheric diamonds is not statistically meaningful given the extremely small size of the dataset. It is important to note that some diamonds (24 samples) with a low N content (<50 at.ppm) shows a high N aggregation state (%B >90). This, as stated above (section 3.2) is not a proof of the sub-lithospheric origin but may support a relatively high number of sub-lithospheric diamonds from the Rae craton.

Based on the available data for diamonds from the Rae craton, a 1:1 peridotitic:eclogitic ratio is observed, with 47% eclogitic and 53% peridotitic diamonds. Two websteritic diamonds are observed from the Rae craton.

The $\delta^{13}C$ values for 185 diamonds from the Rae craton show a range in $\delta^{13}C$ from −29.7‰ to −1.7‰, with an average of −7.7‰, a mode at −5.1‰, and the median at −5.7‰ (Fig. 31). Of these diamonds, 72.4% have values that fall within the mantle range. The relatively low percent of diamonds in accord with the $\delta^{13}C$ mantle range (compared to Slave and Superior cratons, and with the full database) may suggest that the high abundance of eclogitic diamonds observed from mineral inclusions is possibly representative for the Rae craton. Nevertheless, new analyses are needed to understand whether the relatively abundance of eclogitic diamonds observed in the Rae craton is real or an artifact of the small dataset.

3.8.4. Nain

A very limited number of specimens (143), constituting 4% of the diamonds in this work, were collected in the Nain craton. All diamonds were analyzed for their N content and only 4.2% were classified as Type II, the other 95.3% are Type I. Nain diamonds show a very high N content, with a median value of 1295 at.ppm and a maximum value of 3171 at.ppm, which is one of the highest values in this study. The N content of most diamonds has been analyzed by SIMS, and therefore a limited number of data regarding the aggregation state of N is available. Moreover, these data were collected on fibrous diamonds that show low degrees of N aggregation and cannot be assumed as representative of the entire diamond population.

No information regarding the paragenesis of Nain diamonds are available, as no mineral inclusions are reported in the literature.

A total of 128 diamonds from Nain have been analyzed for their C isotopic composition. A range of $\delta^{13}C$ from −28.4‰ to −1.9‰ is observed with 74.2% of the diamonds having $\delta^{13}C$ values in the mantle range (Fig. 31). The average $\delta^{13}C$ for Nain diamonds is −7.6‰, the mode is at −5.7‰, and the median is −6.1‰. This data possibly suggest a prevalence of eclogitic diamonds, similar to what is observed in the Rae craton, but this can only be confirmed by including more data for diamonds with mineral inclusions from the Nain craton.

4. Conclusions

The Canadian Shield is composed of different cratonic cores that, based on the studied samples, exhibit significant differences in their petrology and geochemistry. On average the cratonic lithosphere beneath Canada comprises 64.3% peridotite, 34.8% eclogite, and a very small amount of websterite. Without considering the Nain and Rae cratons, for which data from mineral inclusions in diamonds are not available or very scarce, the Slave and Superior cratons present very different petrological characteristics. The former has a harzburgitic-lherzolitic ratio in agreement with the global database (Stachel et al., 2022b) and a higher-than-average abundance of eclogitic inclusions. The latter shows a very small number of eclogitic inclusions, and a higher-than-average abundance of lherzolitic diamonds. Despite these differences, thermobarometric calculations show similar thermal conditions between the two cratons. The average diamond formation temperatures and pressures from mineral inclusions are 1185 °C, 5.6 GPa and 1190 °C, 6.3 GPa for Slave and Superior cratons, respectively.

A comparison of geothermometric data from mineral inclusions and N aggregation states suggests that Canadian diamonds formed at temperatures higher than their residence temperature, as large discrepancies between the diamond formation temperatures and the residence temperatures are observed. These differences could be due to diamonds forming during short-lived positive thermal anomalies, or to diamonds being transported to lower depths (and therefore lower temperatures) after their formation.

Eclogitic and peridotitic diamonds show similar thermobarometric data, supporting the model developed by Helmstaedt and Schulze (1989), and later used by Stachel and Harris (2008) for the formation of cratons by the imbrication of oceanic lithosphere below early cratonic cores. This model is further supported by the C isotopic signature of eclogitic diamonds combined with their N content, and by the bulk rock REE_N composition calculated from eclogitic garnets and clinopyroxenes that is similar to a N-MORB depleted in LREE. This data suggests eclogitic diamonds form from subducted oceanic crust, a model that has also been recently confirmed for the Slave craton based on geothermometric data from diamonds found in a sedimentary deposit (Timmerman et al., 2022).

Sub-lithospheric Canadian diamonds form throughout the entire sub-lithospheric mantle, from the deep upper mantle to the lower mantle as indicated by the presence of inclusions such as breyite and former bridgmanite associated with ferropericlase, indicative of a lower mantle origin. The pressure of formation of sub-lithospheric diamonds calculated using majoritic garnets ranges from 8.6 to 18.5 GPa, with most of them (88.5%) forming at pressures <17 GPa, in the deep upper mantle or in the shallow transition zone. However, these pressure data represent only the diamonds with majoritic garnet inclusions as diamonds with inclusions of former bridgmanite ± breyite ± ferropericlase form at higher pressures in the lower mantle (>22 GPa), although geobarometric methods to estimate the pressure of formation of these diamonds are not available.

Diamond formation in the Slave craton is linked to pervasive metasomatic events by a C-O-H oxidizing fluid (Creighton et al., 2010). Differences in the formation ages of diamonds from this craton (>1 Ga difference in the ages of peridotitic and eclogitic diamonds) suggests that more than a single diamond forming event occurred. Peridotitic

diamond formation has been linked to the formation of the earliest cratonic nucleus by imbrication. Eclogitic diamonds instead may have formed from later subduction events linked to a series of Proterozoic collisions that built the larger present-day Slave craton (Timmerman et al., 2022). In this picture, sub-lithospheric diamonds would have been transported to the cratonic lithosphere by plume upwelling after the Craton formed.

The Superior craton is also characterized by multiple diamond forming events, only one young set of diamonds has been dated from this craton, but the presence of diamonds in the Wawa metaconglomerate (dated 2.7 Ga, Wyman et al., 2002) suggests at least one diamond forming event preceding this younger diamond growth pulse. The oldest diamond formation event took place before the cratonization of the Superior province (Stachel et al., 2006). Subsequently, the Mid-continental Rift at 1.1 Ga imposed a hotter geotherm, leading to a thinning of the lithosphere (which was reduced to a maximum thickness of ~180 km) and creating a narrow diamond window (Stachel et al., 2018). Later, after thermal relaxation (and therefore thickening) of the lithosphere, volatile-rich, oxidized fluid/melts were mobilized by the ~720 Ma Rodinia breakup. These fluids infiltrated in the cratonic lithosphere, leading to refertilization and formation of the young lherzolitic diamonds from Victor in a layer correspondent to the base of the lithosphere during the Midcontinental Rift (Stachel et al., 2018; Aulbach et al., 2018).

Funding

DN thanks the Rita Levi Montalcini program for support. Open access funding provided by Università degli Studi di Padova within the CRUI-CARE Agreement. This work was funded by the European Union (ERC, INHERIT, starting Grant No. 101041620). Views and opinions expressed are, however, those of the author(s) only and do not necessarily reflect those of the European Union or the European Research Council Executive Agency. Neither the European Union nor the granting authority can be held responsible for them. MGP thanks the European Union's Horizon 2020 research and innovation program (Marie Skłodowska-Curie grant no. 796755).

CRediT authorship contribution statement

Andrea Curtolo: Conceptualization, Data curation, Formal analysis, Investigation, Visualization, Writing – original draft. **Davide Novella:** Conceptualization, Supervision, Writing – review & editing. **Alla Logvinova:** Resources, Writing – review & editing. **Nikolay V. Sobolev:** Resources. **Rondi M. Davies:** Resources, Writing – review & editing. **Maxwell C. Day:** Writing – review & editing. **Martha G. Pamato:** Writing – review & editing. **Fabrizio Nestola:** Conceptualization, Supervision, Writing – review & editing.

Declaration of Competing Interest

The authors declare that they have no known competing financial interests or personal relationships that could have appeared to influence the work reported in this paper.

Data availability

Data will be made available on request.

References

Aulbach, S., Stachel, T., Creaser, R.A., Heaman, L.M., Shirey, S.B., Muehlenbachs, K., Eichenberg, D., Harris, J.W., 2009. Sulphide survival and diamond genesis during formation and evolution of Archaean subcontinental lithosphere: a comparison between the Slave and Kaapvaal craton. Lithos 112S, 747–757.

Aulbach, S., Stachel, T., Seitz, H.-M., Brey, G.P., 2012. Chalcophile and siderophile elements in Sulphide inclusions in eclogitic diamonds and metal cycling in a Paleoproterozoic subduction zone. Geochim. Cosmochim. Acta 93, 278–299.

Aulbach, S., Creaser, R.A., Stachel, T., Heaman, L.M., Chinn, I.L., Kong, J., 2018. Diamond ages from Victor (Superior Craton): Intra-mantle cycling of volatiles (C, N, S) during supercontinent reorganization. Earth Planet. Sci. Lett. 490, 77–87.

Aulbach, S., Viljoen, K.S., Gerdes, A., 2020a. Diamondiferous and barren eclogites and pyroxenites from the western Kaapvaal craton record subduction processes and mantle metasomatism, respectively. Lithos 368–369, 105588.

Aulbach, S., Massuyeau, M., Garber, J.M., Gerdes, A., Heaman, L.M., Viljoen, K.S., 2020b. Ultramafic carbonated melt- and auto-metasomatism in mantle eclogites: compositional effects and geophysical consequences. Geochem. Geophys. Geosyst. 21 (5) e2019GC008774.

Banas, A., Stachel, T., Muehlenbachs, K., McCandless, T.E., 2007. Diamonds from the Buffalo Head Hills, Alberta: Formation in a non-conventional setting. Lithos 93, 199–213.

Brey, G.P., Köhler, T., 1990. Geothermobarometry in four-phase lherzolites II. New thermobarometers and practical assessment of existing thermobarometers. J. Petrol. 31 (6), 1353–1378.

Brown, T.J., Idoine, N.E., Wrighton, C.E., Raycraft, E.R., Hobbs, S.F., Shaw, R.A., Everett, P., Deady, E.A., Kresse, C., 2021. World Mineral Production, 2015–2019. British Geological Survey, Keyworth, Nottingham.

Bruce, L.F., Kopylova, M.G., Longo, M., Ryder, J., Dobrzhinetskaya, L.F., 2011. Luminescence of diamonds from metamorphic rocks. Am. Mineral. 96 (1), 14–22.

Bulanova, G.P., 1995. The formation of diamond. J. Geochem. Explor. 53, 1–23.

Bulanova, G.P., Griffin, W.L., Ryan, C.G., Shestakova, O.Ye., Barnes, S.-J., 1996. Trace elements in sulfide inclusions from Yakutian diamonds. Contrib. Mineral. Petrol. 124, 111–125.

Burgess, R., Cartigny, P., Harrison, D., Hobson, E., Harris, J.W., 2009. Volatile composition of microinclusions in diamonds from the Panda kimberlite, Canada: implications for chemical and isotopic heterogeneity in the mantle. Geochim. Cosmochim. Acta 73, 1779–1794.

Bussweiler, Y., Brey, G.P., Pearson, D.G., Stachel, T., Stern, R.A., Hardman, M.F., Kjarsgaard, B.A., Jackson, S.E., 2017. The aluminium-in-olivine thermometer for mantle peridotites – experimental versus empirical calibration and potential applications. Lithos 272–273, 301–314.

Cartigny, P., Harris, J.W., Javoy, M., 2001. Diamond genesis, mantle fractionation and mantle nitrogen content: a study of δ13C-N concentrations in diamonds. Earth Planet. Sci. Lett. 185, 85–98.

Cartigny, P., 2005. Stable isotopes and the origin of diamond. Elements 1, 79–84.

Cartigny, P., Farquhar, J., Thomassot, E., Harris, J.W., Wing, B., Masterson, A., McKeegan, K., Stachel, T., 2009. A mantle origin for Paleoarchean peridotitic diamonds from the Panda kimberlite, Slave Craton: evidence from 13C-, 15N-, and 33,34S-stable isotope systematics. Lithos 112S, 852–864.

Cartigny, P., Marty, B., 2013. Nitrogen isotopes and mantle geodynamics: the emergence of life and the atmosphere-crust-mantle connection. Elements 9 (5), 359–366.

Cartigny, P., Palot, M., Thomassot, E., Harris, J.W., 2014. Diamond formation: a stable isotope perspective. Annu. Rev. Earth Planet. Sci. 42, 699–732.

Chinn, I.L., Perrit, S.H., Stiefenhofer, J., Stern, R.A., 2018. Diamonds from Orapa Mine show a clear subduction signature in SIMS stable isotope data. Mineral. Petrol. 112, S197–S207.

Clifford, T.N., 1966. Tectono-metallogenic units and metallogenic provinces of Africa. Earth Planet. Sci. Lett. 1, 421–434.

Craig, H., 1957. Isotopic standards for carbon and oxygen and correction factors for mass-spectrometric analysis of carbon dioxide. Geochim. Cosmochim. Acta 12, 133–149.

Creighton, S., Stachel, T., McLean, H., Muehlenbachs, K., Simonetti, A., Eichenberg, D., Luth, R., 2008. Diamondiferous peridotitic microxenoliths from the Diavik Diamond Mine, NT. Contrib. Mineral. Petrol. 155, 541–554.

Creighton, S., Stachel, T., Eichenberg, D., Luth, R.W., 2010. Oxidation state of the lithospheric mantle beneath Diavik diamond mine, central Slave craton, NWT, Canada. Contrib. Mineral. Petrol. 159, 645–657.

Czas, J., Pearson, D.G., Stachel, T., Kjarsgaard, B.A., Read, G.H., 2020. A Palaeoproterozoic diamond-bearing lithospheric mantle root beneath the Archean Sask Craton, Canada. Lithos 356–357, 105301.

Davies, R., Griffin, W., Pearson, N., Andrew, A., Doyle, B., O'Reilly, S., 1998. Diamonds from the deep: Pipe DO-27, Slave Craton,Canada. International Kimberlite Conference: Extended Abstracts 7 (1), 170–172.

Davies, R.M., Griffin, W.L., O'Reilly, S.Y., McCandless, T.E., 2004a. Inclusions in diamonds from the K14 and K10 kimberlites, Buffalo Hills, Alberta, Canada: diamond growth in a plume? Lithos 77, 99–111.

Davies, R.M., Griffin, W.L., O'Reilly, S.Y., Doyle, B.J., 2004b. Mineral inclusions and geochemical characteristics of microdiamonds from the DO27, A154, A21, A418, DO18, DD17 and Ranch Lake kimberlites at Lac de Gras, Slave Craton, Canada. Lithos 77, 39–55.

Day, H.W., 2012. A revised diamond-graphite transition curve. Am. Mineral. 97, 52–62.

De Stefano, A., Lefebvre, N., Kopylova, M., 2006. Enigmatic diamonds in Archean calc-alkaline lamprophyres of Wawa, southern Ontario, Canada. Contrib. Mineral. Petrol. 151, 158–173.

De Stefano, A., Kopylova, M.G., Cartigny, P., Afanasiev, V., 2009. Diamonds and eclogites of the Jericho kimberlite (Northern Canada). Contrib. Mineral. Petrol. 158, 295–315.

Deines, P., 1980. The carbon isotopic composition of diamonds: relationship to diamond shape, color, occurrence and vapor composition. Geochim. Cosmochim. Acta 44, 943–961.

Deines, P., Harris, J.W., Gurney, J.J., 1993. Depth-related carbon isotope and nitrogen concentration variability in the mantle below the Orapa kimberlite, Botswana, Africa. Geochim. Cosmochim. Acta 57, 2781–2796.
Deines, P., Harris, J.W., 1995. Sulfide inclusion chemistry and carbon isotopes of african diamonds. Geochim. Cosmochim. Acta 59 (15), 3173–3188.
Donnelly, C.L., Stachel, T., Creighton, S., Muehlenbachs, K., Whiteford, S., 2007. Diamonds and their mineral inclusions from the A154 South pipe, Diavik Diamond Mine, Northwest territories, Canada. Lithos 98, 160–176.
Doroshev, A.M., Brey, G.P., Girnis, A.V., Turkin, A.I., Kogarko, L.N., 1997. Pyrope-knorringite garnets in the Earth's upper mantle: experiments in the MgO-Al2O3-SiO2-Cr2O3 system. Russ. Geol. Geophys. 38, 559–586.
Droop, G.T.R., 1987. A general equation for estimating Fe3+ in ferromagnesian silicates and oxides from microprobe analyses, using stoichiometric criteria. Mineral. Mag. 51, 431–435.
Dyer, H.B., Raal, F.A., Du Preez, L., Loubser, J.H.N., 1965. Optical absorption features associated with paramagnetic nitrogen in diamond. Philos. Mag. 11 (112), 763–774.
Eeken, T., Goes, S., Petrescu, L., Altoe, I., 2020. Lateral variations in thermochemical structure of the Eastern Canadian Shield. Journal of Geophysical Research: SolidEarth 125 (7) e2019JB018734.
Elazar, O., Grütter, H.S., Weiss, Y., 2022. The a B C's of metasomatism in the North Atlantic Craton during Pangea breakup; characterized by fluid inclusions in Chidliak diamonds. Lithos 422–423, 106725.
Evans, T., Harris, J.W., 1986. Nitrogen aggregation, inclusion equilibration temperatures and the age of diamonds. International Kimberlite Conference: Extended Abstracts 4 (1), 386–388.
Fedortchouk, Y., Zhang, Z., 2011. Diamond resorption: link to metasomatic events in the mantle or record of magmatic fluid in kimberlitic magma? Can. Mineral. 49, 707–719.
Gale, A., Dalton, C.A., Langmuir, C.H., Su, Y., Schilling, J.-G., 2013. The mean composition of ocean ridge basalt. Geochem. Geophys. Geosyst. 14 (3), 489–518.
Garber, J.M., Maurya, S., Hernandez, J.-A., Duncan, M.S., Zeng, L., Zhang, H.L., Faul, U., McCammon, C., Montagner, J.-P., Moresi, L., Romanowicz, B.A., Rudnick, R.L., Stixrude, L., 2018. Multidisciplinary constraints on the abundance of diamond and eclogite in the cratonic lithosphere. Geochem. Geophys. Geosyst. 19 (7), 2062–2086.
Green, B.L., Collins, A.T., Breeding, C.M., 2022. Diamond spectroscopy, defect centers, color, and treatments. In: Smit, K., Shirey, S., Pearson, G., Stachel, T., Nestola, F., Moses, T. (Eds.), Diamond: Genesis, Mineralogy and Geochemistry. Mineralogical Society of America, Chantilly, pp. 637–688.
Gress, M.U., Timmerman, S., Chinn, I.L., Koornneef, J.M., Thomassot, E., van der Valk, E. A.S., van Zuilen, K., Bouden, N., Davies, G.R., 2021. Two billion years of episodic and simultaneous websteritic and eclogitic diamond formation beneath the Orapa kimberlite cluster,Botswana. Contrib. Mineral. Petrol. 176, 54.
Griffin, W.L., Doyle, B.J., Ryan, C.G., Pearson, N.J., O'Reilly, S.Y., Davies, R., Kivi, K., Van Achterbergh, E., Natapov, L.M., 1999. Layered mantle lithosphere in the Lac de Gras area, Slave Craton: composition, structure and origin. J. Petrol. 40 (5), 705–727.
Grütter, H.S., Gurney, J.J., Menzies, A.H., Winter, F., 2004. An updated classification scheme for mantle-derived garnet, for use by diamond explorers. Lithos 77, 841–857.
Harris, J.W., 1987. Recent physical, chemical, and isotopic research of diamond. In: Nixon, P.H. (Ed.), Mantle Xenoliths. John Wiley & Sons Ltd., Chichester, pp. 477–500.
Harris, J.W., Duncan, D.J., Zhang, F., Mia, Q., Zhu, Y., 1991. The physical characteristics and syngenetic inclusion geochemistry of diamonds from Pipe 50, Liaoning province, People's Republic of China. International Kimberlite Conference: Extended Abstracts 5, 160–162.
Harris, G.A., Pearson, D.G., Liu, J., Hardman, M.F., Snyder, D.B., Kelsch, D., 2018. Mantle composition, age and geotherm beneath the Darby kimberlite field, west central Rae Craton. Mineral. Petrol. 122 (S1), S57–S70.
Harte, B., 2010. Diamond formation in the deep mantle: the record of mineral inclusions and their distribution in relation to mantle dehydration zones. Mineral. Mag. 74 (2), 189–215.
Hasterok, D., Chapman, D.S., 2011. Heat production and geotherms for the continental lithosphere. Earth Planet. Sci. Lett. 307, 59–70.
Hayman, P.C., Kopylova, M.G., Kaminsky, F.V., 2005. Lower mantle diamonds from Rio Soriso (Juina area, Mato Grosso, Brazil). Contrib. Mineral. Petrol. 149, 430–445.
Heaman, L.M., Philips, D., Pearson, D.G., 2019. Dating kimberlites: methods and emplacement patterns through time. Elements 15 (6), 399–404.
Helmstaedt, H., Schulze, D.J., 1989. Southern African kimberlites and their mantle sample: implications for Archaean tectonics and lithosphere evolution. In: Ross, J., Jaques, A.L., Ferguson, J., Green, D.H., O'Reilly, S.Y., Danchin, R.V., Janse, A.J.A. (Eds.), Kimberlites and Related ROCKS. Geological Society of Australia Special Publications 14. Blackwell, Carlton, pp. 358–368.
Helmstaedt, H., Pehrsson, S.J., Stubley, M.P., 2021. GAC special Paper 51: the Slave Province, Canada. Geological Evolution of a Archean Diamondiferous Craton. Geological Association of Canada, St. John's.
Hoffman, P.F., 1988. United Plates of America, the birth of a craton: early proterozoic assembly and growth of Laurentia. Annu. Rev. Earth Planet. Sci. 16, 543–603.
Hogberg, K., Stachel, T., Stern, R.A., 2016. Carbon and nitrogen isotope systematics in diamond: different sensitivities to isotopic fractionation or a decoupled origin? Lithos 265, 16–30.
Howell, D., Stachel, T., Stern, R.A., Pearson, D.G., Nestola, F., Hardman, M.F., Harris, J. W., Jaques, A.L., Shirey, S.B., Cartigny, P., Smit, K.V., Aulbach, S., Brenker, F.E., Jacob, D.E., Thomassot, E., Walter, M.J., Navon, O., 2020. Deep carbon through time: Earth's diamond record and its implications for carbon cycling and fluid speciation in the mantle. Geochim. Cosmochim. Acta 275, 99–122.
Hunt, L., Stachel, T., McCandless, T.E., Armstrong, J., Muehlenbachs, K., 2012. Diamonds and their mineral inclusions from the Renard kimberlites in Quebec. Lithos 142–143, 267–284.
Hutchinson, M.T., Cartigny, P., Harris, J.W., 1998. Carbon and nitrogen compositions and physical characteristics of transition zone and lower mantle diamonds from São Luiz,Brazil. International Kimberlite Conference: Extended Abstracts 7 (1), 336–338.
Ivanova, O.A., Logvinova, A.M., Pokhilenko, N.P., 2017. Inclusions in diamonds from Snap Lake kimberlites (Slave Craton, Canada): geochemical features of crystallization. Dokl. Earth Sci. 474 (1), 490–493.
Johnson, C.N., Stachel, T., Muehlenbachs, K., Stern, R.A., Armstrong, J.P., EIMF, 2012. The micro-/macro-diamond relationship: a case study from the Artemisia kimberlite (Northern Slave Craton, Canada). Lithos 148, 86–97.
Kaminsky, F.V., Khachatryan, G.K., 2001. Characteristics of nitrogen and other impurities in diamond, as revealed by infrared absorption data. Can. Mineral. 39, 1733–1745.
Kirkley, M.B., Gurney, J.J., Otter, M.L., Hill, S.J., Daniels, L.R., 1991. The application of C isotope measurements to the identification of the sources of C in diamonds: a review. Appl. Geochem. 6, 477–494.
Klein-BenDavid, O., Izraeli, E.S., Hauri, E., Navon, O., 2007. Fluid inclusions in diamonds from the Diavik mine, Canada and the evolution of diamond-forming fluids. Geochim. Cosmochim. Acta 71, 723–744.
Klemme, S., 2004. The influence of Cr on the garnet-spinel transition in the Earth's mantle: experiments in the system MgO-Cr2O3-SiO2 and thermodynamic modelling. Lithos 77, 639–646.
Kopylova, M.G., Caro, G., 2004. Mantle xenoliths from the Southeastern Slave craton: evidence for chemical zonation in a thick, cold lithosphere. J. Petrol. 45 (5), 1045–1067.
Krebs, M.Y., Pearson, D.G., Stachel, T., Stern, R.A., Nowicki, T., Cairns, S., 2016. Using microdiamonds in kimberlite diamond grade prediction: a case study of the variability in diamond population characteristics across the size range 0.2 to 3.4 mm in misery kimberlite, Ekati Mine, NWT,Canada. Econ. Geol. 111, 503–525.
Krebs, M.Y., Pearson, D.G., Stachel, T., Laiginhas, F., Woodland, S., Chinn, I., Kong, J., 2019. A common parentage-low abundance trace element data of gem diamonds reveals similar fluids to fibrous diamonds. Lithos 324–325, 356–370.
Krogh, E.J., 1988. The garnet-clinopyroxene Fe-Mg geothermometer – a reinterpretation of existing experimental data. Contrib. Mineral. Petrol. 99, 44–48.
Kueter, N., Schmidt, M.W., Lilley, M.D., Bernasconi, S.M., 2020. Kinetic carbon isotope fractionation links graphite and diamond precipitation to reduced fluid sources. Earth Planet. Sci. Lett. 529, 115848.
Lai, M.Y., Stachel, T., Breeding, C.M., Stern, R.A., 2020. Yellow diamonds with colourless cores – evidence for episodic diamond growth beneath Chidliak and the Ekati Mine, Canada. Mineral. Petrol. 114, 91–103.
Li, K., Li, L., Pearson, D.G., Stachel, T., 2019. Diamond isotope compositions indicate altered igneous oceanic crust dominates deep carbon recycling. Earth Planet. Sci. Lett. 516, 190–201.
Li, Z., Fedortchouk, Y., Fulop, A., Chinn, I.L., Forbes, N., 2018. Positively oriented trigons on diamonds from the Snap Lake kimberlite dike, Canada: implications for fluids and kimberlite cooling rates. Am. Mineral. 103, 1634–1648.
Lorenzon, S., Wenz, M., Nimis, P., Jacobsen, S.D., Paqualetto, L., Pamato, M.G., Novella, D., Zhang, D., Anzolini, C., Regier, M., Stachel, T., Pearson, D.G., Harris, J. W., Nestola, F., 2023. Dual origin of ferropericlase inclusions within super-deep diamonds. Earth Planet. Sci. Lett. 608, 118081.
Mariotti, A., 1984. Natural 15N abundance measurements and atmospheric nitrogen standard calibration. Nature 311 (5983), 251–252.
McDonough, W.F., Sun, S.-S., 1995. The composition of the Earth. Chem. Geol. 120, 223–253.
Melton, G.L., Stachel, T., Stern, R.A., Carlson, J., Harris, J.W., 2013. Infrared spectral and carbon isotpic characteristics of micro- and macro-diamonds from the Panda kimberlite (Central Slave Craton, Canada). Lithos 177, 110–119.
Meyer, H.O.A., Boyd, F.R., 1972. Composition and origin of crystalline inclusions in natural diamonds. Geochim. Cosmochim. Acta 36, 1255–1273.
Meyer, H.O.A., 1987. Inclusions in diamond. In: Nixon, P.H. (Ed.), Mantle Xenoliths. John Wiley & Sons Ltd., Chichester, pp. 501–522.
Mikhail, S., Howell, D., 2016. A petrological assessment of diamond as a recorder of the mantle nitrogen cycle. Am. Mineral. 101, 780–787.
Milledge, H.J., Mendelssohn, M.J., Seal, M., Rouse, J.E., Swart, P.K., Pillinger, C.T., 1983. Carbon isotopic variation in spectral type II diamonds. Nature 303, 791–792.
Miller, C.E., Kopylova, M.G., Ryder, J., 2012. Vanished diamondiferous cratonic root beneath the Southern Superior province: evidence from diamond inclusions in the Wawa metaconglomerate. Contrib. Mineral. Petrol. 164, 697–714.
Mints, M.V., 2017. The composite north American Craton, Superior Province: Deep Crustal structure and mantle-plume model of Neoarchaean evolution. Precambrian Res. 302, 94–121.
Moore, A., Helmstaedt, H., 2023. Origin of framesite revisited: possible implications for the formation of CLIPPIR diamonds. Earth Sci. Rev. 241, 104434.
Navon, O., 1999. Diamond Formation in the Earth's Mantle. In: Gurney, J.J., Gurney, J. L., Pascoe, M.D., Richardson, S.H. (Eds.), Proceedings of the VIIth International Kimberlite Conference, vol. 2.. Red Roof Design cc, Cape Town, pp. 584–604.
Nestola, F., Merli, M., Nimis, P., Parisatto, M., Kopylova, M., De Stefano, A., Longo, M., Ziberna, L., Manghnani, M., 2012. In situ analysis of garnet inclusion in diamond using single-crystal X-ray diffraction and X-ray micro-tomography. Eur. J. Mineral. 24, 599–606.
Nestola, F., Jung, H., Taylor, L.A., 2017. Mineral inclusions in diamonds may be synchronous but not syngenetic. Nat. Commun. 8, 14168.

Nestola, F., Jacob, D.E., Pamato, M.G., Paqualetto, L., Oliveira, B., Greene, S., Perrit, S., Chinn, I., Milani, S., Kueter, N., Sgreva, N., Nimis, P., Secco, L., Harris, J.W., 2019. Protogenetic garnet inclusions and the age of diamonds. Geology 47 (5), 431–434.
Nickel, K.G., Green, D.H., 1985. Empirical geothermobarometry for garnet peridotites and implications for the nature of the lithosphere, kimberlites and diamonds. Earth Planet. Sci. Lett. 73, 158–170.
Nimis, P., Taylor, W.R., 2000. Single clinopyroxene thermobarometry for garnet peridotites. Part I. Calibration and testing of a Cr-in-Cpx barometer and an enstatite-in-Cpx thermometer. Contrib. Mineral. Petrol. 139, 541–554.
Nimis, P., Grütter, H., 2010. Internally consistent geothermometers for garnet peridotites and pyroxenites. Contrib. Mineral. Petrol. 159, 411–427.
Nimis, P., Preston, R., Perritt, S.H., Chinn, I.L., 2020. Diamond's depth distribution systematics. Lithos 376–377, 105729.
Nimis, P., 2022. Pressure and temperature data for diamonds. In: Smit, K., Shirey, S., Pearson, G., Stachel, T., Nestola, F., Moses, T. (Eds.), Diamond: Genesis, Mineralogy and Geochemistry. Mineralogical Society of America, Chantilly, pp. 533–565.
O'Hara, M.J., Richardson, S.W., Wilson, G., 1971. Garnet-peridotite stability and occurrence in crust and mantle. Contrib. Mineral. Petrol. 32, 48–68.
O'Neill, H.St.C., 1981. The transition between spinel lherzolite and garnet lherzolite, and its use as a geobaromether. Contrib. Mineral. Petrol. 77, 185–194.
Pamato, M.G., Novella, D., Jacob, D.E., Oliveira, B., Pearson, D.G., Greene, S., Afonso, J. C., Favero, M., Stachel, T., Alvaro, M., Nestola, F., 2021. Protogenetic sulfide inclusions in diamonds date the diamond formation event using Re-Os isotopes. Geology 49, 941–945.
Pasqualetto, L., Nestola, F., Jacob, D.E., Pamato, M.G., Oliveira, B., Perritt, S., Chinn, I., Nimis, P., Milani, S., Harris, J.W., 2022. Protogenetic clinopyroxene inclusions in diamond and Nd diffusion modeling - implications for diamond dating. Geology 50 (9), 1038–1042.
Pearson, D.G., Shirey, S.B., Harris, J.W., Carlson, R.W., 1998. Sulphide inclusions in diamonds from the Koffiefontein kimberlite, S Africa: constraints on diamond ages and mantle Re-Os systematics. Earth Planet. Sci. Lett. 160, 311–326.
Pearson, D.G., Shirey, S.B., 1999. Isotopic dating of diamonds. In: Lambert, D.D., Brown, P.E. (Eds.), Applications of Radiogenic Isotopes to Ore Deposit Research and Exploration. Reviews in Economic Geology 12, pp. 143–171.
Pearson, D.G., Shirey, S.B., Bulanova, G.P., Carlson, R.W., Milledge, H.J., 1999. Re-Os isotope measurements of single sulfide inclusions in a Siberian diamond and its nitrogen aggregation systematics. Geochim. Cosmochim. Acta 63 (5), 703–711.
Pearson, D.G., Canil, D., Shirey, S.B., 2003. Mantle samples included in volcanic rocks: Xenoliths and diamonds. In: Turekian, K.K., Holland, H.D. (Eds.), The Mantle and Core. Treatise on Geochemistry 2, pp. 171–275.
Pearson, D.G., Scott, J.M., Liu, J., Schaeffer, A., Wang, L.H., van Hunen, J., Szilas, K., Chacko, T., Kelemen, P.B., 2021. Deep continental roots and cratons. Nature 596, 199–210.
Peats, J., Stachel, T., Stern, R.A., Muehlenbachs, K., Armstrong, J., 2012. Aviat diamonds: a window into the deep lithospheric mantle beneath the Northern Churchill province, Melville peninsula, Canada. Can. Mineral. 50, 611–624.
Pedregosa, F., Varoquaux, G., Gramfort, A., Michel, V., Thirion, B.V., Grisel, O., Blondel, M., Prettenhofer, P., Weiss, R., Dubourg, V., Vanderplas, J., Passos, A., Cournapeau, D., Brucher, M., Perrot, M., Duchesnay, É., 2011. Scikit-learn: machine learning in python. J. Mach. Learn. Res. 12, 2825–2830.
Petts, D.C., Chacko, T., Stachel, T., Stern, R.A., Heaman, L.M., 2015. A nitrogen isotope fractionation factor between diamond and its parental fluid derived from detailed SIMS analysis of a gem diamond and theoretical calculations. Chem. Geol. 410, 188–200.
Petts, D.C., Stachel, T., Stern, R.A., Hunt, L., Fomradas, G., 2016. Multiple carbon and nitrogen sources associated with the parental mantle fluids of fibrous diamonds from Diavik, Canada, revealed by SIMS microanalysis. Contrib. Mineral. Petrol. 171, 17.
Pokhilenko, N.P., Sobolev, N.V., McDonald, J.A., Hall, A.E., Yefimova, E.S., Zedgenizov, D.A., Logvinova, A.M., Reimers, L.F., 2001. Crystalline inclusions in diamonds from kimberlites of the Snap Lake area (Slave craton, Canada): new evidence for the anomalous lithospheric structure. Dokl. Earth Sci. 380 (7), 806–811.
Pokhilenko, N.P., Sobolev, N.V., Reutsky, V.N., Hall, A.E., Taylor, L.A., 2004. Crystalline inclusions and C isotope ratios in diamonds from the Snap Lake/King Lake kimberlite dyke system; evidence of ultradeep and enriched lithospheric mantle. Lithos 77, 57–67.
Promprated, P., Taylor, L.A., Anand, M., Floss, C., Sobolev, N.V., Pokhilenko, N.P., 2004. Multiple-mineral inclusions in diamonds from the Snap Lake/King Lake kimberlite dike, Slave craton, Canada: a trace-element perspective. Lithos 77, 69–81.
Reutsky, V.N., Shiryaev, A.A., Titkov, S.V., Wiedenbeck, M., Zudina, N.N., 2017. Evidence for Large Scale Fractionation of Carbon Isotopes and of Nitrogen Impurity during Crystallization of Gem Quality Cubic Diamonds from Placers of North Yakutia. Geochem. Int. 55 (11), 988–999.
Richardson, S.H., Gurney, J.J., Erlank, A.J., Harris, J.W., 1984. Origin of diamonds in old enriched mantle. Nature 310, 198–202.
Richardson, S.H., Harris, J.W., Gurney, J.J., 1993. Three generations of diamonds from old continental mantle. Nature 366, 256–258.
Richardson, S.H., Shirey, S.B., Harris, J.W., Carlson, R.W., 2001. Archean subduction recorded by Re-Os isotopes in eclogitic sulfide inclusions in Kimberley diamonds. Earth Planet. Sci. Lett. 191, 257–266.
Robertson, R., Fox, J.J., Martin, A.E., 1934. Two types of diamond. Philos. Trans. Roy. Soc. Lond. 232, 463–535.
Ryan, C.G., Griffin, W.L., Pearson, N.J., 1996. Garnet geotherms: pressure-temperature data from Cr-pyrope garnet xenocrysts in volcanic rocks. J. Geophys. Res. 101 (B3), 5611–5625.
Schidlowski, M., 2001. Carbon isotopes as biogeochemical recorders of life over 3.8 Ga of Earth history: evolution of a concept. Precambrian Res. 106, 117–134.
Scott Smith, B.H., 2008. Canadian kimberlites: Geological characteristics relevant to emplacement. J. Volcanol. Geotherm. Res. 174 (1–3), 9–19.
Shirey, S.B., Cartigny, P., Frost, D.J., Keshav, S., Nestola, F., Nimis, P., Pearson, D.G., Sobolev, N.V., Walter, M.J., 2013. Diamonds and the geology of mantle carbon. In: Hazen, R.M., Jones, A.P., Baross, J.A. (Eds.), Carbon in Earth. Reviews in Mineralogy and Geochemistry 75, pp. 355–421.
Shirey, S.B., Smit, K.V., Pearson, D.G., Walter, M.J., Aulbach, S., Brenker, F.E., Bureau, H., Burnham, A.D., Cartigny, P., Chacko, T., Frost, D.J., Hauri, E.H., Jacob, D.E., Jacobsen, S.D., Kohn, S.C., Luth, R.W., Mikhail, S., Navon, O., Nestola, F., Nimis, P., Palot, M., Smith, E.M., Stachel, T., Stagno, V., Steele, A., Stern, R.A., Thomassot, E., Thomson, A.R., Weiss, Y., 2019. Diamonds and the mantle geodynamics of carbon: Deep mantle carbon evolution from the diamond record. In: Orcutt, B.N., Daniel, I., Dasgupta, R. (Eds.), Deep Carbon: Past to Present. Cambridge University Press, Cambridge, pp. 89–128.
Smart, K.A., Chacko, T., Stachel, T., Muehlenbachs, K., Stern, R.A., Heaman, L.M., 2011. Diamond growth from oxidized carbon sources beneath the Northern Slave Craton, Canada: a δ13C-N study of eclogite-hosted diamonds from the Jericho kimberlite. Geochim. Cosmochim. Acta 75, 6027–6047.
Smart, K.A., Chacko, T., Stachel, T., Tappe, S., Stern, R.A., Ickert, R.B., EIMF, 2012. Eclogite formation beneath the northern Slave craton constrained by diamond inclusions: Oceanic lithosphere origin without a crustal signature. Earth Planet. Sci. Lett. 319–320, 165–177.
Smit, K.V., Stachel, T., Stern, R.A., 2014. Diamonds in the Attawapiskat area of the Superior craton (Canada): evidence for a major diamond-forming event younger than 1.1 Ga. Contrib. Mineral. Petrol. 167, 962.
Smit, K.V., Timmerman, S., Aulbach, S., Shirey, S.B., Richardson, S.H., Phillips, D., Pearson, D.G., 2022a. Geochronology of diamonds. In: Smit, K., Shirey, S., Pearson, G., Stachel, T., Nestola, F., Moses, T. (Eds.), Diamond: Genesis, Mineralogy and Geochemistry. Mineralogical Society of America, Chantilly, pp. 567–636.
Smit, K., Shirey, S., Pearson, G., Stachel, T., Nestola, F., Moses, T., 2022. Diamond: Genesis, Mineralogy and Geochemistry. Mineralogical Society of America, Chantilly.
Smith, E.M., Shirey, S.B., Nestola, F., Bullock, E.S., Wang, J., Richardson, S.H., Wang, W., 2016. Large gem diamonds from metallic liquid in Earth's deep mantle. Science 354 (6318), 1403–1405.
Snyder, D.B., Hillier, M.J., Kjarsgaard, B.A., De Kemp, E.A., Craven, J.A., 2014. Lithospheric architecture of the Slave craton, Northwest Canada, as determined from an interdisciplinary 3-D model. Geochem. Geophys. Geosyst. 15 (5), 1895–1910.
Sobolev, N.V., 1977. The facies of diamond-bearing eclogites and peridotites. In: Sobolev, N.V., Brown, D.A., Boyd, F.R. (Eds.), Deep-Seated Inclusions in Kimberlites and the Problem of the Composition of the Upper Mantle. American Geophysical Union, Washington, Washington, pp. 83–153.
Sobolev, N.V., Lavrent'ev, Yu.G., Pokhilenko, N.P., Usova, L.V., 1973. Chrome-rich garnets from the kimberlites of Yakutia and their parageneses. Contrib. Mineral. Petrol. 40, 39–52.
Sobolev, N.V., Logvinova, A.M., Zedgenizov, D.A., Pokhilenko, N.P., Kuzmin, D.V., Sobolev, A.V., 2008. Olivine inclusions in Siberian diamonds: high-precision approach to minor elements. Eur. J. Mineral. 20, 305–315.
Sobolev, N.V., Wirth, R., Logvinova, A.M., Yelisseyev, A.P., Kuzmin, D.V., 2016. Retrograde isochemical phase transformations of majoritic garnets included in diamonds: a case study of subcalcic Cr-rich majoritic pyrope from a Snap Lake diamond, Canada. Lithos 265, 267–277.
Stachel, T., Harris, J.W., Aulbach, S., Deines, P., 2002. Kankan diamonds (Guinea) III: δ13C and nitrogen characteristics of deep diamonds. Contrib. Mineral. Petrol. 142, 465–475.
Stachel, T., Harris, J.W., Tappert, R., Brey, G.P., 2003. Peridotitic diamonds from the Slave and the Kaapvaal cratons – similarities and differences based on a preliminary data set. Lithos 71, 489–503.
Stachel, T., Aulbach, S., Brey, G.P., Harris, J.W., Leost, I., Tappert, R., Viljoen, K.S., 2004. The trace element composition of silicate inclusions in diamonds: a review. Lithos 77, 1–19.
Stachel, T., Brey, G.P., Harris, J.W., 2005. Inclusions in sublithospheric diamonds: glimpses of the deep Earth. Elements 1, 73–78.
Stachel, T., Banas, A., Muehlenbachs, K., Kurszlaukis, S., Walker, E.C., 2006. Archean diamonds from Wawa (Canada): samples from deep cratonic roots predating cratonization of the Superior Province. Contrib. Mineral. Petrol. 151, 737–750.
Stachel, T., Harris, J.W., 2008. The origin of cratonic diamonds – Constraints from mineral inclusions. Ore Geol. Rev. 34, 5–32.
Stachel, T., Harris, J.W., 2009. Formation of diamond in the Earth's mantle. J. Phys. Condens. Matter 21, 364206.
Stachel, T., Banas, A., Aulbach, S., Smit, K.V., Wescott, P., Chinn, I.L., Kong, J., 2018. The Victor Mine (Superior Craton, Canada): Neoproterozoic lherzolitic diamonds from a thermally-modified cratonic root. Mineral. Petrol. 112, 325–336.
Stachel, T., Cartigny, P., Chacko, T., Pearson, D.G., 2022a. Carbon and Nitrogen in mantle-derived diamonds. In: Smit, K., Shirey, S., Pearson, G., Stachel, T., Nestola, F., Moses, T. (Eds.), Diamond: Genesis, Mineralogy and Geochemistry. Mineralogical Society of America, Chantilly, pp. 809–875.
Stachel, T., Aulbach, S., Harris, J.W., 2022b. Mineral inclusions in lithospheric diamonds. In: Smit, K., Shirey, S., Pearson, G., Stachel, T., Nestola, F., Moses, T. (Eds.), Diamond: Genesis, Mineralogy and Geochemistry. Mineralogical Society of America, Chantilly, pp. 307–391.
Sudholz, Z.J., Yaxley, G.M., Jaques, A.L., Chen, J., 2021. Ni-in-garnet geothermometry in mantle rocks: a high pressure experimental recalibration between 1100 and 1325°C. Contrib. Mineral. Petrol. 176, 32.
Tappert, R., Stachel, T., Harris, J.W., Shimizu, N., Brey, G.P., 2005. Mineral inclusions in diamonds from the Panda kimberlite, Slave Province, Canada. Eur. J. Mineral. 17, 423–440.

Tappert, R., Foden, J., Stachel, T., Muehlenbachs, K., Tappert, M., Wills, K., 2009. Deep mantle diamonds from South Australia: a record of Pacific subduction at the Gondwanan margin. Geology 37 (1), 43–46.
Taylor, L.A., Liu, Y., 2009. Sulfide inclusions in diamonds: not monosulfide solid solution. Russ. Geol. Geophys. 50, 1201–1211.
Taylor, W.R., Jaques, A.L., Ridd, M., 1990. Nitrogen-defect aggregation characteristics of some Australasian diamonds: time-temperature constraints on the source regions of pipe and alluvial diamonds. Am. Mineral. 75, 1290–1310.
Taylor, W.R., 1998. An experimental test of some geothermometer and geobarometer formulations for upper mantle peridotites with application to the thermobarometry of fertile lherzolite and garnet websterite. Neues Jahrbuch für Mineralogie – Abhandlungen 172, 381–408.
Thomson, A.R., Kohn, S.C., Prabhu, A., Walter, M.J., 2021. Evaluating the formation pressure of diamond-hosted majoritic garnets: a machine learning majorite barometer. Journal of Geophysical Research: SolidEarth 126 (3) e2020JB020604.
Timmerman, S., Reimink, J.R., Vezinet, A., Nestola, F., Kublik, K., Banas, A., Stachel, T., Stern, R.A., Luo, Y., Sarkar, C., Ielpi, A., Currie, C.A., Mircea, C., Jackson, V., Pearson, D.G., 2022. Mesoarchean diamonds formed in thickened lithosphere, caused by slab-stacking. Earth Planet. Sci. Lett. 592, 117633.
Tomlinson, E.L., Jones, A.P., Harris, J.W., 2006. Co-existing fluid and silicate inclusions in mantle diamond. Earth Planet. Sci. Lett. 250, 581–595.
Van Rythoven, A.D., Schulze, D.J., 2009. In-situ analysis of diamonds and their inclusions from the Diavik Mine, Northwest Territories, Canada: mapping diamond growth. Lithos 112S, 870–879.
Van Rythoven, A.D., McCandless, T.E., Schulze, D.J., Bellis, A., Taylor, L.A., Liu, Y., 2011. Diamond crystals and their mineral inclusions from the Lynx kimberlite dyke complex, Central Quebec. Can. Mineral. 49, 691–706.
Van Rythoven, A.D., Schulze, D.J., Hauri, E.H., Wang, J., Shirey, S., 2017. Intra-crystal co-variations of carbon isotopes and nitrogen contents in diamond from three north american cratons. Chem. Geol. 467, 12–29.
Van Rythoven, A.D., Schulze, D.J., Stern, R.A., Lai, M.Y., 2022. Composition of diamond from the 95–2 pipe, Lake Timiskaming kimberlite cluster, Superior craton,Canada. Can. Mineral. 60 (1), 67–90.
Walter, M.J., Thomson, A.R., Smith, E.M., 2022. Geochemistry of silicate and oxide inclusions in sublithospheric diamonds. In: Smit, K., Shirey, S., Pearson, G., Stachel, T., Nestola, F., Moses, T. (Eds.), Diamond: Genesis, Mineralogy and Geochemistry. Mineralogical Society of America, Chantilly, pp. 393–450.
Webb, S.A.C., Wood, B.J., 1986. Spinel-pyroxene-garnet relationship and their dependence on Cr/Al ratio. Contrib. Mineral. Petrol. 92, 471–480.
Westerlund, K.J., Shirey, S.B., Richardson, S.H., Carlson, R.W., Gurney, J.J., Harris, J.W., 2006. A subduction wedge origin for Paleoarchean peridotitic diamonds and harzburgites from the Panda kimberlite, Slave craton: evidence from Re-Os isotope systematics. Contrib. Mineral. Petrol. 152, 275–294.
Whitmeyer, S.J., Karlstrom, K.E., 2007. Tectonic model for the Proterozoic growth of North America. Geosphere 3 (4), 220–259.
Wold, S., Esbensen, K., Geladi, P., 1987. Principal component analysis. Chemom. Intell. Lab. Syst. 2, 37–52.
Woodland, A.B., Gräf, C., Sandner, T., Höfer, H.E., Seitz, H.-M., Pearson, D.G., Kjarsgaard, B.A., 2021. State and metasomatism of the lithospheric mantle beneath the Rae Craton, Canada: strong gradients reflect craton formation and evolution. Sci. Rep. 11, 3684.
Wyman, D.A., Kerrich, R., 1993. Archean shoshonitic lamprohyres of the Abitibi Subprovince, Canada: petrogenesis, age and tectonic. J. Petrol. 34 (6), 1067–1109.
Wyman, D.A., Kerrich, R., Polat, A., 2002. Assembly of Archean cratonic mantle lithosphere and crust: plume-arc interaction in the Abitibi-Wawa subduction-accretion complex. Precambrian Res. 115, 37–62.
Zhang, Z., Fedortchouk, Y., 2012. Records of mantle metasomatism in the morphology of diamonds from the Slave craton. Eur. J. Mineral. 24, 619–632.
Ziberna, L., Nimis, P., Kuzmin, D., V.G., 2016. Error sources in single-clinopyroxene thermobarometry and a mantle geotherm for the Novinka kimberlite, Yakutia. Am. Mineral. 101, 2222–2232.